Out-of-Autoclave Manufacturing of Aerospace Representative Parts

by

Julien Cauberghs

Ingénieur diplômé de l'Ecole Polytechnique, 2009

Department of Mechanical Engineering

McGill University, Montreal

A thesis submitted to

McGill University

in partial fulfillment of the requirements of the degree of

Master of Engineering

McGill

July 2011

Abstract

The use of carbon fibre reinforced composites for aerospace structures has seen a high increase in recent years, and is still growing. The high stiffness-to-weight ratio of these materials makes them ideal for primary structures on airplanes, satellites, and spacecrafts. Nevertheless, the manufacturing of composites remains very costly since it requires equipment investment such as an autoclave, and very qualified workers. Out-of-autoclave manufacturing technology is very promising since it only requires a traditional oven, while still aiming at similar part quality. However, the absence of positive pressure compared with an autoclave makes it more difficult to achieve low porosity parts.

This research investigates the manufacturing of complex features with out-of-autoclave prepreg technology. The features studied are tight-radius corners with a curvature change, and ply drop-offs. Ply drop-offs tests were conducted to identify if porosity is higher at ply terminations. In corners, the bagging arrangement was modified to achieve the most uniform thickness in areas of curvature change, even with small radii. The conclusions from these studies provided us with guidelines to manufacture larger representative parts, which included these features. The representative parts were tested for porosity, thickness uniformity, mechanical performance, and glass transition temperature (T_g). A total of four representative parts were manufactured with out-of-autoclave technology, and one more was manufactured with an autoclave to allow for a proper comparison between the two processes. The materials used were MTM45-1 5 harness satin and CYCOM5320 plain weave for the out-of-autoclave parts, and CYCOM5276-1 plain weave for the autoclave part. The effect of ply drop-offs on porosity was found to be negligible. Thickness deviation in corners was attributed to a combination of consumable bridging, prepreg's bulk factor and inter-ply shear. Overall, out-of-autoclave prepregs showed performance similar to autoclave prepregs.

Sommaire

L'utilisation de matériaux composites en fibres de carbone pour des structures aéronautiques a connu une croissance rapide ces dernières années, et continue de croitre. Le rapport raideur/masse de ce type de matériaux en fait une solution idéale pour les structures primaires d'avions, de satellites, ou de navettes spatiales. Toutefois, la fabrication de ces pièces en composites demeure extrêmement couteuse puisqu'elle nécessite de lourds investissements d'équipement tels que l'acquisition d'un autoclave, ainsi que de la main-d'œuvre qualifiée. La technologie hors autoclave semble très prometteuse puisqu'elle ne requiert que l'utilisation d'un four traditionnel, tout en visant à obtenir des pièces de qualité similaire. Cependant, l'absence de pression extérieure provenant de l'autoclave rend plus délicate l'obtention de pièces ayant une faible porosité.

Cette recherche a pour thème la fabrication d'éléments complexes avec la technologie hors autoclave. Les éléments étudiés sont des angles convexes et concaves ayant de faibles rayons de courbure, ainsi que des plis partiels. Des tests sur les plis partiels ont été réalisés pour déterminer si ils sont associés à une augmentation de la porosité. Dans les angles, l'arrangement des consommables a été modifié pour obtenir l'épaisseur la plus uniforme possible dans les zones de changement de courbure, et cela même pour de faibles rayons. Les conclusions de ces tests nous ont permis de considérer la fabrication de pièces représentatives de plus grande taille, et qui contiennent les éléments précédemment étudiés. Les pièces représentatives ont été testées pour déterminer leur niveau de porosité, l'uniformité de leur épaisseur, leur performance mécanique, et leur température de transition vitreuse. Au total, quatre pièces représentatives ont été fabriquées par technologie hors autoclave, et une a été fabriquée dans un autoclave afin de permettre une comparaison de bon aloi entre ces deux procédés de fabrication. Les matériaux utilisés pour cette recherche étaient du MTM45-1 5 harness satin et du CYCOM5320 plain weave pour les pièces hors autoclave, ainsi que du CYCOM5276-1 plain weave pour la pièce autoclave. La présence de plis partiels n'a pas été associable à une augmentation notable de la porosité. L'uniformité

d'épaisseur s'est révélée être une combinaison de pontage des consommables, du facteur de foisonnement du pré-imprégné, et du cisaillement entre les plis de fibre. Globalement, les pré-imprégnés hors autoclave ont montré des performances similaires aux pré-imprégnés autoclave.

Acknowledgements

I would like to thank all those people who supported me through the duration of my master's program and who are still present by the end of this period of my life. A special thank goes to my parents for their material support and moral presence in the last twenty four years.

I would like to acknowledge my supervisor Professor Pascal Hubert for giving me the opportunity to work on this project and to be part of the Structures and Composite Materials Laboratory. My experience at McGill University was full of lessons and discoveries.

This research was made possible thanks to the financial support of NSERC, CRIAQ, Bell Helicopter Textron, Bombardier, and Delastek.

I would like to express my gratitude to Daniel Poirier from the Center for the Development of Composites in Quebec (CDCQ), for his continuous help, advices, and availability, and for understanding that people being formed make mistakes. I also thank all the technicians who helped me: Martine Pelletier, Raphaël Chamberland Girardin, Franck Segara, and Jean-François Corbeil for the mechanical tests.

I would like to thank Philip Barsalou from Bell Helicopter for his patience, his help with material supplies and ply cutting for the representative parts.

Many thanks go to Xavier Gagné Brulotte for his help with the little things and ideas that make your life easier, as well as for the Tg measurements.

I sincerely thank my colleagues working in FDA 015 for the lively environment and the even more lively discussions, as well as for the team moments.

Finally, special thanks go to Sophie Bussières for her support, patience, love and presence in my life.

Table of contents

List of Tables

List of Figures

Nomenclature

B_f: Bulk factor

K: Permeability coefficient of the prepreg

L: Length of the part

m/m_0: Mass fraction of gas remaining in the laminate

off0: Offset in ambient conditions

P: Measured pressure

P_0: Initial pressure in the bag

$\mathrm{R_i}$: Initial radius on the bag side

$\mathrm{R_f}$: Final radius on the bag side

sens0: Sensitivity at room temperature

Sout: Output signal from pressure cell

t: Vacuum hold time

$\mathrm{t_i}$: Initial flange thickness

$\mathrm{t_f}$: Final flange thickness

$\mathrm{t_i^M}$: Initial corner thickness

$\mathrm{t_f^M}$: Final corner thickness

TCO: Thermal coupling of the offset

TCS: Thermal coupling of the sensitivity

$\mathrm{T_g}$: Glass transition temperature

V_{void}: Void content (porosity)

β: Deformation angle

μ: Dynamic viscosity of air

1 Introduction

1.1 Composite Materials

Since the emergence of composite materials in the 1940s, improvements in advanced polymers and high-performance fibres led to an increasing number of applications. From the horizontal stabilizer of the F-111 in the 1960s to the primary structure of the Boeing 787 in 2009, the aerospace industry used more and more composite materials to reduce the aircraft weight [1]. Weight reduction goes along with improved fuel efficiency, a critical objective for aircraft manufacturers. Composite materials not only have a higher specific modulus and specific strength compared to steel or aluminum, they also have a better resistance to corrosion and fatigue.

The outstanding properties of composite materials are the result of the combination of reinforcement (fibres) in a matrix system (polymer resin). Fibres can be of different materials; fibreglass, carbon fibre and aramid fibre are the most commonly used. They give the composite its high strength and stiffness, while the resin gives the shape of the part and ensures load transfer between fibres. The best mechanical properties are obtained using continuous fibres. Fibres have a very small diameter (approximately $6x10^{-6}$m for carbon fibres [2]) and they are bundled together to form a fibre tow, as shown in Figure 1.1. A tow usually contains 3000, 6000 or 12000 fibres. Tows are kept aligned to form unidirectional plies or they are woven like a textile to form fabric plies.

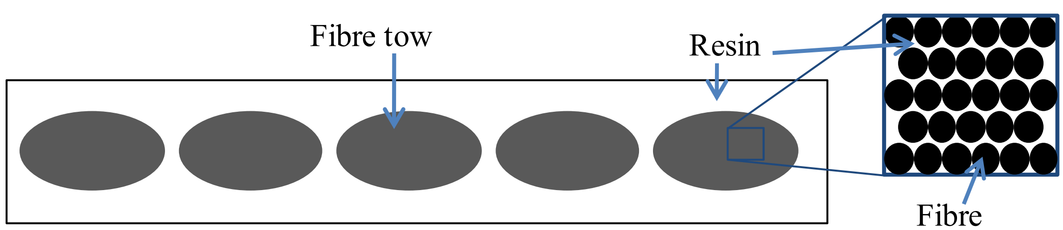

Figure 1.1: Cross-sectional view of a unidirectional composite ply and detail of a fibre tow.

Plies of fibre are stacked to form a laminate (Figure 1.2). By varying the number of plies and their angles, a laminate can be designed to resist the loads it will have to face. Because they have a high specific strength, carbon fibre composites are an important category of composite materials. They are widely used in aerospace parts.

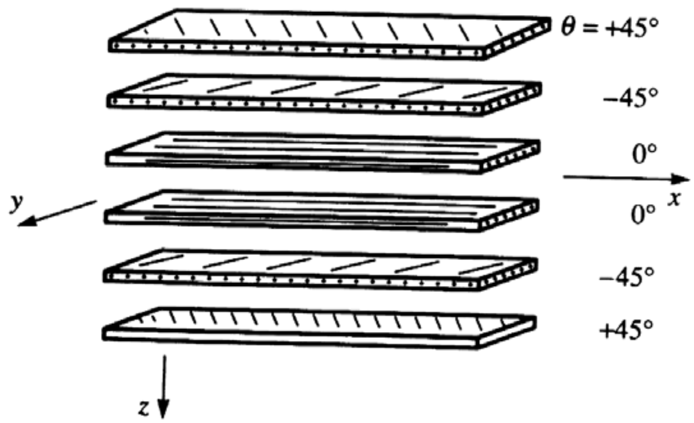

Figure 1.2: Exploded view of a laminate [3].

When a high bending stiffness is required, the laminate should be very thick. To reduce even more the weight of such a part, a core is usually placed between two skins of composite material, resulting in a sandwich panel. An important type of core consists of a honeycomb, made of hexagonal cells. To ensure a good bonding between the honeycomb and the composite skins a layer of adhesive material is placed on each side of the honeycomb core (Figure 1.3).

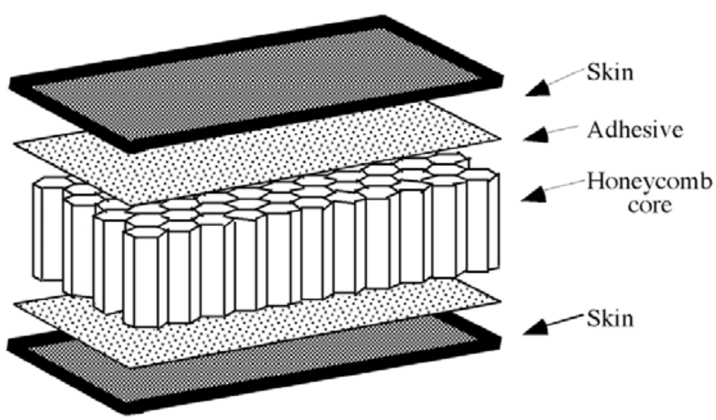

Figure 1.3: Exploded view of a honeycomb core sandwich structure [4].

1.2 Autoclave Manufacturing

Several manufacturing methods are used for composite materials. An overview can be found in [5]. The choice of a manufacturing method is a balance between the expected properties and production costs. For high performance composites, like aerospace parts, weight reduction and mechanical performance are the driving factors. The manufacturing process can start with dry fibres that are later impregnated with resin, but a more convenient material form is prepreg. The later is composed of fibre pre-impregnated with resin. One advantage of prepreg is that it already contains an amount of matrix material, which ensures a good distribution of resin, diminishing the risk of dry regions. And more practically, it is easy to handle since it does not require injecting liquid resin in a dry fibre bed.

The objectives to achieve through the manufacturing process are 1) a homogeneous part without resin accumulation or dry regions, 2) a high fibre volume fraction (ratio of fibre volume over total volume), 3) the absence of defects like delamination zones, 4) a low void content.

Autoclave manufacturing proved its efficiency to meet these objectives. An autoclave can be basically described as a pressurized oven. In autoclave manufacturing, prepreg plies are stacked on the mould, and a vacuum bag is sealed around the plies. The autoclave is then heated, and pressurized (typically at 4 to 8 atm). The pressure in the autoclave provides compaction to the laminate. The curing of the resin is activated by the heat. Cross-links between chains of polymers are created and the resin gels to become solid. Finally, the part is cooled down to room temperature and taken out of the autoclave.

A typical bagging arrangement for autoclave curing is shown in Figure 1.4. The mould surface is treated with a release agent so that the part can be easily removed after cure. A bleeder cloth is placed above the laminate. Autoclave prepregs usually have an excess of resin which gets evacuated in the bleeder during cure. Dams are placed at the edges of the laminate to avoid resin loss on the sides of the part. A breather cloth ensures the distribution of vacuum in the bag. The vacuum bag is sealed-off around the part with sealant tape.

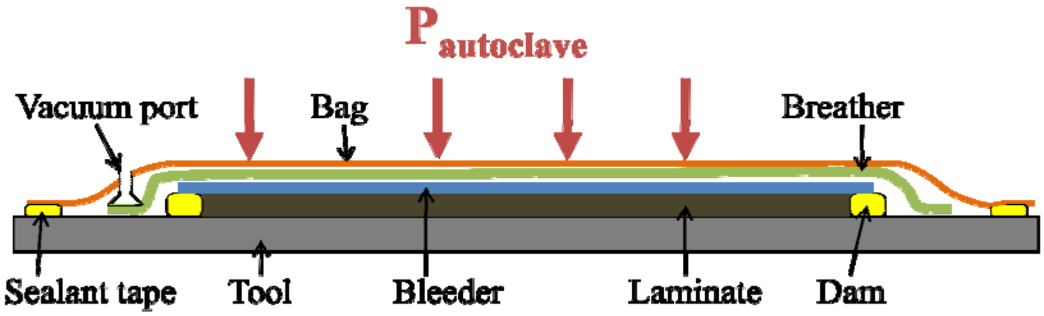

Figure 1.4: Schematic of bagging arrangement for autoclave manufacturing.

1.3 Out-of-Autoclave Manufacturing

Despite their capacity to manufacture good parts, autoclaves are very costly and represent a prohibitive investment. Also, the size of the part is limited to the size of the autoclave. For these reasons, prepreggers put a lot of effort into the development of prepregs that can be cured under vacuum pressure only, in a traditional oven. Out-of-autoclave manufacturing (OOA) was born, with carbon epoxy prepregs that could be cured at a lower temperature than autoclave prepregs. However, the mechanical properties were not as good as with autoclave prepregs. New prepregs were then produced with toughened epoxy resin, resulting in parts with improved mechanical properties and a higher glass transition temperature (T_g) which allowed for a higher service temperature [6]. The glass transition temperature is the temperature above which the material changes from a solid state to a rubbery state. Contrary to the early autoclave prepreg systems, OOA prepregs directly have the right amount of resin; they are “no-bleed systems”. Note that some autoclave prepregs recently developed are also no-bleed systems. The main challenge with OOA prepregs is to evacuate the air that is entrapped between or within the plies. Indeed, only 1 atm of pressure is available (vacuum pressure). In autoclaves, the high pressure applied on the bag can dissolve the entrapped air into the resin. In out-of-autoclave manufacturing, the air needs to be physically removed from the laminate. To enable air removal, prepreggers made their prepregs porous with evacuation channels (EVaC). These channels can be seen as an interconnected 3D network (see Figure 1.5).

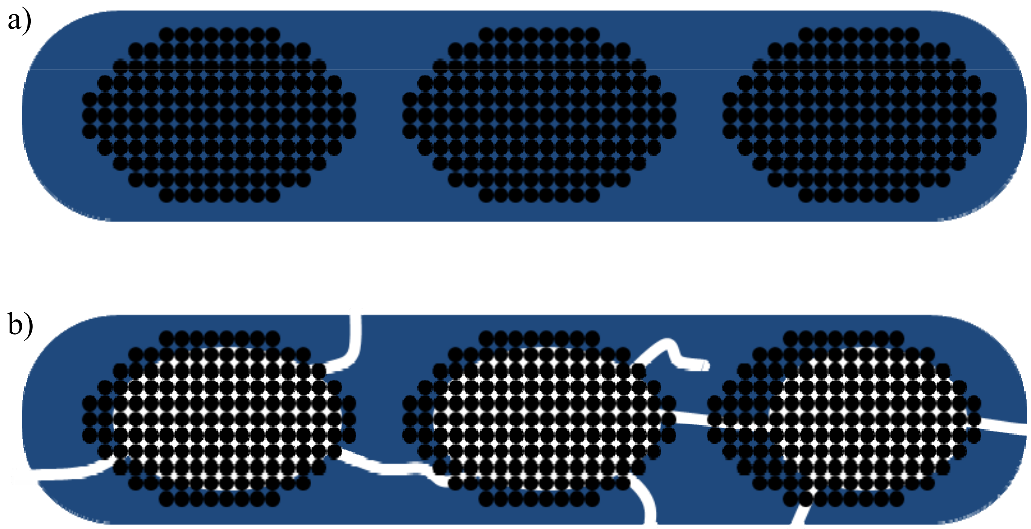

Figure 1.5: Schematic of fibre tows a) in a no-bleed prepreg b) in an out-of-autoclave prepreg. Black, blue and white represent the fibres, resin and air respectively.

Several details in the bagging arrangement and the manufacturing steps in OOA manufacturing differ from autoclave manufacturing. They are further discussed in the literature review.

1.4 Motivation and Thesis Organization

Although out-of-autoclave manufacturing looks very attractive, the influence of the different process variables is not yet fully understood, and it is difficult to consistently make low porosity parts (void content < 1%).

This research focuses on the manufacturing of a representative sub-component. It is part of a large project that investigates the effect of the processing parameters in order to optimise them, establish the relationship between part quality and production costs, and determine and test a suitable representative sub-component using out-of-autoclave technology.

Two out-of-autoclave resin systems were selected for this project: MTM45-1 manufactured by The Advanced Composites Group, and CYCOM5320 manufactured by Cytec Industries. Initial studies covered some fundamental understanding of the materials like resin cure kinetics, resin viscosity through the cure cycle, the effect of vacuum level on part quality, etc [7]. These studies allowed the manufacturing of parts like sandwich panels and curved parts [8-11].

The next step was to select a representative part; a sub-component that could demonstrate the capacities of out-of-autoclave manufacturing and show that this technology is suitable for aerospace grade composite parts. The chosen mould featured manufacturing challenges like tight concave and convex corners, and double curvatures. It was larger than the parts previously manufactured in this project. It was also decided to manufacture autoclave parts with an autoclave prepreg on the same mould to allow an objective comparison between OOA and autoclave technologies. The approach is summarized in the flow chart Figure 1.6.

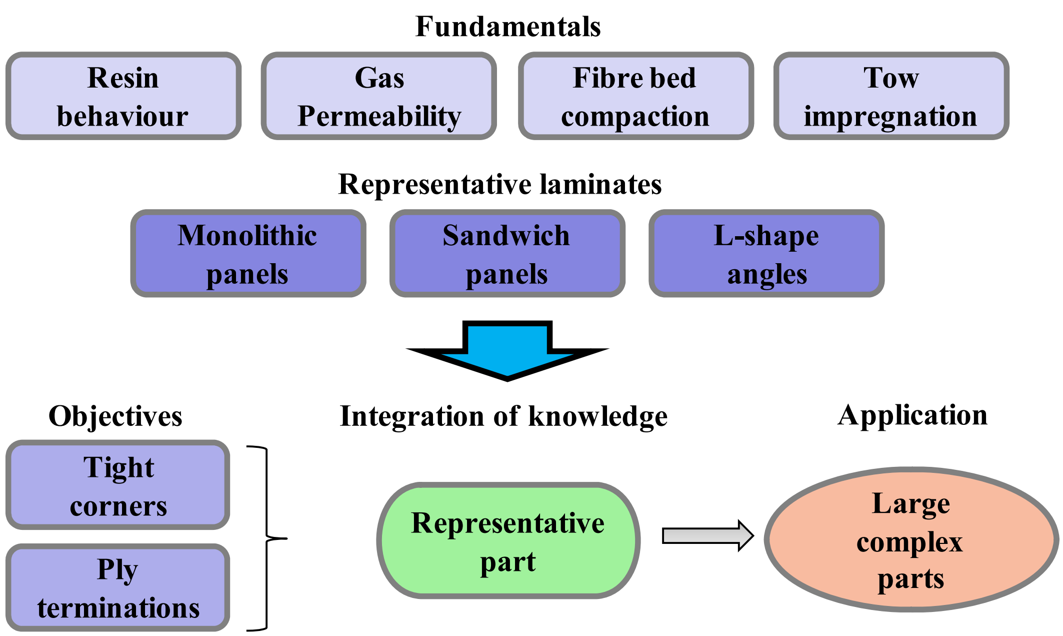

Figure 1.6: Project overview.

The representative part included several manufacturing challenges. Some of them had already been studied but others had to be further investigated before manufacturing a complete part. The effect of two features on part quality was studied. The first feature was ply drop-offs, also called ply terminations. They are partial plies that do not stretch on the entire surface of the part. The end of the ply is in the middle of the laminate. The second feature is tight corners with curvature changes, and more especially the succession of a concave, a convex, and a second concave corner.

The objective of this research is to design, manufacture and test representative parts in order to evaluate and compare the capacities of autoclave and out-of-autoclave manufacturing. The part quality will be assessed through porosity measurements, thickness measurements in tight corners, mechanical testing, and evaluation of the glass transition temperature (T_g).

Chapter 2 presents a review of the literature on manufacturing of complex shape laminates, theories on void formation, as well as a summary of the previous research work on out-of-autoclave technology that is useful to the manufacturing of the representative part. Chapter 3 presents results from experiments on tight corners and Chapter 4 discusses the effect of ply drop-offs. Chapter 5 details the design of the representative parts, their manufacturing, and a comparison with autoclave-manufactured parts. Conclusions on out-of-autoclave capacities and limitations are discussed in Chapter 6.

2 Literature Review

Manufacturing a composite part is always a challenge, even with an autoclave. Numerous factors can impact the final quality of the part. Early research works tried to identify these factors and to control their influence. This literature review does not cover all the phenomena involved in prepreg manufacturing technology, but focuses on the aspects that are most relevant for the manufacturing of the representative parts.

2.1 Resin Properties

The mechanical performance of a composite material depends on the fibres, the resin, and their interaction. While the fibres give the tensile properties of the material, the resin is more responsible for the compression and shear properties. The resins used in this project are epoxy resins. They are polymer chains that are initially uncured. When heated, cross-links are created and a 3D network is formed (see Figure 2.1). The control of resin cure kinetics, viscosity and degree of cure are of high importance. Loos and Springer [12] modelled the kinetics and viscosity of an autoclave resin system. They created a numerical model to tailor the cure cycle so that the desired material properties are met. Modelling the curing process avoids adopting a trial and error approach and thus allows for important time and cost savings. A review by Hubert and Poursartip [13] presents a general model that links degree of cure, resin viscosity and resin flow in the prepreg stack during cure.

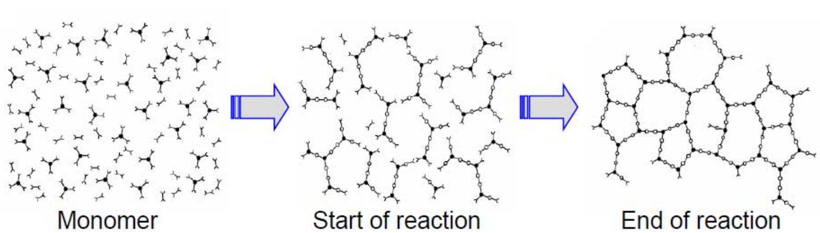

Figure 2.1: Schematic of resin cure [14].

Another important resin property is glass transition temperature (T_g). The glass transition temperature should be significantly higher than the service temperature of the material. The first generation of out-of-autoclave prepregs used un-toughened epoxy resins and had significantly lower glass transition temperatures compared to autoclave systems, limiting the application of such materials. The second generation of out-of-autoclave prepregs such as the ones studied in this project uses toughened epoxy resins with a T_g comparable to autoclave prepregs T_g [15]. Typical evolutions of the degree of cure, the resin viscosity, and T_g during cure are shown in Figure 2.2.

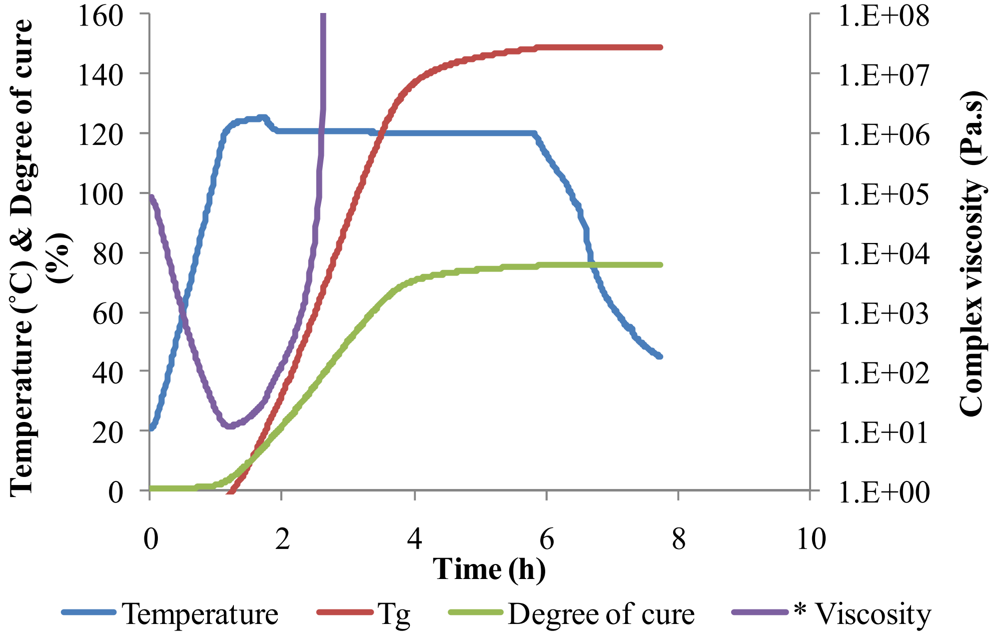

Figure 2.2: Evolution of resin properties during cure (MTM45-1).

Out-of-autoclave materials were designed by prepreggers to be cured at low temperature on low cost tooling. To develop full mechanical performance and high T_g, the parts should be post-cured. To do so, the part is removed from the mould after cure and placed back in the oven with sufficient support to avoid part distortion. The oven is heated to a higher temperature than during cure and the resin gets fully cured. Degree of cure, viscosity, and glass transition temperature were investigated and modelled for MTM45-1 and CYCOM 5320 [7].

2.2 Porosity

2.2.1 Void Formation and Growth

Voids are defects consisting of small cavities that are found in cured composite laminates. The void content of a composite is the ratio between the volume occupied by voids and the total volume of the composite. Porosity is used as a synonym to void content. Voids were quickly found to reduce the mechanical performance of a material, mainly compression and shear properties, since they are a source of stress concentration. The shear strength, for example, decreases when void content is higher than 1%. At 4% void content, shear strength can be reduced by as much as 20% [16]. Voids can be of different shape and size and are usually found in resin rich regions, i.e. between plies and between fibre tows (see Figure 2.3).

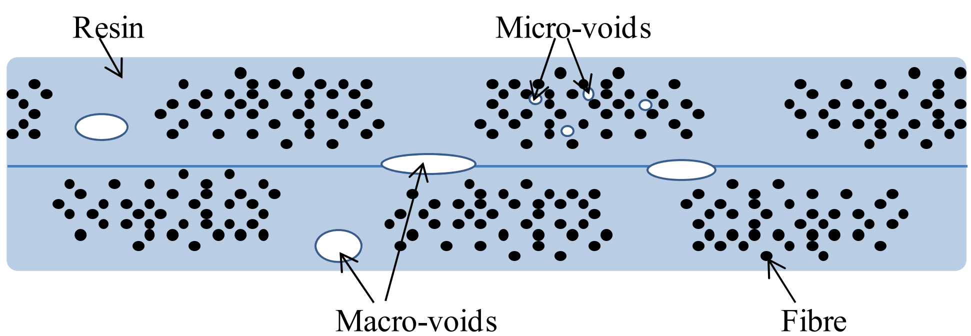

Figure 2.3: Schematic of voids typically found in composite laminates.

Voids formation and growth have been investigated in several research works [17-20]. An important source of voids is the air entrapped in or between plies of prepreg during lay-up. Moisture was also found to generate voids as the water turns into vapour above a certain temperature, depending on the pressure level. Also, the chemical reaction can generate volatiles that are part of the reaction products. A more marginal void nucleation mechanism was reported in [17] and described as stress-initiated void formation. When epoxy resin cures, it undergoes a volumetric shrinkage that can be as high as 10%. The resin being displacement-constrained, the shrinkage creates internal stresses that can lead to the formation of voids.

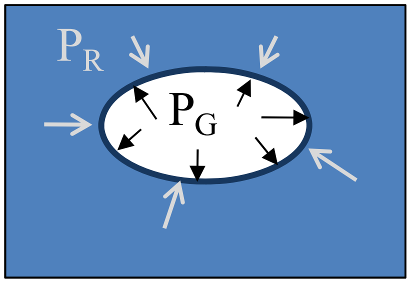

Figure 2.4: Forces acting on a void in partially cured resin.

Once a void has formed, its evolution depends on the pressure differential between the gas in the void and in the resin surrounding the void, and on the surface tension at the resin/gas interface, as shown in Figure 2.4. This balance of forces defines a radius for the void to be at equilibrium. If resin pressure is high enough, the void can collapse and the gases are dissolved in the resin. If not, the void will remain stable, or will even grow.

In autoclaves, the external pressure applied on the vacuum bag increases the resin pressure and voids are likely to be dissolved. In out-of-autoclave technology, the resin pressure is not always high enough to remove all the voids. The best solution to this issue is to remove a maximum of air from the laminate prior to the cure, or during cure before the resin gels.

2.2.2 Permeability

Permeability is a measure of the ability of fluids or gases to flow through a porous medium. Out-of-autoclave prepregs show permeability to air in the uncured state. Because of their anisotropic structure, the in-plane permeability of prepregs is usually very different from their through thickness (Z direction) permeability. Researchers started to study prepreg permeability with autoclave prepregs. Ahn and Seferis [21] examined the permeability of three different autoclave prepregs; a porous, a fully resin-impregnated, and a particulate surface toughened prepreg. They found that the porous and particulate surface toughened prepreg had a higher permeability to air than the fully impregnated prepreg, and under "the same operating conditions, prepregs of higher permeation consistently resulted in the production of void-free laminates"[21]. The advantage of a permeable prepreg over an impermeable one is that the entrapped air can be evacuated instead of forming voids that need to be dissolved in the resin.

Out-of-autoclave prepregs are permeable to air and, once the vacuum bag is ready and before starting the cure, the laminate is placed under full vacuum for a certain period called vacuum hold. The objective of this operation is to remove as much air as can be removed from the prepreg stack. Vacuum hold can last for several hours; the duration depends on the part size and complexity. A large part with several curvatures will require a longer vacuum hold than a small flat part.

Permeability of prepregs is commonly used along with Darcy's law to model fluid transport within a fibrous medium. Arafath et al. exposed a 1D model for gas transport [22]. They derived a simple equation to predict the vacuum hold time necessary to remove a desired portion of gas.

$$t = \frac{\mu}{P_0}\frac{L^2}{K}\left[-\frac{1}{0.9}\ln\left(\frac{m}{m_0}\right)\right]^{\frac{1}{0.6}} \tag{2.1}$$

where t is the vacuum hold time, μ the dynamic viscosity of air, P_0 the initial pressure in the bag (atmospheric), L the length of the part, K the permeability coefficient of the prepreg, and m/m_0 the mass fraction of gas remaining in the laminate. This equation shows that the vacuum hold time does not evolve linearly with L, but with L^2.

The same approach was applied to MTM45-1 in [23]. The order of magnitude of the permeability of the prepregs used in this project was measured and is reported in Table 2.1.

Table 2.1: Order of magnitude of permeability for the prepregs used in this project [7, 11, 23-25].

Material	In-plane permeability [m^2]	Through thickness permeability [m^2]
MTM45-1 5HS	10^{-14}	10^{-18}
CYCOM5320 PW	10^{-14}	10^{-16}

The in-plane permeability is comparable for both materials, whereas the through thickness permeability of CYCOM5320 Plaine Weave (PW) is 2 orders of magnitude higher than MTM45-1 5 Harness Satin (5HS). In both cases, the in-plane permeability is much higher than the through thickness permeability. This means that, except for large parts, the gases are essentially evacuated through the edges of the laminate, and not through its thickness.

2.2.3 OOA Bagging Arrangement

The phenomenon presented in the previous paragraph has a direct influence on the bagging arrangement used in out-of-autoclave manufacturing. To enhance the gas evacuation at the edges of the laminate, and take advantage of the high in-plane permeability of out-of-autoclave prepregs, edge breathing is used. It consists of dry fibreglass placed on the edge of the laminate. Two different configurations can be used and are shown in Figure 2.5. In Configuration A) a dry fibreglass fabric is wrapped around sealant tape and placed against the edge of the laminate. The fabric continuously surrounds the part. The fibreglass provides a path for air and volatiles from the laminate to the breather. In configuration B) dry fibreglass tows are placed over cork dams and between the plies of the laminate, and are regularly spaced [15]. The fibreglass tows also serve as a passage from the laminate to the breather. In configurations A) and B), sealant tape or cork dam prevents the resin to bleed in the plane of the laminate. It was also found that the tape/dam should be at least as thick as the laminate to avoid any pinching of the edge of the laminate that could partially block the evacuation paths. Both configurations were tested in [26] and there was no clear sign that one leads to higher quality laminates than the other.

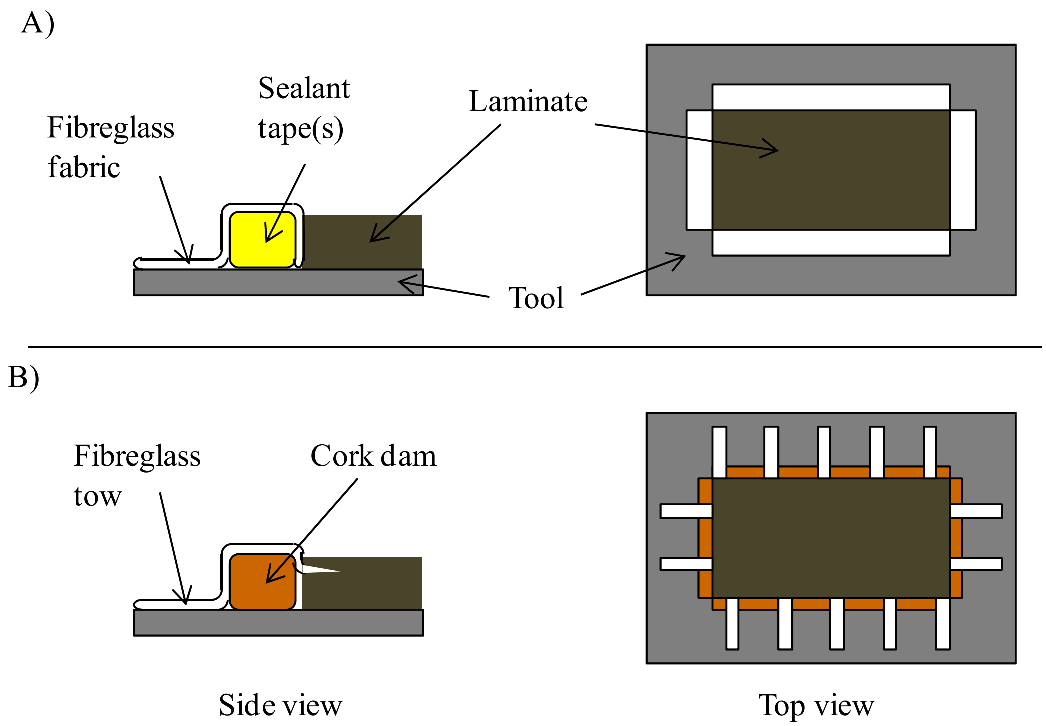

Figure 2.5: Top and side views of two edge breathing configurations A) tacky tape and fibreglass cloth, B) cork dam and fibreglass tows (from [8]).

In out-of-autoclave manufacturing, the bagging arrangement is similar to the one used in autoclave manufacturing except for two important details: there is no bleeder because the prepreg already contains the right amount of resin, and dams are replaced with edge breathing (see Figure 2.6). To prevent the breather from sticking on the laminate, a ply of release film is placed above the laminate. It can be perforated or not. Perforated release film might be of interest because it allows the air to flow in the through thickness direction. If a purely in-plane evacuation approach is chosen, non-perforated release film is used.

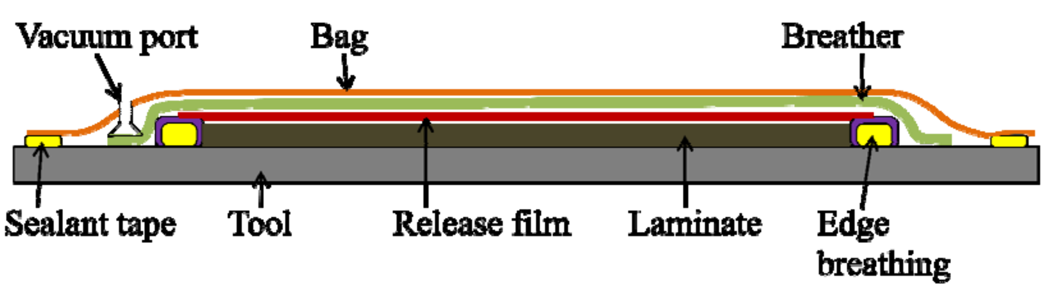

Figure 2.6: Schematic of bagging arrangement for out-of-autoclave manufacturing

During the lay-up of the plies, it is recommended to perform a debulk every 4 plies approximately. A debulk consists in keeping the laminate under vacuum for 5 to 10 minutes. This operation is time consuming since it requires to place release film, breather cloth, and a sealed vacuum bag above the prepreg stack, and then to remove it to continue laying up the plies of prepreg. Still, debulks ensure that the prepreg stack conforms to the mould shape and consolidate the prepreg stack.

2.3 Sandwich Structures

To reduce the weight of a part that requires high flexural stiffness, a honeycomb core is inserted between two skins of prepreg, with a ply of adhesive between the core and each prepreg skin. One of the issues is that the honeycomb core is a large volume of air, initially at atmospheric pressure. Depending on the prepreg and adhesive permeability and on the duration of the vacuum hold before cure, the pressure can be reduced in the core. Early research work concluded that leaving the air in the core at a high pressure led to a poor skin/core adhesion but to low porosity in the skin. On the contrary, decreasing the air pressure prior to the cure was beneficial to the skin/core adhesion, but led to high skin porosity because of a low compaction due to a low pressure differential between the bag and the core [27]. The trade-off between porosity and skin/core bonding was later studied in [10, 28, 29]. The phenomenon is complex and depends on the materials and the cure cycle used. The existence of an optimal core pressure at the beginning of the cure cycle was described:

- If the initial pressure in the core is too high, the air forces its way through the bag side skin when the laminate is heated and the resin viscosity is low, resulting in skins with high porosity, adhesive push-through in the skin on the bag side, and even void channels linking the core to the bag side facesheet [10].
- If the initial pressure in the core is too low, the fracture energy in delamination Mode I was found to decrease [28, 29].

The pressure level in the core at the end of the vacuum hold is directly related to the skin through thickness permeability. The layer of adhesive was found to be fairly impermeable to air. Consequently, if a ply of adhesive and several plies of prepreg are laid down on the honeycomb core, the pressure might not decrease during vacuum hold. To increase the through thickness permeability of the skin, the plies can be spiked with needles [7, 10, 30]. It is very effective to reduce the pressure in the core, but has to be adapted to the permeability of the materials. The operator can choose to spike only the adhesive layer, the prepreg plies before laying them down, or to spike the whole skin. Overall, high quality is difficult to consistently achieve in out-of-autoclave manufacturing of sandwich structures.

2.4 Complex Shape Laminates

Real parts manufactured to answer industrial needs are usually not flat. They can feature concave and convex corners, and double curvatures. Concave and convex corners were studied with autoclave technology [31, 32]. The issues raised in these studies also apply to out-of-autoclave technology, but the absence of positive pressure from the autoclave makes the problems slightly different.

Because they are partially impregnated with resin, out-of-autoclave prepregs are thinner after cure than during the lay-up. This is not a problem on flat parts, but becomes one on curvy parts. To quantify this reduction in thickness, the bulk factor (B_f) is the ratio of the thickness reduction over the initial thickness.

$$B_f = \frac{initial\ thickness - cured\ thickness}{initial\ thickness} \tag{2.2}$$

The bulk factor of out-of-autoclave prepregs is typically 20%. The bulk factors of the materials used in this project are 19% for the MTM45-1, and 23% for the CYCOM5320. Some autoclave prepregs are also semi-impregnated and have similar bulk factors.

In a corner, the surface close to the center of the corner is smaller than the surface far away from the center of the corner (see Figure 2.7). In a concave corner (A), the tool surface (S_T) is larger than the bag surface (S_P). In a convex corner (B), the tool surface (S_T) is smaller than the bag surface (S_P). The bag surface is always exposed to 1 atm of pressure (P). To satisfy the balance of forces, the reaction pressure from the tool in a concave corner is less than 1 atm (P-ΔP), whereas the reaction pressure from the tool in a convex corner is more than 1 atm (P+ΔP). Consequently, concave corners are usually subject to corner thickening, and convex corners usually exhibit corner thinning [31, 32].

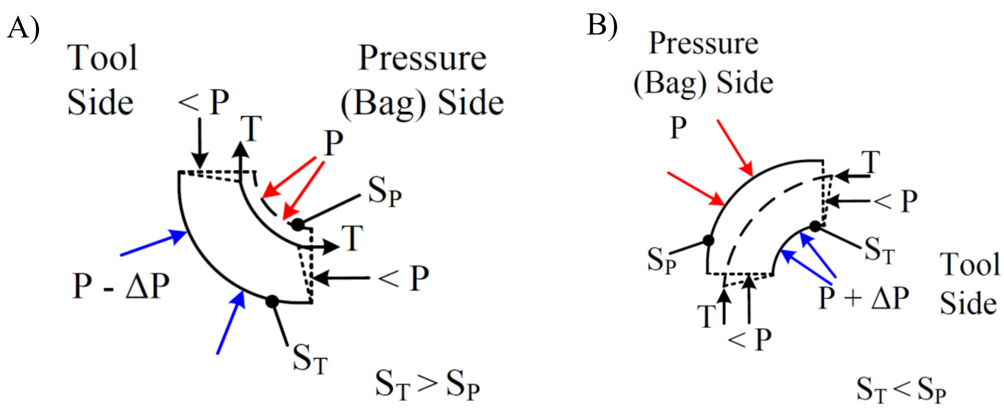

Figure 2.7: Forces acting on a laminate over A) a concave tool and B) a convex tool [8].

The shearing capability of the prepreg was also found to play an important role. Indeed, since the fibres are very stiff, plies of prepreg on the flanges of corners cannot be stretched and need to slide towards the corner for a concave tool and toward the extremities of the flanges for a convex tool (see lines with small dashes in Figure 2.7). This effect combined with the high bulk factor of semi-impregnated prepregs increases corner thickening, and corner thickening was even observed on convex corners for out-of-autoclave prepregs [8, 9]. When the thickness-to-radius ratio increases, thickness variations also increase. A critical ratio can be experimentally determined for every prepreg.

To add an extra-compaction force on the bag side, pressure intensifiers can be used. They are local counter moulds and, depending on their size, are called pressure strips, pressure pads, or caul-sheets. They should have the dimensions of the final part on the bag side. Their ability to improve thickness uniformity in corners is directly related to their stiffness. A thin cured composite caul-sheet was shown to be much more efficient than a soft rubber caul-sheets, but also more efficient than a thick cured composite caul-sheet [31]. Pressure intensifiers were found to be particularly efficient on concave corners, if they have the appropriate geometry [8, 9].

Recent research works by *The Boeing Company* reported the manufacturing of more complex parts featuring hats, ribs, and stiffeners, but they only provide limited details contributing to fundamental understanding of phenomena at work in out-of-autoclave technology [33, 34].

2.5 Ply Drop-offs

In a laminate, all the plies do not necessarily cover all the surface of the part. The thickness of a laminate can be non-constant by design; such a laminate is called a tapered laminate, and an example is shown in Figure 2.8.

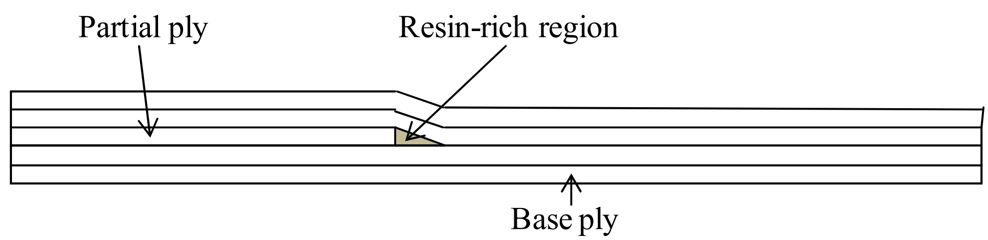

Figure 2.8: Schematic of a ply drop-off in a tapered laminate.

Also, prepreg is supplied in rolls and some plies are larger than the roll width, which implies that one layer is made of 2 or more plies. The transition between two plies can be done by just putting the plies against each other (butt joint) or by overlapping the two plies on a certain distance (overlap). These two types of joints are displayed on Figure 2.9. Whereas an overlap creates two resin-rich regions, it ensures the transmission of stresses between the two plies and is usually recommended for aerospace composite parts.

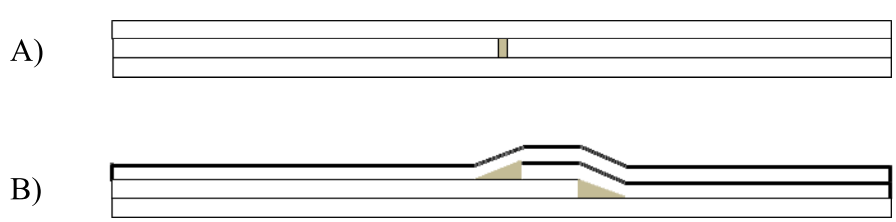

Figure 2.9: Plies junction using A) a butt joint, and B) an overlap.

In the cases of a tapered laminate or of overlaps, the laminate contains ply drop-offs, also called ply terminations. Ply drop-offs are known to affect the delamination strength of laminates [35]. Experiments and numerical models provide guidelines for ply drop-offs [36]. Plies should be dropped-off individually, with a stagger distance between two successive drop-offs that depends on the ply thickness. A common rule of thumb for ply drop-offs is to respect a 12mm (.5”) stagger distance. This rule was shown to be fairly conservative and a minimum stagger distance of eight times the ply thickness is recommended in [36].

2.6 Research Objectives

The present research aims at integrating the knowledge recently gained in out-of-autoclave technology to face multiple challenges of out-of-autoclave manufacturing and to allow the manufacturing of representative parts, in the continuity of previous research works performed in this collaborative project. More precisely, the following aspects are developed in this thesis:

1. Conduct experiments on the effects of ply drop-offs and tight corners with curvature changes on part quality. Establish manufacturing guidelines for these features.
2. Design the representative parts with a specialized CAD software and make manufacturing choices to optimize the part quality.
3. Manufacture the parts and test them for porosity, thickness uniformity in corners, mechanical performance and T_g. Compare the results with the differences between the materials.
4. Discuss the limitations of out-of-autoclave technology and compare it with autoclave technology.

3 Tight corners study

3.1 Experiments

3.1.1 Geometry

The mould of the representative part features tight corners with 6.4 mm (¼”) radii. Although simple concave and convex corners have already been studied, the geometry investigated here is a convex corner between two concave corners. The tight corners are surrounded with red in Figure 3.1.

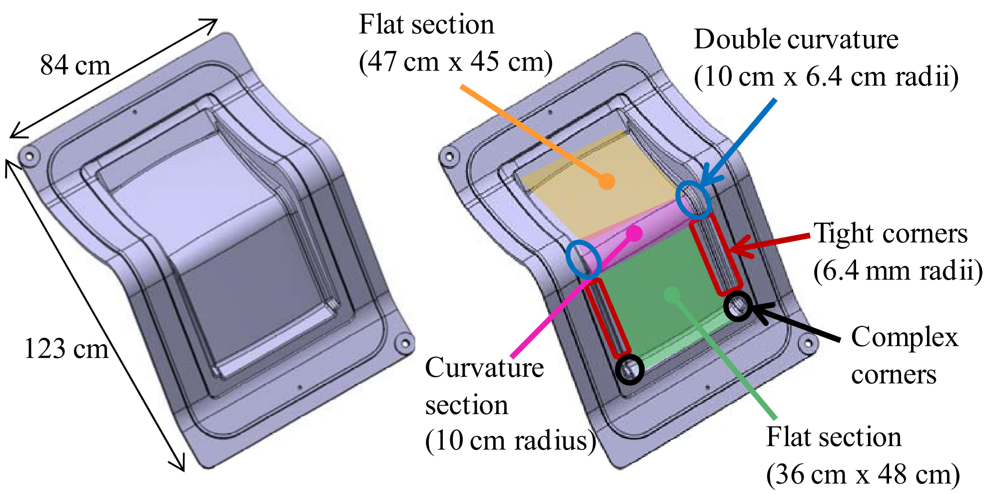

Figure 3.1: CAD drawing of the mould of the representative parts (left) and positions of several features on the mould (right).

The parts manufactured in these tests are a portion of the representative parts. They have a “rectangular” shape and stretch from side to side of the bottom of the seat, in order to fully cover the tight corner regions while avoiding the double curvature and complex corner regions. Since the part is symmetric, two different bagging configurations can be tested simultaneously, one on each side of the part.

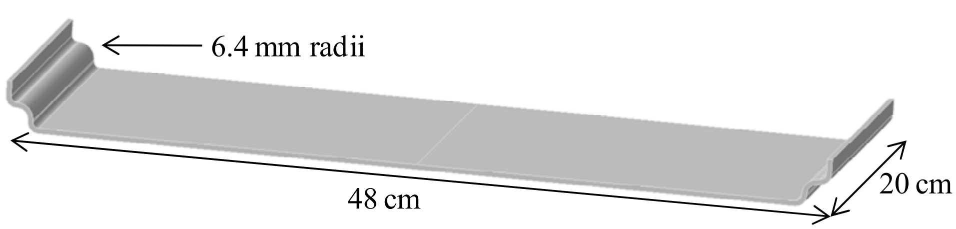

Figure 3.2: CAD drawing of a part manufactured in the tight corners tests.

3.1.2 *Materials and Layup*

The prepreg used for the tight corner tests is MTM45-1 5HS. It was preferred over CYCOM5320 PW because MTM45-1 5HS is approximately twice thicker, which means the thickening or thinning effects would be more pronounced with MTM45-1 5HS. When prepreg plies are applied over a concave corner, the inner radius decreases when the laminate thickness increases. Thus, a thick laminate is a "worst case scenario" since the last plies of prepreg will have to conform to a very tight corner for the thickness to remain constant. The consumables used are detailed in Table 3.1.

Table 3.1: Materials used in the tight corner experiments.

Item	Supplier	Description
MTM45-1 5HS prepreg	The Advanced Composites Group	5 harness satin fabric, 6K tows, 36% weight content MTM45-1 resin, areal weight 375 g/m^2
Edge breathing	Unknown	Dry fibreglass, plain weave fabric, 10cm wide, areal weight 203g/m^2
Non-perforated release film	Airtech	Wrightlon 5200
Breather cloth	Airtech	Airweave N4
Bagging film	Airtech	Wrightlon 8400 blue
Sealant tape	Airtech	AT 200 Y
Rubber pressure intensifiers	Airtech	Aircast 3700

Pressure intensifiers were developed with Aircast 3700, a silicone rubber material. Pressure intensifiers were used in corners to increase the applied pressure. They were moulded using calibrated wax placed on the mould to simulate the final part thickness. Aircast 3700 is initially in a liquid state. The liquid is mixed with a curing agent before being injected between the calibrated wax and a local counter-mould. It can cure at room temperature.

The parts were 8 plies thick. To avoid part distortion, a symmetric, balanced, quasi-isotropic layup was chosen: $[(+45/-45)/(0/90)/(90/0)/(-45/+45)]_S$. The uncured thickness of the laminates was 3.9 mm, which implies that on the bag side the theoretical radius was 2.5 mm for concave corners and 10.3 mm for convex corners.

3.1.3 Experimental Plan

The objective of the tight corner tests was to determine the optimal bagging arrangement that leads to the most uniform thickness in corners. Three parts were manufactured, allowing for the testing of five different bagging arrangements, summarized in Table 3.2.

Table 3.2: Tight corner tests matrix.

Part#	**Configuration**	**Description**
1	Breather	Nominal consumable arrangement
2	No breather	Breather removed in concave corners
	Bleeder	Breather replaced by bleeder in corners
3	Pressure strips	Small strips placed in concave corners
	Pressure pad	Pad covering the corners area

The consumables on top of the laminate, namely the release film, the breather, and the vacuum bag are known to be subject to consumable bridging. Consumable bridging occurs when a consumable does not conform to a concave corner, and prevent the vacuum bag from fully applying a 1 atm compaction pressure on the laminate. The consumable has the shape of a bridge that stretches over the corner. This phenomenon is illustrated in Figure 3.3.

Figure 3.3: Schematics of a concave corner with a consumable well adjusted (left), and a bridging consumable (right).

The first two parts (#1 and #2) investigate the effect of breather bridging. To prevent bridging from other consumables, the release film was cut and overlapped in concave corners, and the bagging film was pleated in these corners so that both consumables could move by some millimetres.

In the nominal bagging arrangement (Part #1) one piece of breather cloth is placed above the whole corner area (see Figure 3.4 & Figure 3.7). Bleeder cloth was used on one side of Part #2 as an alternative to breather cloth to investigate the possible advantage from its low thickness. The other side of Part #2 had no breather at all (see Figure 3.5 & Figure 3.8). Pressure strips and a pressure pad were used in Part #3 to try to increase the applied pressure in concave corners (see Figure 3.6 & Figure 3.9).

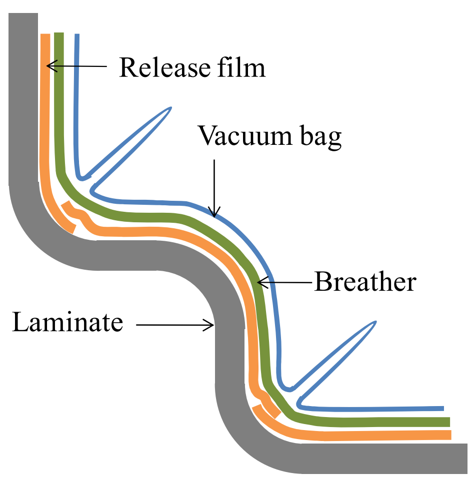

Figure 3.4: Schematic of the nominal bagging arrangement for the tight corner tests (Part #1).

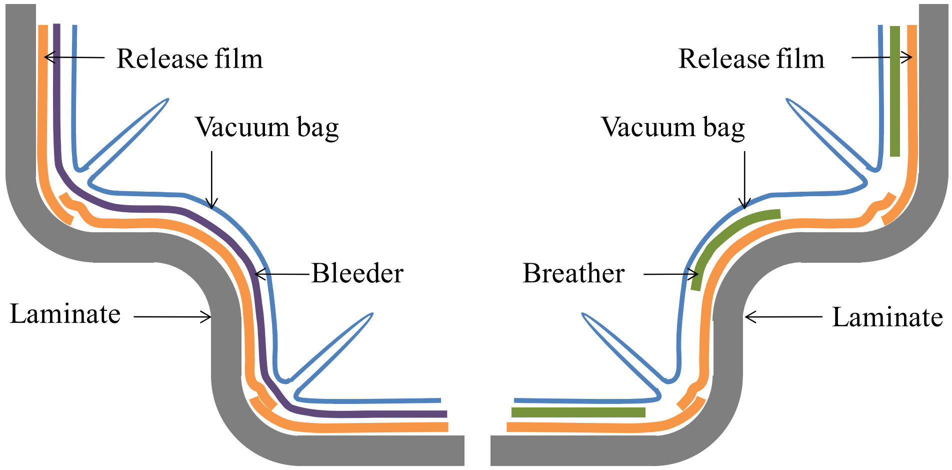

Figure 3.5: Schematic of the bagging arrangement for Part #2. Bleeder (left) and no breather in concave corners (right).

Figure 3.6: Pressure pad (left) and pressure strips (right) used in Part #3.

Figure 3.7: Details of Part #1: Breather cloth covering the entire part.

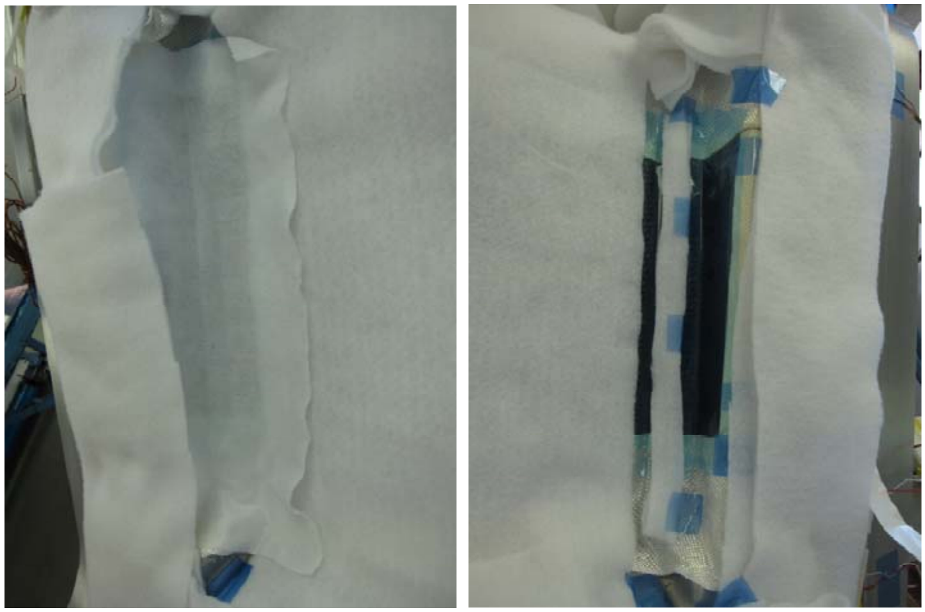

Figure 3.8: Details of Part #2: no breather in concave corners (left), and bleeder in corners (right).

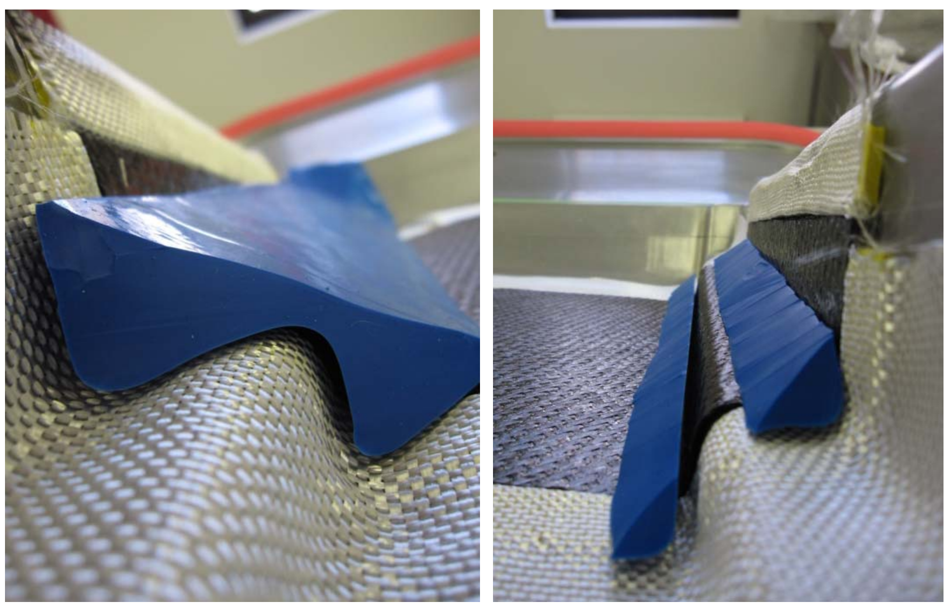

Figure 3.9: Details of Part #3: pressure pad (left), and pressure strips (right).

The cure cycle consisted of a ramp at 1.7˚C/min (3˚F/min) up to 120˚C (250˚F), followed by a dwell of 4h once the part temperature has reached 120˚C. Then the part was cooled down to room temperature. The cure cycle is shown in Figure 3.10.

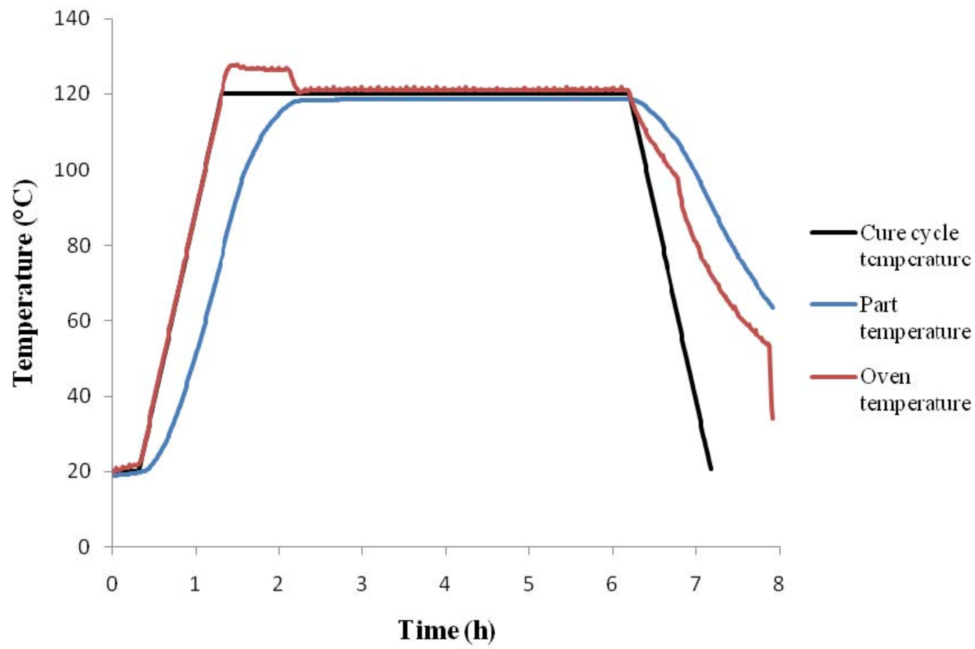

Figure 3.10: Cure cycle and temperature measurements during cure. The part temperature was taken between the 4^{th} and the 5^{th} ply of the laminate.

As it can be seen in Figure 3.10, there is a thermal lag between the part and oven temperatures. The mould of the representative part is a large mass of aluminum that has a significant thermal inertia. Note that, to reduce this lag, the oven is overheated at the end of the first ramp. This temperature overshoot makes the part reach 120˚C faster.

3.2 Measurement Techniques

To quantify the differences between the parts in terms of quality, two types of measurement were performed: void content and thickness measurements.

3.2.1 Thickness

To measure the thickness, the cured parts were cut as depicted in Figure 3.11 and Figure 3.12. One side of the tight corner coupons was polished for void content measurement (see 3.2.2) and scanned with an Epson Perfection scanner with a resolution of 1200 dpi.

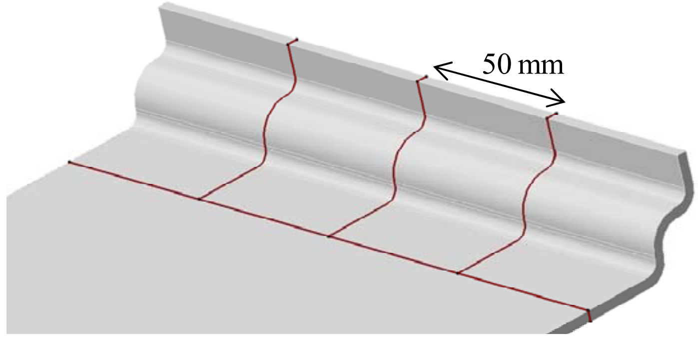

Figure 3.11: Cut positions on tight corners parts.

Figure 3.12: Part #2 after cutting.

Each scan was placed above a template to ensure that the measurements were taken at the same location for every coupon (see Figure 3.13). Twenty measurements per coupon were taken with the image analysis software ImageJ. The numerical measurements were verified by taking some measurements directly on the coupons with a digital calliper.

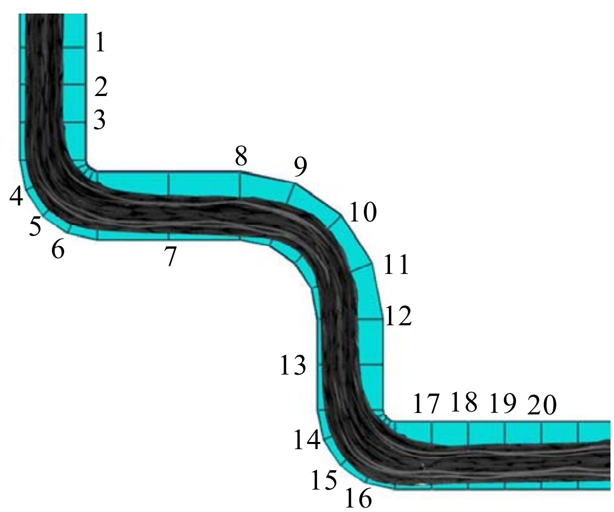

Figure 3.13: Thickness measurements positions.

3.2.2 Void Content

Void content is very representative of the quality of a part. While measuring the total volume of a composite is easy, evaluating the volume occupied by voids with precision is difficult. Destructive methods like resin removal by pyrolysis or chemical digestion can be used [37], but they are not always precise enough for aerospace grade composites, which have a very low void content. To overcome this difficulty, it is common to deduce void content from 2D measurements. A uniform void distribution is assumed and when looking at the cross section of a composite, the void content is given by the following equation:

$$V_{void} = \frac{\sum void\ areas}{total\ cross - sectional\ area} \quad \textbf{(3.1)}$$

Since the porosity of aerospace grade composites is low, several cross sections are inspected to determine the porosity of a region. In this work, three coupons are usually inspected for one region.

The void content was determined for the coupons introduced in 3.2.1. The side of the coupons were polished on a Buehler wet polishing machine, scanned with an Epson Perfection scanner with a resolution of 1200 dpi to determine the total cross-sectional area of the coupon, and then the area of every void was measured using a Nikon Eclipse L150 microscope with a magnification of 50x or 100x. The shape of each void was manually selected with the software ImageJ to determine its area.

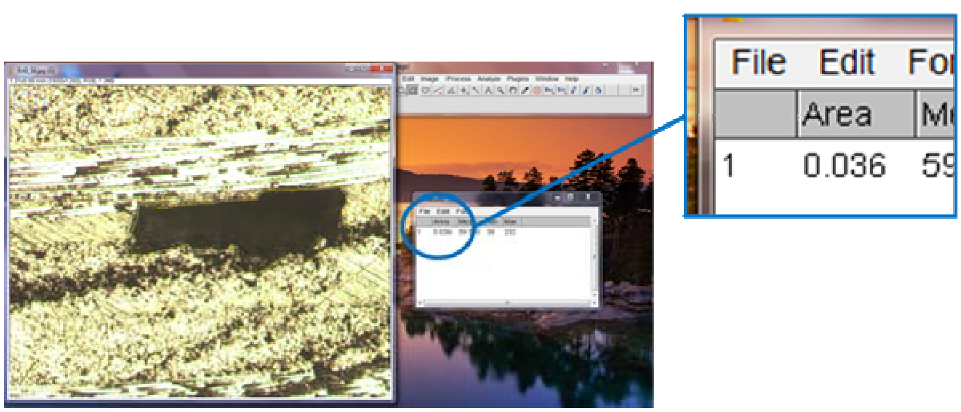

Figure 3.14: Measuring the area of a void with the software ImageJ.

3.3 Results

3.3.1 Thickness

Figure 3.15 shows cross-sectional views of parts manufactured with different bagging configurations. Corner thinning and thickening were the most common defects observed. Thickening was always observed in concave corners. In some cases, resin accumulations were found (breather, bleeder and pressure pad configurations). The use of pressure intensifiers created resin fillets at their edges.

Figure 3.16 shows the average thicknesses deviation with respect to the bagging arrangement. The thickness deviation is the percentage of difference between the flange thickness (nominal thickness) and the local thickness. The average thickness at the flange was 3.1mm. The measured thickness is very dependent on the bagging arrangement. The nominal bagging arrangement led to an average thickness deviation of + 57% in the concave corners and - 6% in the convex corner. The no breather case gave a + 34% thickness deviation in the concave corners and less than - 2% in the convex corner. The bleeder case gave a + 82% thickness deviation in the concave corners and - 11% in the convex corner. The pressure strips led to a + 37% thickness deviation in the concave corners and - 12% in the convex corner. The pressure pad gave a + 82% thickness deviation in the concave corners and - 14% in the convex corner.

The best results were obtained for the no breather case. Replacing the breather by bleeder led to bad corners. Pressure intensifiers did not give better results compared to the no breather case.

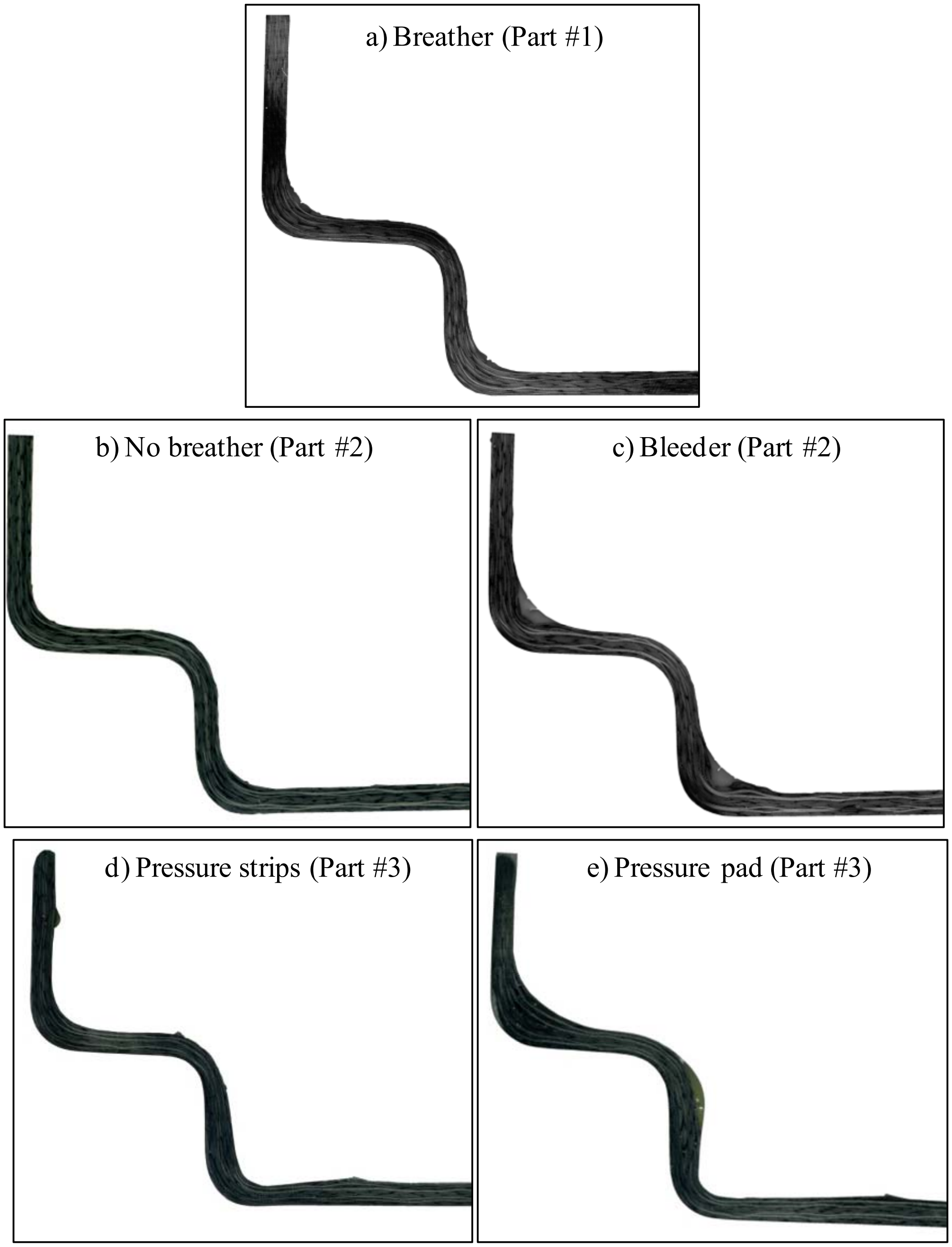

Figure 3.15: Tight corner scan for each consumable configuration. Some images were horizontally flipped to facilitate comparisons.

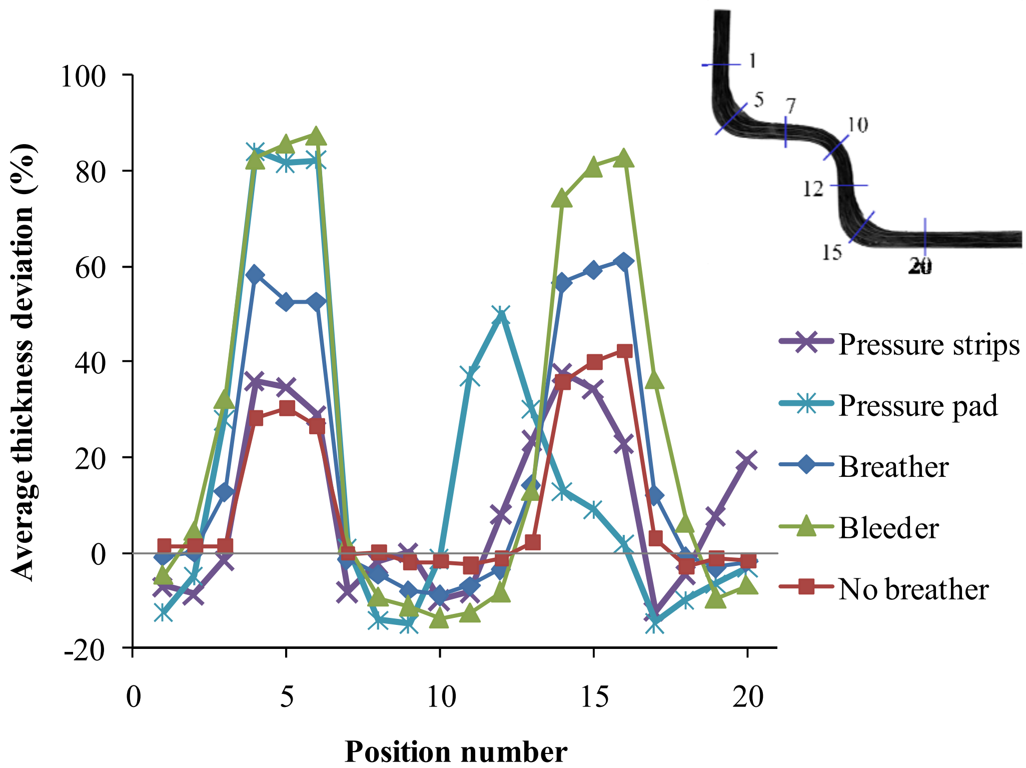

Figure 3.16: Average thickness deviation of laminates with tight corners.

The bleeder material was thinner and stiffer compared to the breather. Thus, the higher stiffness prevented the bleeder from extending into the concave corners. This created consumable bridging as the bleeder was not able to follow the change in laminate's shape during cure. Without any consumable in tension (no breather) corner thickening was still observed. The problem underlined for consumables is the same for the outer plies of the laminate. If the plies cannot slide between each other because of high inter-ply shear, the outer plies will not be able to conform in the concave corners. Figure 3.15 a) and c) show resin accumulation in concave corners with breather or bleeder in tension. Without breather, fibres are less compacted, but there is no resin accumulation, which is an improvement in terms of stress distribution.

Pressure intensifiers gave extra compaction, but they were difficult to manufacture with an accurate geometry for such tight corners. As shown in Figure 3.15 e), the corners covered by a pressure pad had poor compaction in the first concave corner and severe resin accumulation zones. Pressure strips were more efficient, but not more than the no breather configuration. In both cases, resin fillets were observed at the edges of the pressure intensifiers. Also, for this geometry, compacting the concave corners implies stretching the fibres from the convex corner, resulting in corner thinning in the convex corner.

3.3.2 Void Content

The void content was evaluated for each bagging arrangement. Results are given in Figure 3.18. The bars are the plus/minus one standard deviation of the measurements. Typical images of the cross sections are given in Figure 3.17 for the no breather configuration and the pressure pad configuration.

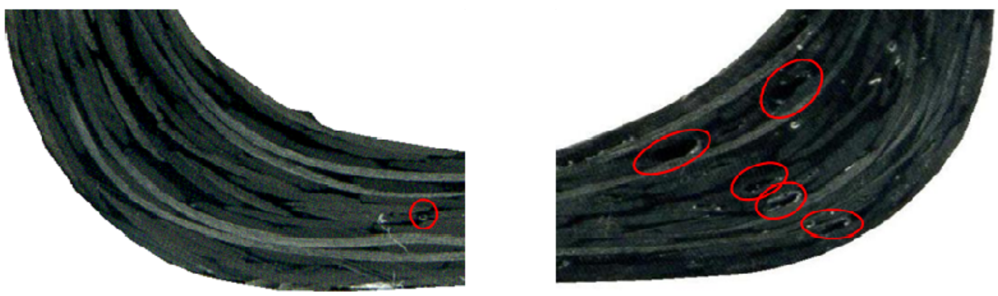

Figure 3.17: Detail of scans of coupons from the no breather configuration (left) and the pressure pad configuration (right). Main voids are surrounded in red.

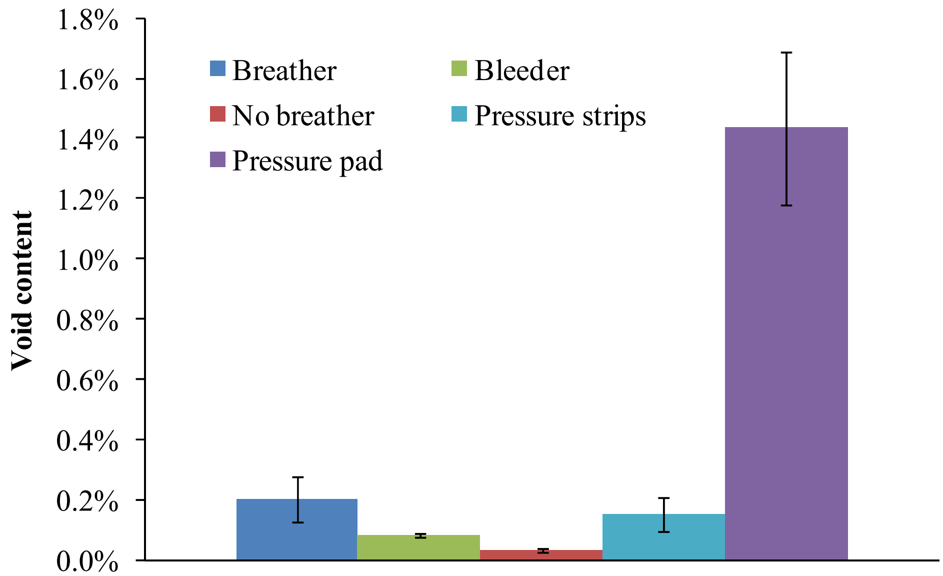

Figure 3.18: Average void content of tight corners regions for the different tested configurations.

The results correlate well with the thickness measurements. The no breather case gave the lowest porosity. The breather, bleeder, and pressure strips cases have higher porosities, but still below 0.2%. The use of a pressure pad was very detrimental to the part quality; with porosity as high as 1.4%. The voids were mainly found in the concave corners, where compaction was lower. These porosity measurements correspond to visual observations of the surface finish on the tool side of the parts.

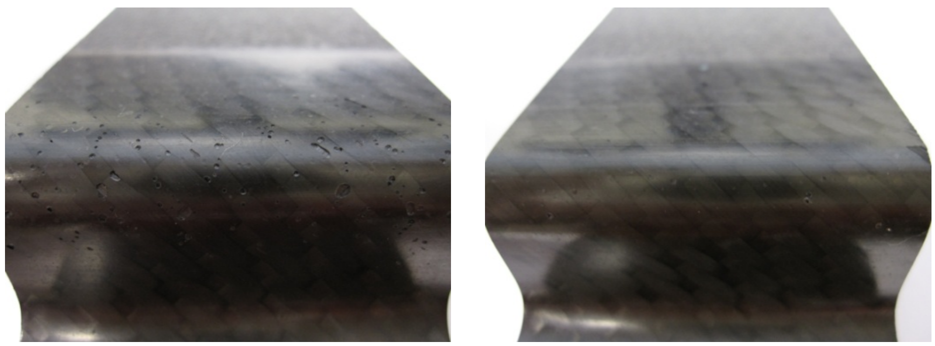

Figure 3.19: Surface finish on the tool side of a concave corner manufactured with bleeder (left) and without breather (right). Pin holes are seen on the left picture whereas the right picture shows a glossy surface without defects.

It is essential for the corners to be placed under a high compaction force. Cases with consumable bridging (breather case and bleeder case) resulted in higher void content than in the no breather case. The pressure pad and the pressure strips were not developed with a sufficiently accurate geometry to be able to increase the pressure at the right locations. Pressure pad led to poor compaction and, consequently, high porosity. Also, the pressure intensifiers had a low stiffness, which made it difficult to transfer the applied pressure properly.

3.4 Kinematic Corner Compaction Model

Consumable bridging is likely to happen with prepregs that have a high bulk factor like out-of-autoclave prepregs. Indeed, in concave corners, the length that a consumable has to cover is longer at the end of the cure than before cure. This additional length might come from the flanges of the corner. But because of the applied pressure on the flanges and of the consumable stiffness, the consumable is kinematically constrained.

A simple kinematic model is presented to evaluate the influence of consumable bridging on corner thickening in concave corners, assuming that the laminate's outer shape in the corner is dictated by the consumables. To do so, the worst case scenario of an infinitely stiff material is considered. The experiments with laminates featuring tight corners gave values for an infinitely compliant consumable (no breather case) and also a stiff consumable (bleeder case). A comparison is made between these values and the idealized case of an infinitely stiff consumable.

Let us consider a concave corner modelled by a quarter-circle surrounded by straight flanges. Before cure, the laminate is assumed to have a uniform thickness except in the concave corner and the consumable is directly placed on top of it without any wrinkles. On the flange, the applied pressure forbids the consumable from sliding on the laminate. This is the boundary condition. As the consumable is infinitely stiff its length remains constant. During cure, the thickness of the laminate decreases and the consumable is not long enough to remain in contact with the laminate. Knowing the final thickness of the laminate and using the constant length of the consumable, it is possible to determine the quarter-circle that describes the consumable after cure. Using the assumption that the laminate's outer shape is dictated by the consumable, the theoretical final thickness of the laminate in the corner is determined. This can be visualized in Figure 3.20.

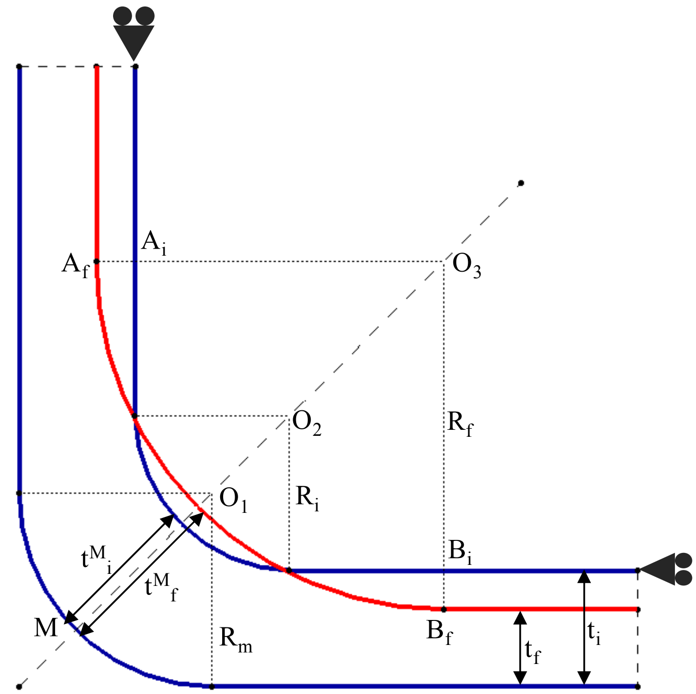

Figure 3.20: Kinematic corner compaction model for consumable bridging.

The laminate is described on the tool side by a quarter-circle with center O_1 and radius R_m. Its bag side is initially described by the quarter-circle with center O_2 and radius R_i, and by the quarter-circle with center O_3 and radius R_f in the final state. t_i and t_f are respectively the initial and final thicknesses of the laminate on the flange. $t^M{}_i$ and $t^M{}_f$ are respectively the initial and final thickness along the dashed line that goes through M. With a hand layup process it is difficult to reach a constant thickness in tight concave corners and an initial manufacturing thickening is observed. Thus, $t^M{}_i$ is slightly larger than t_i. (an average of 28% was measured).

The radii and thicknesses are related by the following equations

$$t_i^M = \sqrt{2} \times t_i + \left(\sqrt{2} - 1\right) \times (R_i - R_m) \quad \textbf{(3.2)}$$

$$t_f^M = \sqrt{2} \times t_f + \left(\sqrt{2} - 1\right) \times \left(R_f - R_m\right) \quad \textbf{(3.3)}$$

The constant length of the consumable between points A and B leads to

$$R_f = R_i + \frac{1}{1 - \pi/4}\left(t_i - t_f\right) \quad \textbf{(3.4)}$$

This finally gives

$$t_f^M = t_i^M + \left(\frac{\sqrt{2}-1}{1-\pi/4} - \sqrt{2}\right)\left(t_i - t_f\right) \approx t_i^M + .5 \times \left(t_i - t_f\right) \tag{3.5}$$

Within this model, the final thickness in the corner is the initial thickness plus the thickness reduction on the flange multiplied by a geometrical factor, which is close to 0.5. For out-of-autoclave prepregs, the bulk factor is typically 20%. If B_f designates the bulk factor of the material, the equation becomes:

$$t_f^M \approx t_i^M + t_i \times \frac{B_f}{2} \tag{3.6}$$

The predicted thickness is compared to an ideal uniform thickness in Figure 3.21. In this model, the thickness increase evolves linearly with the laminate thickness.

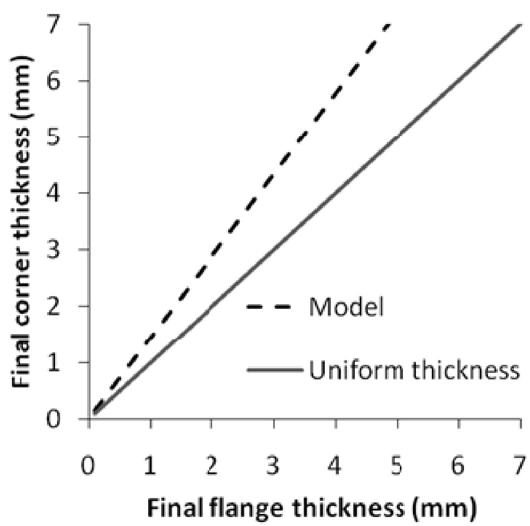

Figure 3.21: Final corner thickness as a function of the final flange thickness according to the kinematic model.

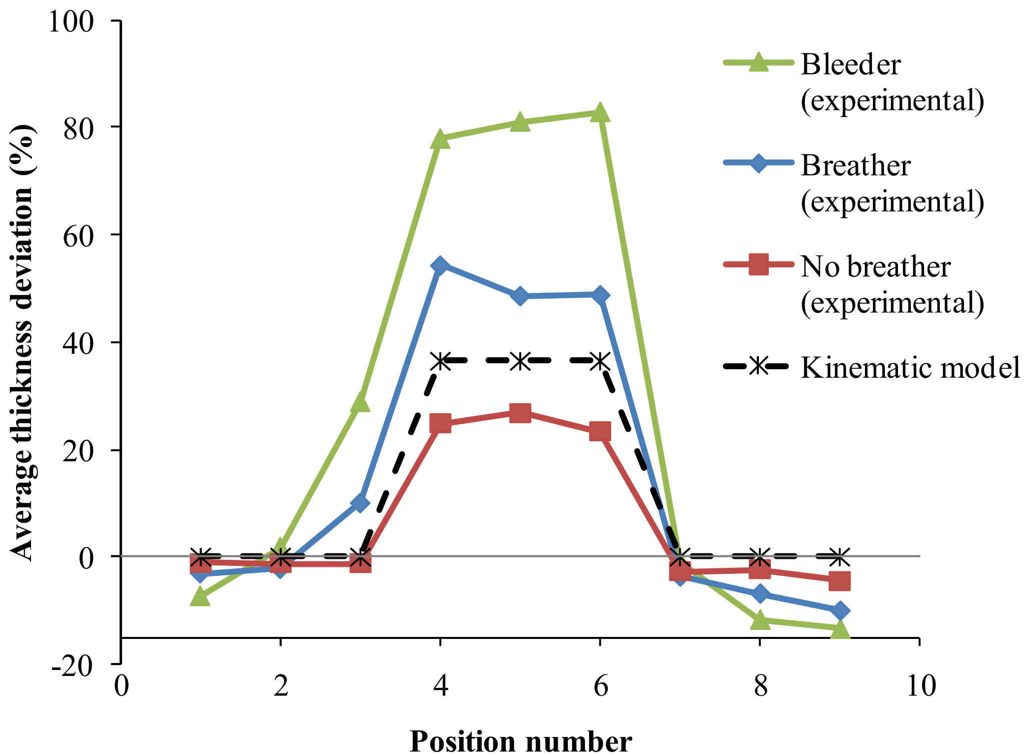

Figure 3.22: Kinematic corner compaction model versus experimental results.

The model prediction can be visualized in Figure 3.22. According to this model, the bridging phenomenon for an infinitely stiff bagging material leads to a corner thickening that is half of the bulk factor. For out-of-autoclave prepregs, it corresponds approximately to a 10% thickening. Adding the initial manufacturing thickening gives a 38% increase at the corner. However, a thickening up to 82% is experimentally observed when using a stiff bleeder as consumable. This shows that the assumption that the consumable's shape dictates the shape of the laminate does not stand. The phenomenon is not purely kinematic. The stiffness of the consumable does affect the corner thickening, but the mechanism is not direct: as the stiffness of the consumable increases, its tension in the corner region also increases resulting in a low normal pressure applied on the prepreg stack. Consequently a resin pressure gradient takes place in the laminate and leads to a resin migration from the flange to the corner region, when the resin viscosity drops during cure. This corresponds to experimental observations (see Figure

3.16), where the parts with the highest corner thickening in the concave corners are associated with the highest corner thinning in the convex corner.

3.5 Comparison with L-shape laminates

The thickness results presented in the previous section can be compared to the study conducted by Brillant [8, 9] with L-shape laminates. By extrapolating her results to the radii and the laminate thickness of the tight corner experiments, a thickness increase of +30% in the concave corners and a thickness increase of +12% in the convex corners was expected. Whereas there is a good correspondence for concave corners (+34% in the no breather configuration), the difference is more than significant for convex corners. Indeed, corner thinning was observed in the tight corner experiments when L-shape laminates gave corner thickening.

Consider an L-shape laminate over a convex corner, as seen in Figure 3.23. In the corner region, the tool surface (in blue) is smaller than the bag surface (in red) which undergoes a 1 atm compaction pressure. To satisfy the balance of forces, the tool reaction force has to be higher than 1 atm. The average compaction pressure in the corner region is then higher than on the flange. Thus, corner thinning would be expected. The results on L-shape laminates showed that the boundary conditions of the corner must be taken into account, and that they are related to the shear capacities of the prepreg. Indeed, during cure out-of-autoclave laminate gets thinner (dashed line in Figure 3.23). To keep a constant thickness in the corner region, the plies of prepreg close to the bag surface need to slide towards the flange region. If the shear efforts in the flange are high, the plies cannot slide to compensate for the 20% thickness decrease related to the bulk factor of the material. To put it in a nutshell, convex corners are subject to a competition between a high compaction pressure that tends to give thinning, and shear forces at the boundaries of the corner that tends to give thickening. If the flanges are long – like for L-shape laminates – the shear forces dominate and corner thickening is observed. The convex corner of the tight corner experiments was placed between two concave corners, which did not "lock" the plies and led to corner thinning.

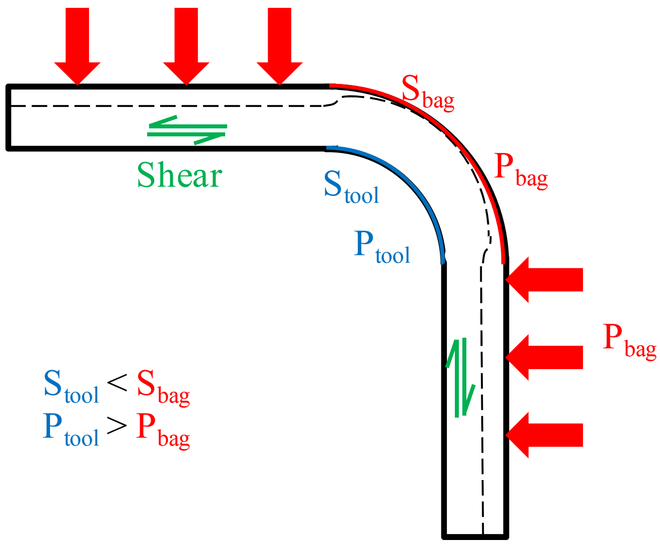

Figure 3.23: Forces acting on a convex L-shape laminate.

In concave corners, the two phenomena previously described also take place, but they combine instead of competing. Consider an L-shape laminate over a concave corner, as seen in Figure 3.24. In the corner region, the tool surface (in blue) is larger than the bag surface (in red) which undergoes a 1 atm compaction pressure. To satisfy the balance of forces, the tool reaction force has to be lower than 1 atm. The average compaction pressure in the corner region is then lower than on the flange. Moreover, because of the significant bulk factor of out-of-autoclave prepregs, the plies of prepreg close to the bag surface need to slide towards the corner region to keep a constant thickness in that region. These two phenomena add up and lead to corner thickening. Since there is no competition between the two phenomena, corner thickening in concave corners is more pronounced than corner thinning in convex corners.

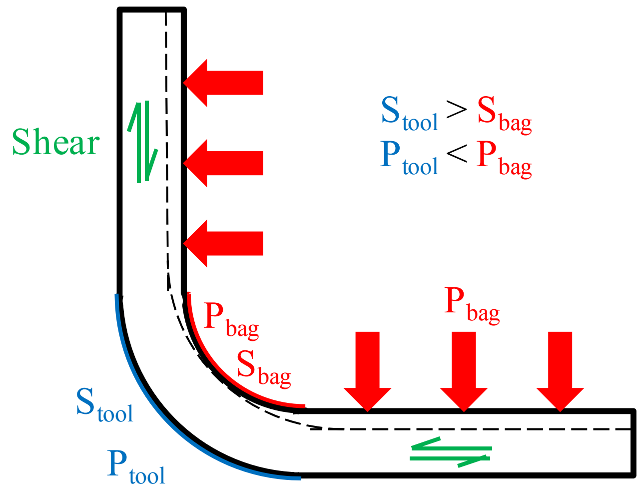

Figure 3.24: Forces acting on a concave L-shape laminate.

Figure 3.25 shows the geometry of the tight corner parts. As discussed in the previous paragraphs, the convex corner is subject to a high compaction pressure whereas the two concave corners undergo a low compaction pressure. Consequently, and since the distance between the corners is short, the plies are likely to slide from the convex corner towards the concave corners (green arrows). Moreover, the pressure gradient between convex and concave corners may induce resin flow towards the concave corners. This was experimentally observed when bridging occurred in concave corners (bleeder configuration), reducing even more the compaction pressure in these corners. The parts with the highest thinning in the convex corner also had the highest thickening in the concave corners, associated with resin accumulation when bridging occurred.

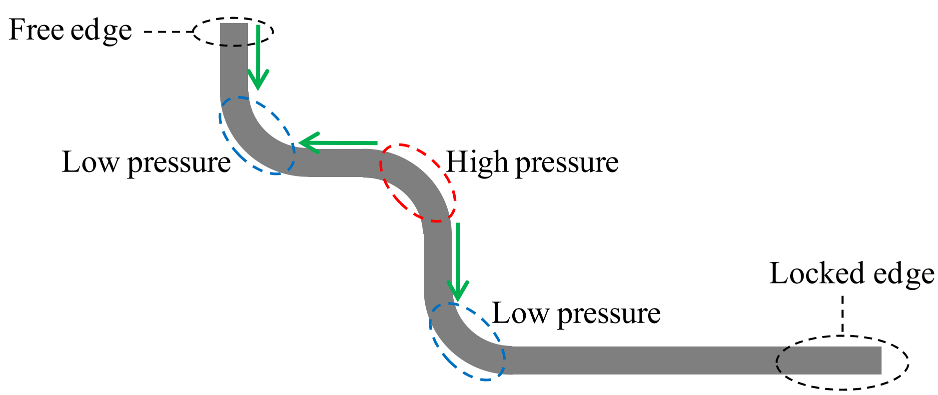

Figure 3.25: Constraints applied to the tight corner parts.

3.6 Summary

Several points can be highlighted thanks to these tight corner experiments.

- Consumables have a significant effect on thickness uniformity. Consumable bridging in concave corners should be avoided.
- The kinematic compaction model showed that when consumable bridging occurs in a concave corner, the final shape of the laminate is not given by the shape of the consumable. Because of the pressure differential between the corner and the flange, resin may migrate into the corner.
- Boundary conditions surrounding a convex corner determine if thinning or thickening will occur. With long flanges (L-shape laminates), the plies were locked and thickening was observed. In these tight corner experiments, thinning was observed.
- With the tight corner configuration, thickening in concave corners could not be avoided with out-of-autoclave prepregs. Thinning in convex corners was almost reduced to zero.

4 Ply Drop-offs Study

4.1 Experiments

4.1.1 Motivation

Ply drop-offs are found in composite parts that require thickness changes or local reinforcement. This feature was investigated with out-of-autoclave technology. One question needed to be answered: how easily can the entrapped air be removed from partial plies? Indeed, let us consider a part that needs a local reinforcement or local stiffening in its centre (Figure 4.1). To minimize weight, the usual solution would be to have partial plies in the centre of the part (Figure 4.2 A)). However, since the through thickness permeability is much lower than the in-plane permeability, air evacuation in the partial plies could be compromised. Possibly, the partial plies need to be extended up to the closest edge of the part so that they are in direct contact with edge breathing during cure (Figure 4.2 B)).

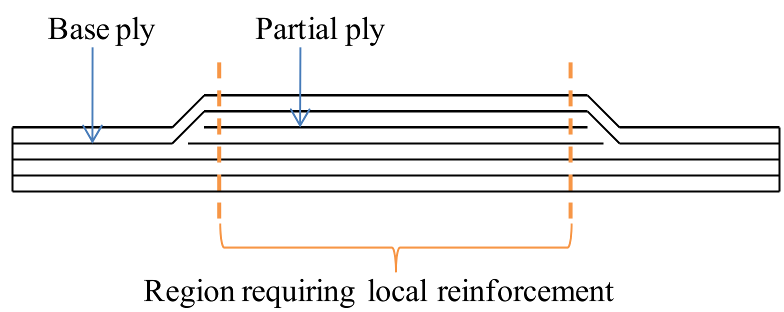

Figure 4.1: Cross sectional view of a part with partial plies

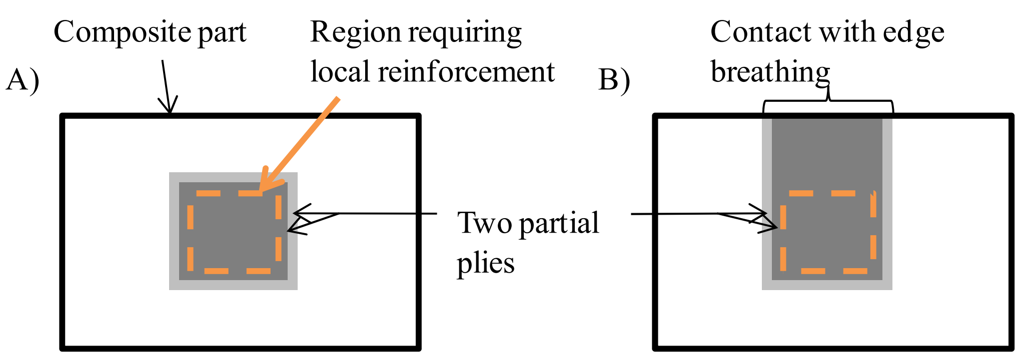

Figure 4.2: Top view of a part with partial plies A) no contact with edge breathing, and B) in contact with edge breathing.

Experiments were designed to investigate the necessity to have partial plies in contact with edge breathing during cure.

4.1.2 Experimental Setup

The problem was reduced to a 1D configuration described in Figure 4.3. The parts had four base plies and four partial plies. Two bagging arrangements were used to investigate the connectivity of dropped plies to vacuum source. Figure 4.3 shows the variation in the bagging on the left side of the laminate used to connect the dropped plies to the vacuum source (edge breathing) or seal the dropped plies from the vacuum source (sealant tape). A total of 8 parts divided in 4 tests were made (see Table 4.1). Each test contained two parts cured on the same tool plate to ensure that the only difference between the two parts was the edge breathing arrangement (see Figure 4.4). One part had only one breathing edge (1BE) on the thin side while the thick side was sealed with sealant tape and the other part had 2 breathing edges (2BE) located on the thin and thick sides. All the parts were 10 cm wide. Two lengths were used; 20 cm for the short parts and 102 cm for the long parts. Two successive ply drop-offs were separated by a distance λ. It is usual to take $\lambda \geq 12.7$ mm to avoid excessive stress concentrations. Pictures of short and long parts are shown in Figure 4.5.

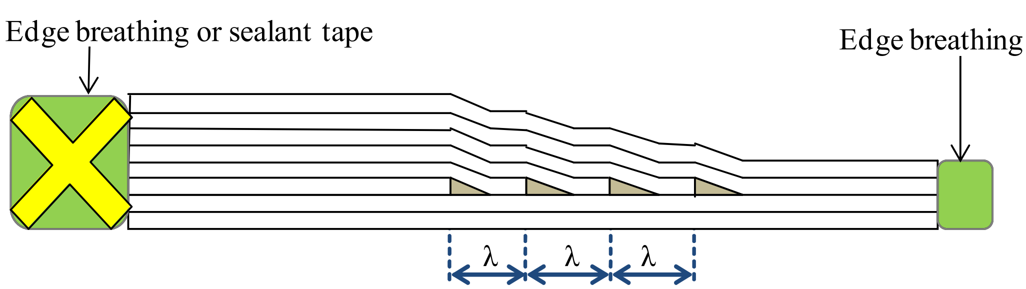

Figure 4.3: Side view of the studied laminate. λ=12.7 mm.

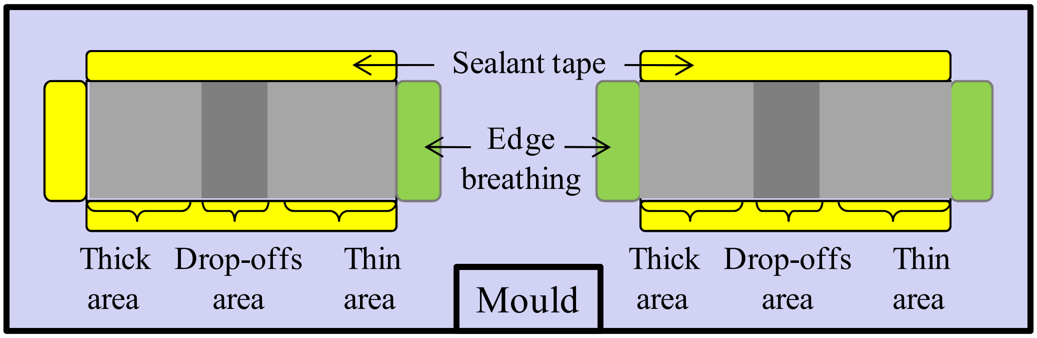

Figure 4.4: Top view of two simultaneously cured parts. Edge breathing (green) is connected to the breather, sealant tape (yellow) blocks air flow to the breather.

Since non-perforated release film was used on the top of the prepreg stack, air evacuation was confined to in-plane air flow in the prepreg. Thus, in-plane permeability is a key parameter that governs air evacuation. The debulk time was determined with a 1-D model based on Darcy's law [23]. The debulk times shown in Table 4.1 were obtained for an air extraction of 99% for the short parts and 95% for the long parts using lower bounds permeability values reported in [10, 23].

Table 4.1: Ply drop-offs vacuum hold time computed with a 1D air evacuation model [23].

Test #	Material	In-plane permeability [10, 23, 25]	Length	Vacuum hold time
1	MTM45-1 5HS	$3.0\text{x}10^{-14}\text{m}^2$	Short	3h
3			Long	14h
2	CYCOM 5320 PW	$1.6\text{x}10^{-13}\text{m}^2$	Short	1h
4			Long	3h

4.1.3 Cure Details

All the plies were (0/90) degree fabric with 4 base plies (20 cm or 102 cm long) and 4 partial plies (~50% length). Thermocouples were placed between the release film and the breather in the thick area of every part to monitor the temperature in the vacuum bag. The consumables are given in Table 4.2.

Table 4.2: Consumables used in the ply drop-off experiments.

Item	Supplier	Description
Edge breathing	Unknown	Dry fibreglass, plain weave fabric, 10cm wide, areal weight 203g/m^2
Non-perforated release film	Airtech	A4000 Red
Breather cloth	Airtech	Ultraweave 606
Bagging film	Airtech	Wrightlon 7400
Sealant tape	General Sealants	GS 213-3

The parts were cured on an aluminum tool plate placed in a Blue M 146 series oven. The cure cycle consisted of a ramp at 1.7˚C/min up to 120˚C, followed by a dwell of 4h, and a cool down to room temperature.

Figure 4.5: Pictures of short (left) and long (right) CYCOM5320 parts. The part at the top of the pictures has one breathing edge and one sealed edge. The part at the bottom of the pictures has two breathing edges.

4.2 Measurements

The difference in quality between the parts was quantified through void content measurements. The laminate porosity was measured in three areas for the short parts (thick, drop-offs and thin) and in four areas for the long parts (thick/end, thick/middle, drop-offs and thin). Three cuts were performed in each zone as shown in Figure 4.6. The coupons obtained were approximately 25 mm by 60 mm. One edge of each coupon was observed according to the procedure described in 3.2.2.

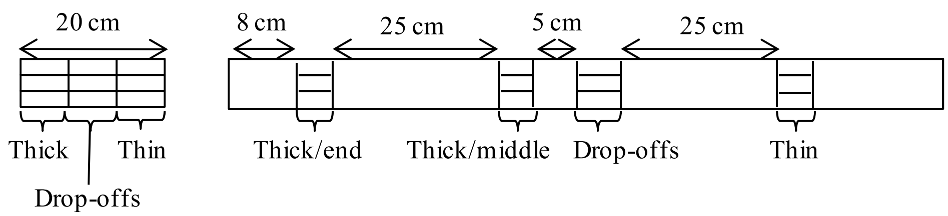

Figure 4.6: Position of tested areas in short parts (left) and long parts (right).

The average void content of the different parts were compared, but also the distribution of these voids was investigated.

4.3 Results

Most of the voids had an elliptical shape and were found between the fibre tows. Figure 4.7 illustrates the typical size of observed voids. Figure 4.8 shows the overall part porosity. The error bars are plus/minus one standard deviation of the measurements. The void content was below 1% and the parts with porosity below 0.1% can be considered as void free as no macro-voids were found (Figure 4.7). Parts with two breathing edges show less porosity than the ones with edge breathing on one side only. One exception was noticed for the long parts made with MTM45-1 5HS prepreg which have a similar void content in both configurations. Because of the very low porosity level, high variability was observed between coupons resulting in high standard deviations. Also, Figure 4.8 shows averages for the entire parts, but the porosity fluctuates a lot between the thin and thick ends of the parts.

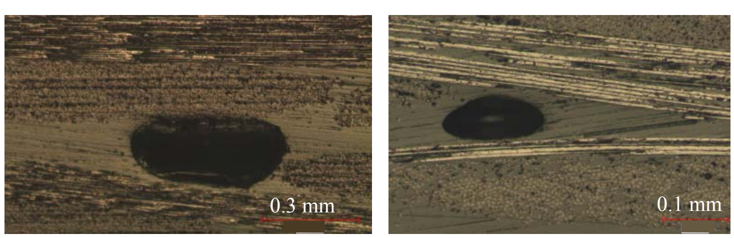

Figure 4.7: Typical micrographs of macro-voids.

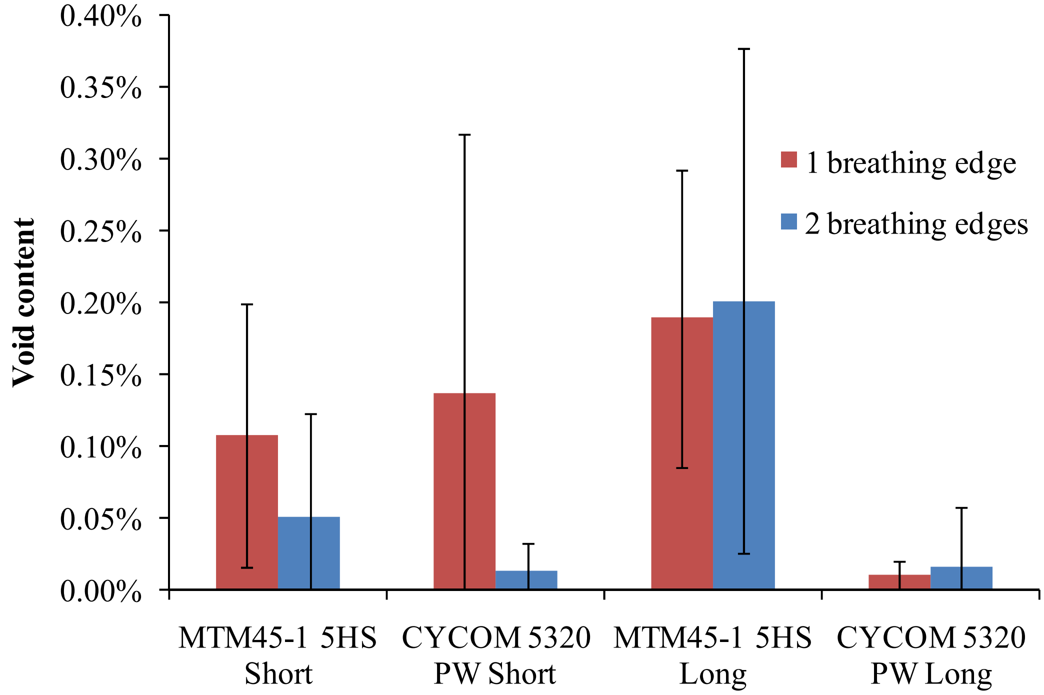

Figure 4.8: Comparison of average porosity of parts with one or two breathing edges. Parts associated with the same colour were simultaneously cured.

Figure 4.9 shows the distribution of voids in the short parts. The thick area was the most porous region, whereas the thin area was void free. The parts with two breathing edges (2BE) were mainly void free everywhere, even if more voids were observed in the thick area (void < 0.1%). The parts with 1BE clearly showed an increase in void content compared to 2BE parts. This means that air evacuation was efficient if all the plies were in contact with edge breathing and air extraction was more difficult in parts with only 1BE. However, the void content remained low in all the areas (void < 0.4%). It looks like the through-thickness permeability of the two prepregs was high enough so that the air entrapped in the partial plies reaches the base plies for which the in-plane permeability is also sufficient for all the air to be extracted through the thin edge.

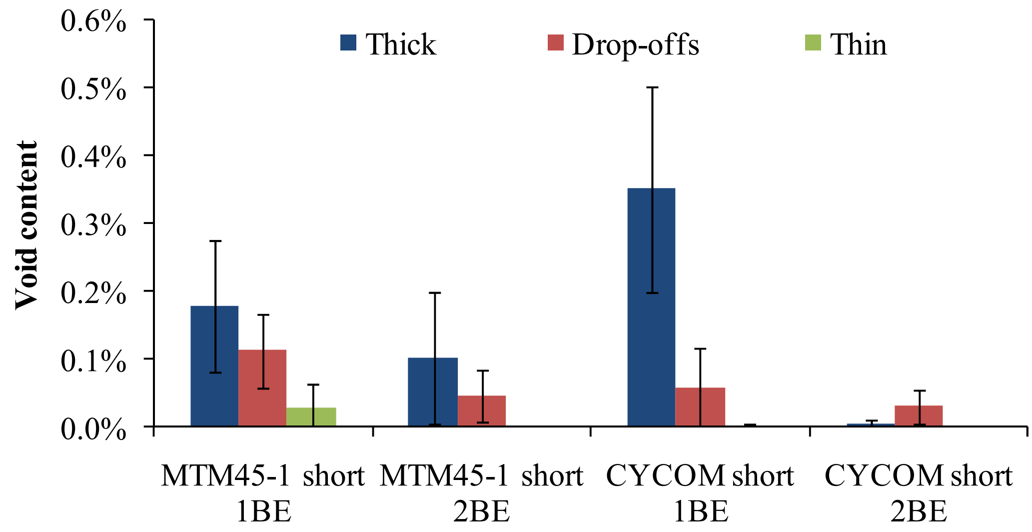

Figure 4.9: Porosity distribution in short parts.

For the long parts, the void distribution is more complex, as shown in Figure 4.10. The CYCOM5320 PW prepreg showed very good results (void < 0.1%). The high through-thickness permeability of the CYCOM5320 PW prepreg led to a thick area with very low porosity even for such a long part. The MTM45-1 5HS part with 2BE had its highest porosity located in the thick area, middle zone where entrapped air is the most present at the beginning of the cure (because of the thickness) and the furthest away from a breathing edge. For the MTM45-1 5HS prepreg part with 1BE the void content measured in the thin and drop-offs areas was surprisingly higher than in the thick area. It looks like the air from the partial plies was blocked in the part while it was being evacuated towards the thin edge. During cure above a certain temperature, the through-thickness permeability increases, allowing air entrapped in the partial plies to reach the base plies. If the part is too long, gelation may occur before this air gets extracted by the edge breathing.

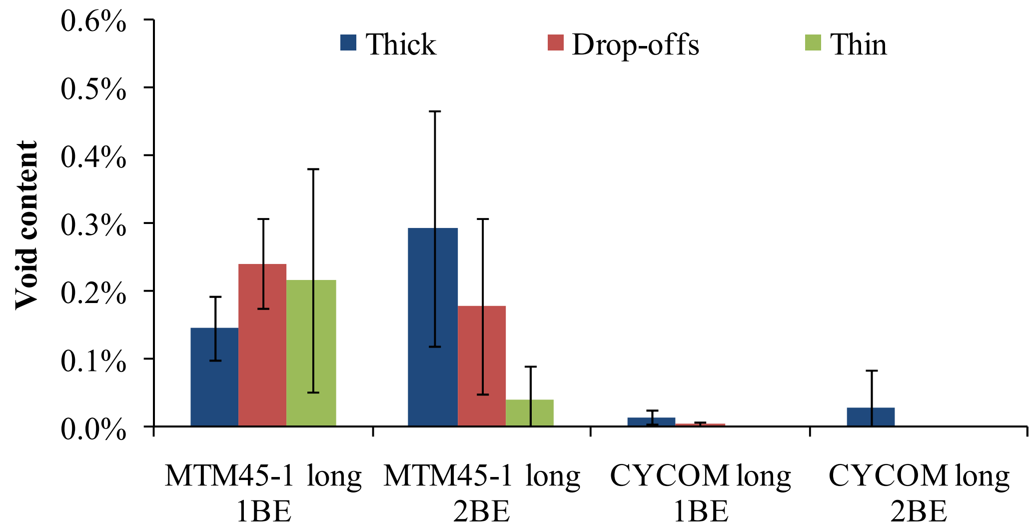

Figure 4.10: Porosity distribution in long parts.

4.4 Summary

This ply drop-off study showed that the air can be extracted from partial plies, even if they are not directly in contact with edge breathing. With both out-of-autoclave prepregs that were used, the average porosity was low (< 0.2%) in all the parts. Porosity distribution revealed that for large parts the onset of resin gelation might leave entrapped porosity in the laminate.

5 Representative Parts

5.1 Definition

5.1.1 Experimental Plan

Representative parts were manufactured to meet several objectives. The two autoclave prepregs chosen for this project were used. The fabric was 5 harness satin (5HS) for the MTM45-1, and plain weave (PW) for the CYCOM5320. For each prepreg, a monolithic part (8 layers) and a sandwich part (8 layers, 6 partial plies, and 1 honeycomb core) were manufactured. Also, to provide a comparison with autoclave technology, one monolithic part was manufactured using CYCOM5276-1 plain weave, an autoclave prepreg. CYCOM5276-1 is a no-bleed prepreg. Like out-of-autoclave prepregs, it already contains the right amount of resin. As a consequence, the use of a bleeder is not necessary, and this prepreg has a bulk factor similar to the OOA prepregs that we used in this research. A total of five parts were made; they are given in Table 5.1.

In this chapter, the word layer is used instead of ply because, in such complex parts, several pieces of prepreg are required to cover the whole surface of the parts. One layer contains one or several plies.

Table 5.1: Representative parts test matrix.

Part	Prepreg	Part type	Description
A	MTM45-1 5HS	Monolithic	OOA cure + post-cure
B		Sandwich	OOA cure
C	CYCOM5320 PW	Monolithic	OOA cure + post-cure
D		Sandwich	OOA cure
E	CYCOM5276-1 PW	Monolithic	Autoclave cure

As presented in the following paragraphs, the monolithic parts will be used for mechanical tests, which requires the resin to be fully cured (100% degree of cure) to develop its maximum mechanical properties. Consequently, Parts A and C were removed from the mould after cure, and placed back in the oven for a free-standing post-cure.

5.1.2 Representative Monolithic Parts

The monolithic parts (A, C and E Parts) were 8 layers thick. To avoid part distortion, a symmetric, balanced, quasi-isotropic layup was chosen: $[(+45/-45)/(0/90)/(90/0)/(-45/+45)]_S$. Figure 5.1 shows the layup surface on which the plies were laid.

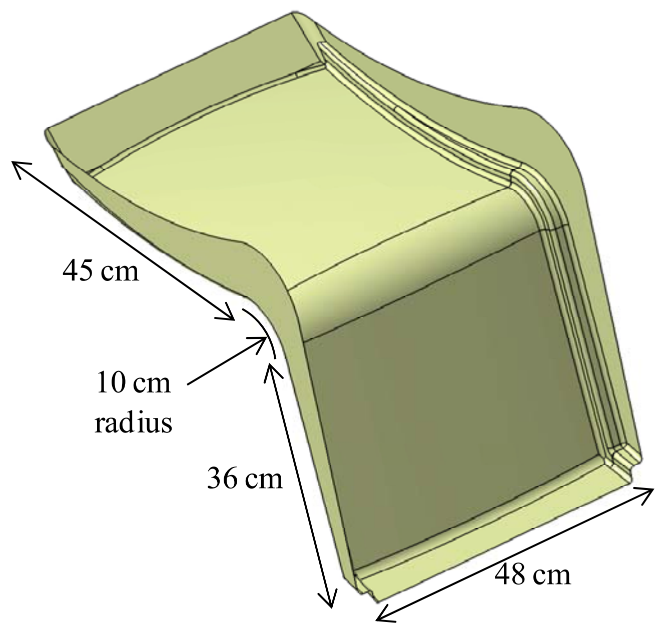

Figure 5.1: CAD drawing of the layup surface of monolithic representative parts.

5.1.3 Representative Sandwich Parts

The sandwich parts (B and D Parts) had 8 base layers, with the same layup than monolithic parts: $[(+45/-45)/(0/90)/(90/0)/(-45/+45)]_S$. On one of the flat area, a honeycomb core was inserted between the 4^{th} and 5^{th} layers. On the other flat area, six partial plies were inserted between the 4^{th} and 5^{th} layers. Figure 5.3 shows the resulting over core layup surface on which the last 4 layers were laid.

The honeycomb was Nomex core, with 3.2 mm diameter cells. The adhesive used was AF 163 manufactured by 3M. The dimensions of the core are given in Figure 5.2.

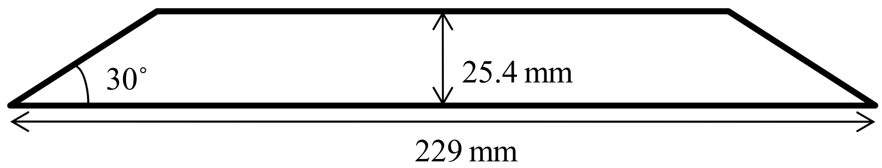

Figure 5.2: Honeycomb core dimensions.

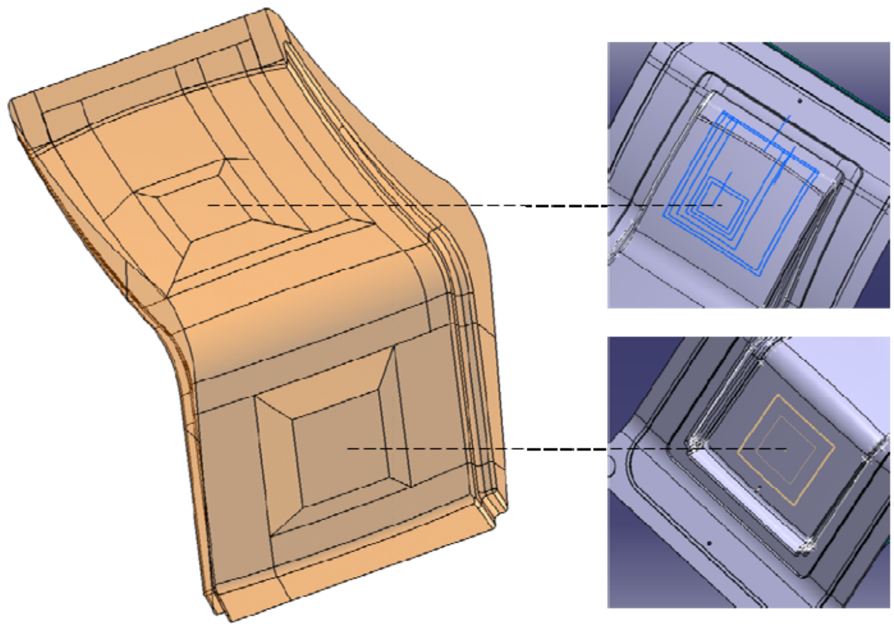

Figure 5.3: Over core layup surface (left), and details of the position of partial plies (top right) and honeycomb core (bottom right).

The dimensions of the partial plies are given in Table 5.2.

Table 5.2: Partial plies dimensions. Plies are numbered from the tool surface towards the bag surface.

Partial ply #	**1**	**2**	**3**	**4**	**5**	**6**
Length (cm)	34	36	30	32	10	12.7
Width (cm)	29	32	15	19	10	12.7

5.2 FiberSIM Designs

5.2.1 Software Principles

FiberSIM is a composite design software edited by Vistagy, that works in the Catia V5 environment. It is a surface-based software that simulates the draping of fibres on a mould and calculates the deformation of the fibre. This software does not allow finite element analysis and is used only for manufacturing design purposes. The end goal is to generate the flat patterns of the plies, which can be transferred to an automated ply cutter or a laser projector for example.

Woven fibres can handle a certain amount of shear deformation. Fibres in the warp and weft directions are initially perpendicular. When placed on a complex shape, the fibres deform and this deformation can be quantified by the angle between the actual fibre orientation and the perpendicular orientation (angle β in Figure 5.4).

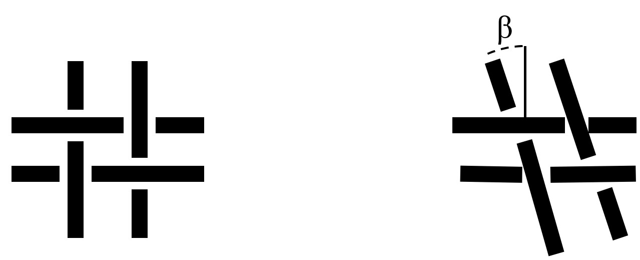

Figure 5.4: Woven fibres without deformation (left) and deformed woven fibres (right). β is the deformation angle.

Each prepreg has a limit angle for deformation. This angle is determined experimentally. Using FiberSIM, the designer defines the layup surface, the laminate boundaries as well as the point of application (where the operator starts to place the ply). By simulating the draping, the software displays the resulting deformations. The zones in blue have a deformation between zero and half of the limit angle, the zones in yellow have a deformation between half of the limit angle and the value of the limit angle. The zones in red have a higher deformation than the limit angle and should be avoided. Figure 5.5 shows the calculated deformations for a hypothetical full ply that would cover the entire layup surface of the representative part. The presence of red zones shows that manufacturing changes have to be made.

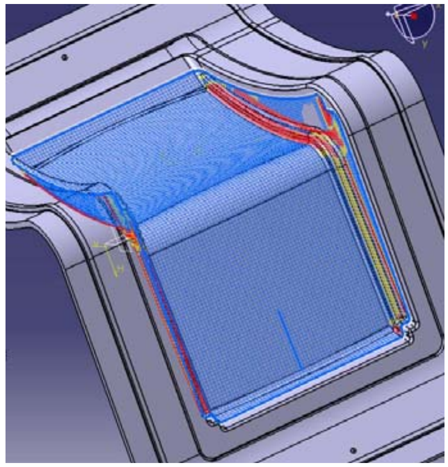

Figure 5.5: Calculated deformation for a full single ply covering the layup surface. The zones in red should be avoided.

To decrease the deformation of the prepreg, different type of cuts can be performed for a layer:

- The layer can be entirely cut in two plies. Such a feature is called a splice. Then the designer has to choose a strategy for joining the two plies. A butt joint gives a uniform thickness, but an overlap is usually preferred since it ensures a continuous distribution of the loads between the two plies. In the aerospace industry, it is usual to have a 12 mm overlap, and to leave 25 mm between two splices in the same laminate.
- The layer can be darted at its edges. A dart is a cut starting on one edge of a ply. If the ply is wrinkling (too much material) a slit dart is performed. It consists in removing a zone in the flat patterns so that when the ply is placed on the mould there is not too much material. If there is not enough material, a V-shape dart is performed. It consists in having a cut in the flat pattern to allow for more deformation. A V-shape dart leaves a zone without prepreg on the mould, and it has a V-shape. A patch of prepreg has to be added to complete the layer. Again, the joint can be a butt joint or an overlap.

With these features, a designer should be able to get rid of any excessive deformation.

From one ply to the next, FiberSIM can take into account the difference in one surface due to the previous ply's thickness. However, if the laminate contains a lot of plies or if a core is inserted, a new layup surface must be defined in Catia V5.

5.2.2 Representative Part Designs

First, the limit angles of the used materials had to be determined. To do so, one ply of prepreg was placed on a complex mould, and cuts had to be performed to suppress wrinkles. Then, the mould geometry was created within Catia V5 and simulations were run with FiberSIM to adjust and determine the limit angle. The limit angles for the prepregs used were 37° for the MTM45-1 5HS, and 39° for the CYCOM5320 PW. Since the autoclave prepreg was not available, a standard value of 30° was taken for the designs.

The designs were the same for the two out-of-autoclave prepregs. The zones with the largest deformations were in the curved area, and in the four corners of the seat. Small slit darts and V-shape darts were added in the corners of the seat. Larger V-shape darts were added in the large curvature region. Deformation when splicing the plies in this curved region. Unfortunately, to respect the 12 mm overlap and the 25 mm interval, only 4 plies could be spliced in that region. As a result, the four ±45°layers were splices in the curved region, and the two 0° layers as well as the two 90° plies had only one main ply. Every ply had four patches to fill in the gaps left by the V-shape darts.

The final calculated deformations of some plies and patches are displayed in Figure 5.6 and Figure 5.7. It can be observed that there was no zone where the limit angle was exceeded.

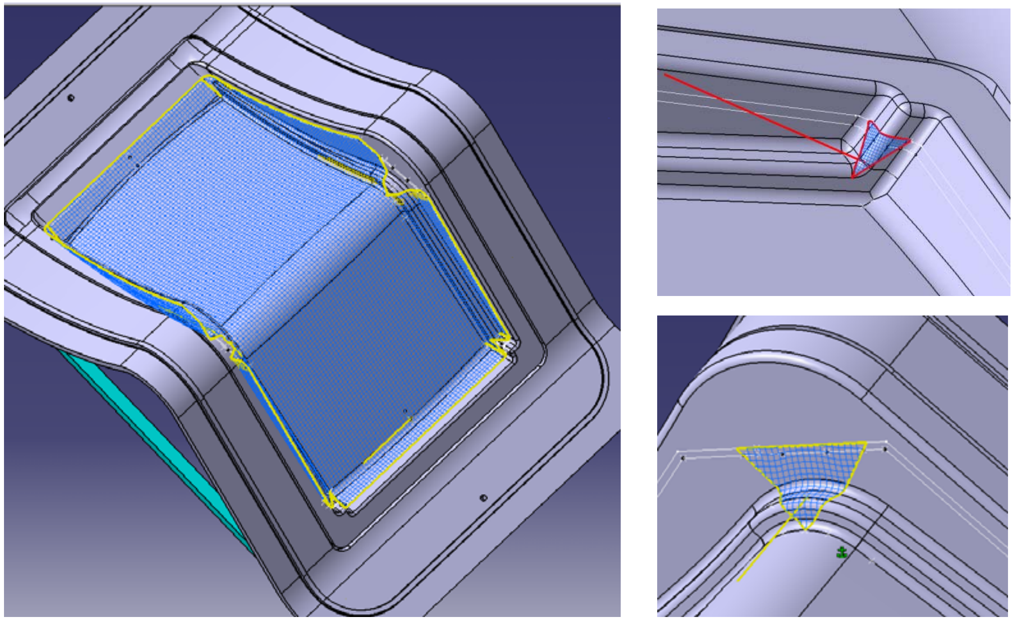

Figure 5.6: Main ply of a 90° layer (left) and V-shape dart (right).

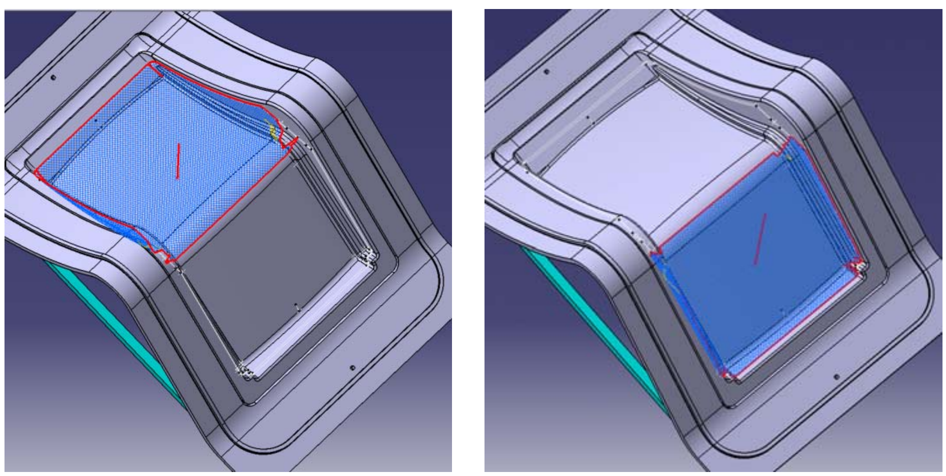

Figure 5.7: Two main plies of a -45° layer.

The end result given by FiberSIM is the flat patterns of the plies. The geometry of the flat patterns was used as an input for an industrial ply cutter. The plies resulting from this operation were ready to be laid up. An example of flat patterns is given in Figure 5.8.

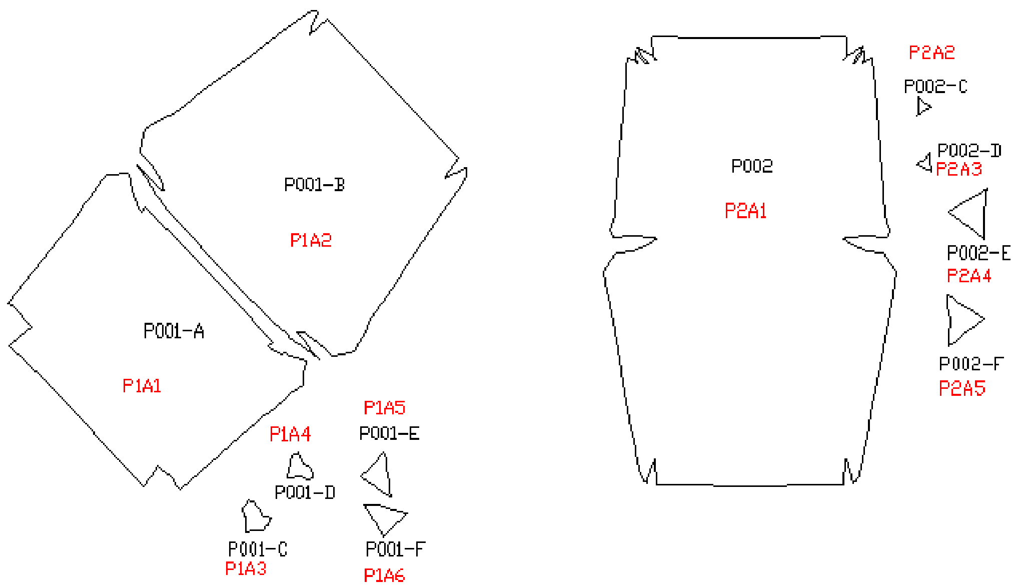

Figure 5.8: Flat patterns of the first two layers for Part A MTM45-1 monolithic.

5.3 Manufacturing

The same consumables were used for the four OOA parts. The autoclave consumables were not exactly the same while having the same function. A stretchy bag was used to reduce the risk of bag bridging, especially in the four corners of the seat. All the consumables are summarized in Table 5.3.

Table 5.3: Consumables used for representative parts manufacturing.

	OOA	**Autoclave**
Release film	Airtech, 5200 Blue P3 (perforated)	Airtech, A4000V (non-perforated)
Breather	Airtech, Airweave N4	Airtech, Airweave N10
Vacuum bag	Airtech, Stretchlon 800	Airtech, Stretchlon 800
Sealant tape	General Sealants, GS 213-3	General Sealants, GS 213-3
Fibreglass (edge breathing)	Dry fibreglass fabric, plain weave, 10 cm wide	Dry fibreglass tow

Because of the results obtained with the tight corner experiments (Chapter 3), it was chosen not to place any breather over the tight corners, except for the autoclave part since it is not recommended to have any surface uncovered by breather. Debulks were usually performed as follows: after the 1^{st} layer, after the 3^{rd} layer, and after the 5^{th} layer. Pictures of the manufacturing steps (layup and bagging) are given in Appendix A. The cure cycles and cure conditions are summarized in Table 5.4.

Table 5.4: Cure conditions for representative parts

Parts	Vacuum hold time	Ramp up rate	Dwell	Pressure	Post-cure
A	16h	1.7˚C/min	4h @ 120˚C	Atmospheric (~1 bar)	3˚C/min to 120˚C 0.3˚C/min to 180˚C 2h @ 180˚C -2˚C to 20˚C
B	16h	1.7˚C/min	4h @ 120˚C	Atmospheric (~1 bar)	None
C	16h	1.7˚C/min	4h @ 120˚C	Atmospheric (~1 bar)	3˚C/min to 120˚C 0.3˚C/min to 180˚C 2h @ 180˚C -2˚C to 20˚C
D	16h	1.7˚C/min	4h @ 120˚C	Atmospheric (~1 bar)	None
E	None required	2.8˚C/min	3h @ 180˚C	6.5 bar	None

5.4 Instrumentation: Miniature Pressure Sensors

5.4.1 Presentation

When curing OOA prepregs, the pressure inside the bag should be as low as possible. The capacity to locally monitor the pressure in the bag is interesting, since it can allow to track any sudden air release from the laminate during cure, or even the pressure in a honeycomb core. By knowing all the manufacturing parameters (temperature, pressure in the bag and in the core) it is possible to get a better idea of the mechanisms taking place during cure.

Miniature pressure sensors were used. They were MS5407 manufactured by Measurement Specialties (MEAS) [38], wired to a National Instruments PC interface. The data acquisition was done by a LabVIEW program. Once calibrated, they measure the absolute pressure. These sensors can be embedded in a vacuum bag or a honeycomb core thanks to their small size (6.2 mm x 6.4 mm).

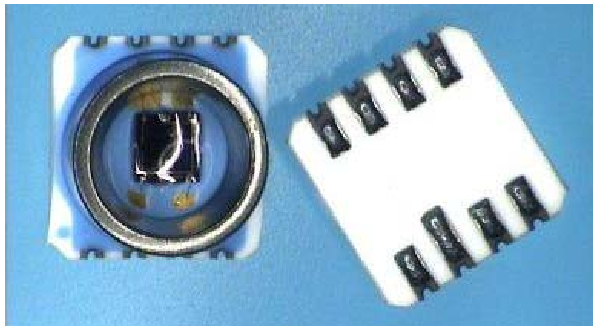

Figure 5.9: Picture of the miniature pressure sensors used.

In a sensor, the deformation of the membrane caused by the outside pressure acts on a full Wheatstone bridge. The Wheatstone bridge is excited by a voltage supplied by the National Instruments interface. The output of the bridge is a voltage that depends on the pressure. The interface divides the output voltage by the excitation voltage so that the acquired signal is in mV/V and does not depend on the value of the excitation voltage. The output signal and the pressure are related by the following equation:

$$P = \frac{Sout - \left(off0 + TCO(T - T1)\right)}{sens0(1 + TCS(T - T1))} \tag{5.1}$$

where P is the measured pressure, Sout is the output signal, off0 is the offset in ambient condition, TCO is the thermal coupling of the offset, sens0 is the sensitivity at room temperature, and TCS the thermal coupling of the sensitivity. T1 is the room temperature during calibration (see next paragraph).

As it can be seen, the output signal depends on the pressure and the temperature. To take the temperature into account a thermocouple has to be placed next to each pressure sensor.

5.4.2 Calibration

Before being used, the pressure sensors need to be calibrated. As presented in the previous paragraph, the pressure is related to the output signal through the temperature and four constants (sens0, off0, TCS and TCO). These four unknowns are determined by taking four values of the output under four different conditions. More precisely, the operator chooses two temperatures (T1 and T2) and two pressures (P1 and P2) and reads the output signal under the four following conditions: [P1,T1], [P1,T2], [P2,T1] and [P2,T2]. The calibration constants are given by the following equations:

$$sens0 = \frac{Sout[P2,T1] - Sout[P1,T1]}{P2 - P1} \tag{5.2}$$

$$TCS = \frac{Sout[P2,T2] - Sout[P1,T2] - Sout[P2,T1] + Sout[P1,T1]}{(T2 - T1)(Sout[P2,T1] - Sout[P1,T1])} \tag{5.3}$$

$$off0 = Sout[P2,T1] - P2 \times sens0 \tag{5.4}$$

$$TCO = \frac{Sout[P2,T2] - P2 \times sens0\big(1 + TCS(T2 - T1)\big) - off0}{T2 - T1} \tag{5.5}$$

5.4.3 Use in Representative Parts

Miniature sensors were used to monitor pressure during cure. Three sensors were placed on top of the laminate, between the release film and the breather to measure the bag pressure. For the sandwich parts, a fourth sensor was placed in the honeycomb core (see Figure 5.10).

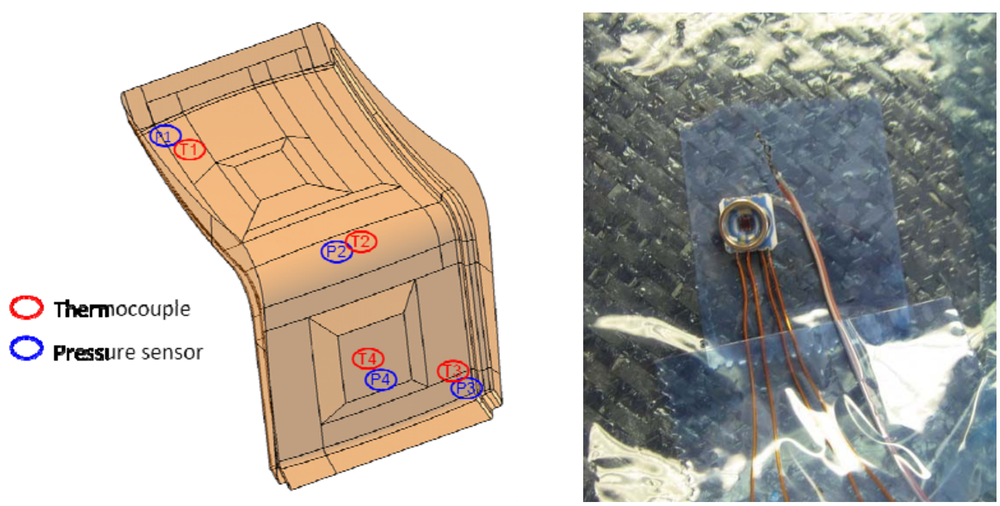

Figure 5.10: Positions of the pressure sensors during cure (left), and picture of a sensor and a thermocouple on the MTM45-1 5HS monolithic part (right).

The measurements for the first part (MTM45-1 5HS monolithic) revealed a problem caused by the bag. The pressure readings were significantly higher than expected (around 100 mbar) and increased with temperature (see Appendix B). Tests were then done on a tool plate without laminate in the bag and showed the same behaviour. It was found that the bag was actually pushing on the silicone membrane of the sensors, artificially increasing the pressure readings. The elasticity of the bag increased during cure and consequently increased even more the pressure readings. A simple and elegant solution to impede the bag from being in contact with the sensor's membrane was found. A small rubber cylinder was placed around the sensor. It was high enough to keep the bag away from the membrane while still allowing any pressure from gas or air to be measured. Pictures of this protective cylinder are shown in Figure 5.11.

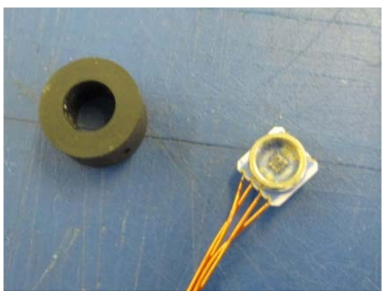
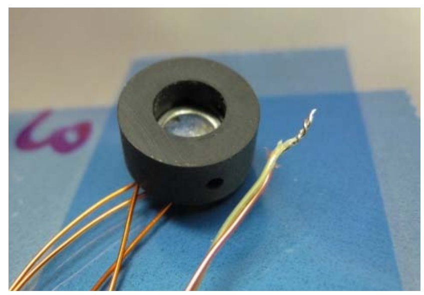

Figure 5.11: Picture of a pressure sensor and a rubber cylinder (left). Picture of a protected pressure sensor (right).

Another problem arose with the part cured in an autoclave. CYCOM5276-1 is an autoclave prepreg cured at 180°C. Unfortunately, the pressure sensors should not be placed above 125°C to ensure proper readings. As a consequence, pressure sensors could not be used for the autoclave part.

5.5 Tests

All the representative parts were destructively tested. The methodology for thickness measurement was the one described in 3.2.1, and porosity was measured following the procedure described in 3.2.2.

5.5.1 Monolithic Representative Parts

After cure and post-cure if applicable, all the monolithic parts were cut tested in the same way. Tests consisted of void content measurements, thickness measurements in tight corners, mechanical tests (compression and three points bending), and T_g determination. The position of the coupons is shown in Figure 5.12.

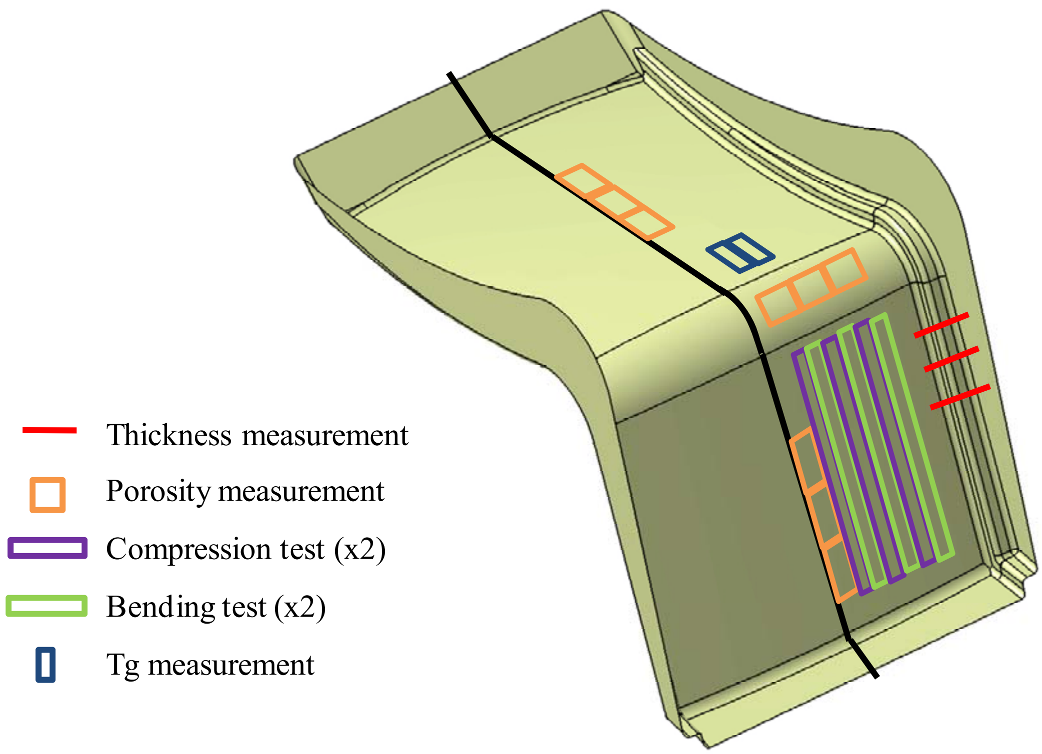

Figure 5.12: Position of tested coupons on monolithic representative parts.

Half of the part was kept for demonstration purposes, and the other half was cut for destructive testing.

5.5.2 Sandwich Representative Parts

After cure, all the sandwich parts were cut and tested in the same way. Tests consisted of void content measurements, thickness measurements in tight corners, and mechanical tests (flatwise tension). The position of the coupons is shown in Figure 5.13.

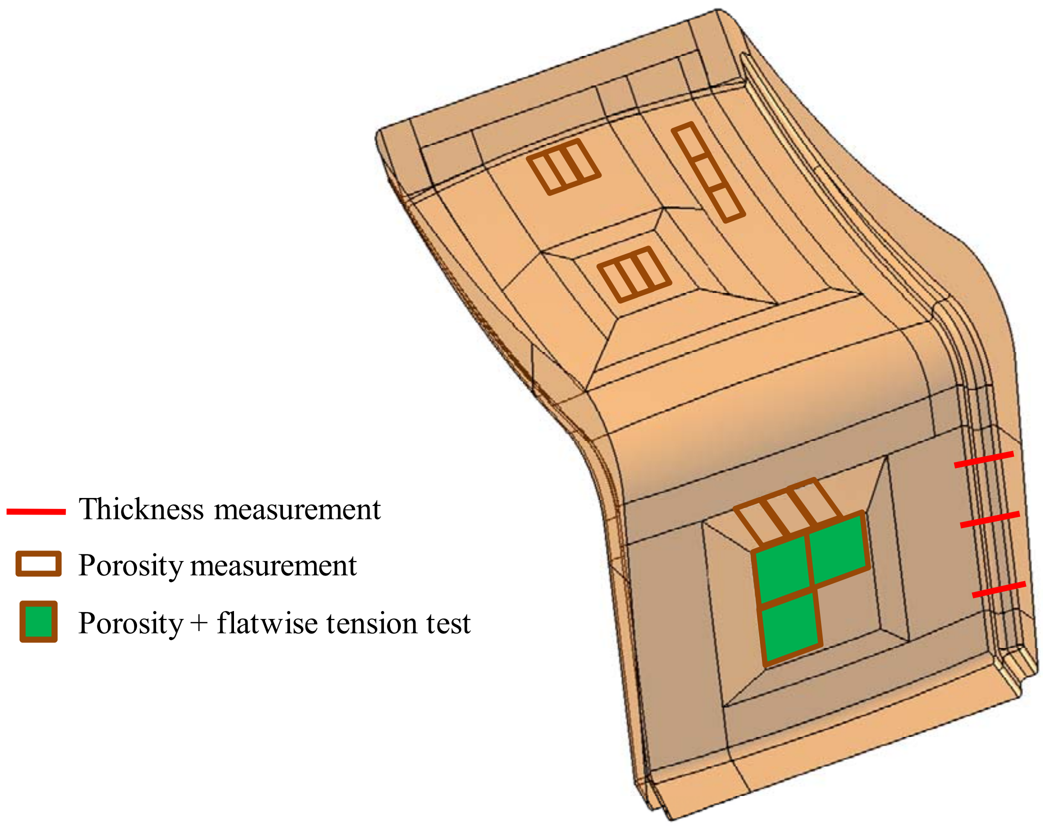

Figure 5.13: Position of tested coupons on sandwich representative parts.

5.5.3 Mechanical Tests

Compression tests and bending tests were performed on the monolithic parts. The compression tests were performed according to the ASTM D695 standard, by compressing a dog bone shaped coupon. The bending tests were 3-point bending tests with coupons having a 32:1 span ratio; they were performed according to the ASTM D790 standard.

On the sandwich parts, 50 mm x 50 mm coupons were cut in the honeycomb core region. They were first analysed for void content, and then mechanically tested for flatwise tension, according to the ASTM C297 standard. The two skins are glued to a fixture, and tension is applied. When doing this test, the main interest is to see if the failure is a pure core failure, or if the bond between a skin and the core failed first, showing a poor adhesion between the honeycomb core and the prepreg.

5.5.4 Glass Transition Temperature (T_g)

The T_g was measured by Dynamic Mechanical Analysis (DMA), with a Q800 DMA from TA Instruments. The procedure was performed as described in ASTM D7028-07 standard. A small coupon (55 mm x 10 mm approximately) was placed on a 3-point bending fixture and was periodically bent at 1 Hz. The fixture was in a heating chamber that was heated up to 250°C. Once at T_g, the storage modulus of the coupon decreased. The T_g was graphically determined by the intersection of the two tangents to the curve right before and after the modulus decrease.

5.6 Results

5.6.1 Void Content

Figure 5.14 shows typical micrographs obtained on the representative parts, and Figure 5.15 shows the average porosity of the representative parts. The parts made with MTM45-1 and CYCOM5276-1 (autoclave) had a very low void content (<0.2%), whereas the parts made with CYCOM5320 had several tested coupons with a void content higher than 1%. This difference is explained by a too long time spent at room temperature. Indeed, OOA prepregs have a limited time during which they can be left at room temperature. The datasheets indicate 10 to 12 days for MTM45-1 and 2 weeks for CYCOM5320. Since the material is received from the partners of the project, it is hard to know or control the time spent by the material at room temperature. However, the CYCOM5320 showed a very low tack, proof of a long time at room temperature.

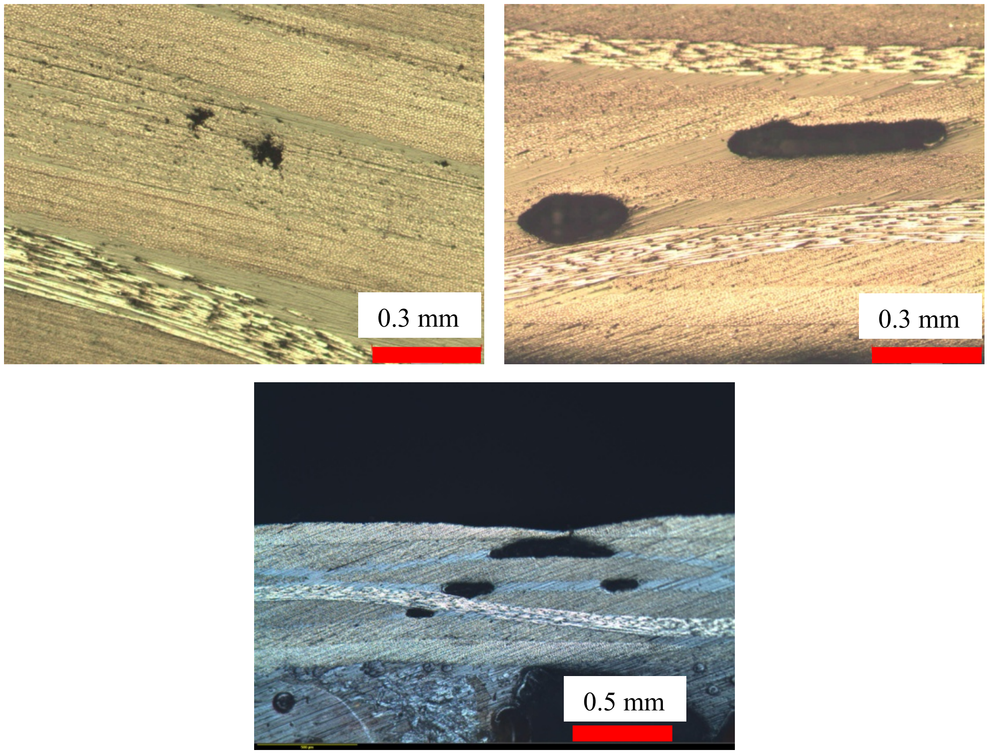

Figure 5.14: Typical micrographs from Part A: MTM45-1 monolithic (top left), Part D: CYCOM5320 sandwich in the partial plies region (top right), and Part D: CYCOM 5320 sandwich in the top skin of the core (bottom).

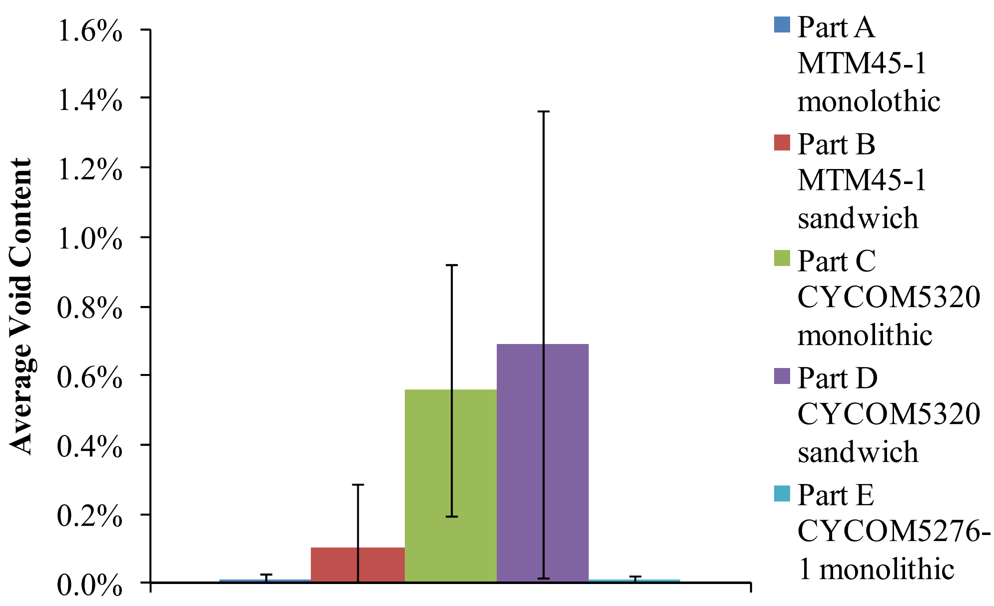

Figure 5.15: Average porosity of representative parts.

These porosity results show that a complex out-of-autoclave laminate can have a porosity as low as the same autoclave laminate. Also, when comparing the sandwich and the monolithic part of the same prepreg, the sandwich part has a higher porosity than a monolithic one. Honeycomb cores have always been challenging for OOA technology because they contain a large quantity of air entrapped in the laminate.

While having different values because of the out time of CYCOM5320, Figure 5.16 and Figure 5.17 show very similar trends. First, the partial plies have a low porosity (all below 0.4%), confirming the results from the ply drop-offs tests (Chapter 4): the air in the partial plies gets evacuated and there is not a clear increase of void content. Second, the core region has a much higher porosity (above 2% for the CYCOM5320). Third, porosity is highest in the top skin of the core (bag side). This may be caused by the air going from the core to the breather during cure and leaving entrapped air. Finally, the bevel region has a porosity between the top and the bottom skin of the core, which is logical since it is the junction of the two skins.

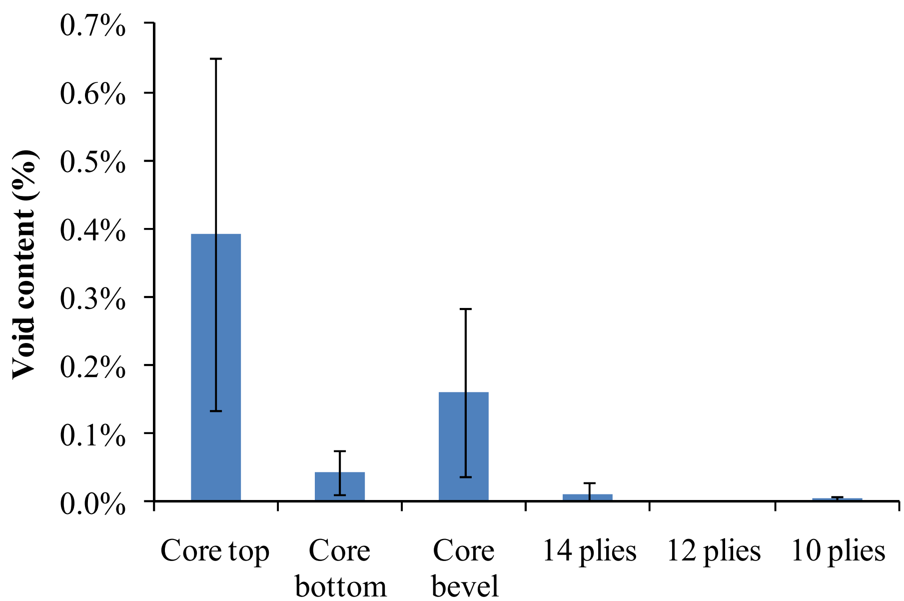

Figure 5.16: Porosity distribution in the MTM45-1 sandwich part.

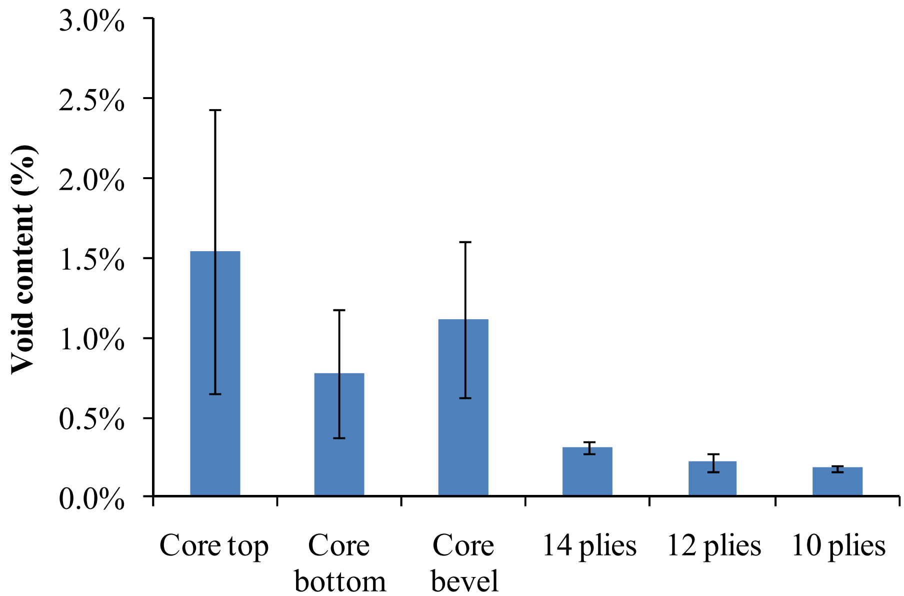

Figure 5.17: Porosity distribution in the CYCOM5320 sandwich part.

5.6.2 Thickness

The thickness deviation was measured in the bottom region of the seats. Average measurements are reported in Figure 5.18. Several observations can be made.

Very similar values were found between the sandwich and the monolithic version of the same prepreg. Thus, the presence of a honeycomb core a few centimetres away from the corners does not have an effect on laminate thickness in the corners.

Comparing MTM45-1 and CYCOM5320, one can see that having a thinner laminate gave better results. CYCOM5320 showed almost no thinning in the convex corner and around 20% thickening in concave corners, whereas MTM45-1 gave 8% thinning in the convex corner and 50% thickening in concave corners. As previously shown by Brillant [8, 9] the thickness becomes less uniform when the ratio Radius/Thickness becomes smaller.

The part made in an autoclave showed very high corner thickening in the concave corners. This is first due to the presence of breather that may have been bridging. Indeed, it is not recommended to leave any surface uncovered with breather in an autoclave to lower the risk of bag punching. Since CYCOM5276-1 has a high bulk factor like OOA prepregs, consumable bridging is likely to happen in concave corners. The difference between the first and the second concave corner (position #5 and position #15) is due to prepreg bridging in the second concave corner. One of the plies was not placed correctly down in the corner during layup. This type of defect is operator dependent.

Overall, a no-bleed autoclave prepreg did not give better results than an out-of-autoclave prepreg.

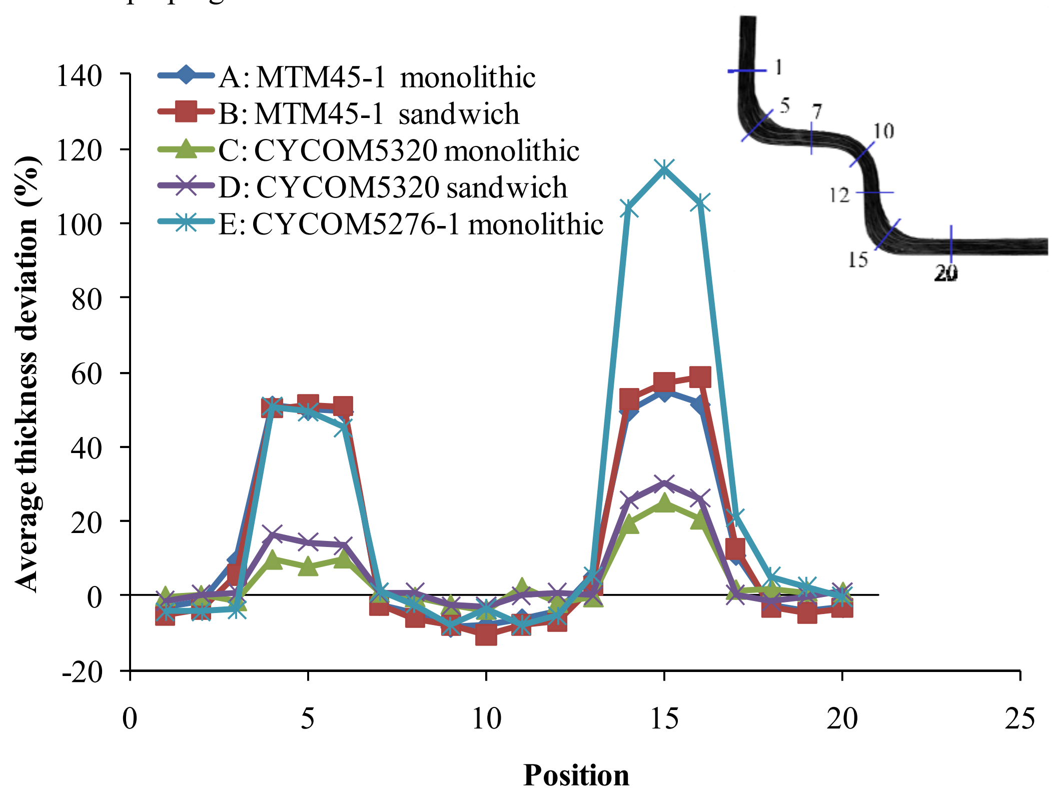

Figure 5.18: Thickness deviation of representative parts.

5.6.3 Mechanical Tests

For each monolithic part, 6 coupons were tested in 3-point bending and 6 other coupons were tested in compression. The results are shown in Figure 5.19 and Figure 5.21.

In 3-point bending, the two OOA prepregs had similar flexural strengths (755 MPa for MTM45-1 and 790 MPa for CYCOM5320). However, failure happened on the compressive side for MTM45-1 and on the tensile side for CYCOM5320.

The autoclave prepreg had a higher flexural strength of 873 MPa, and failure happened on the tensile side (see Figure 5.20).

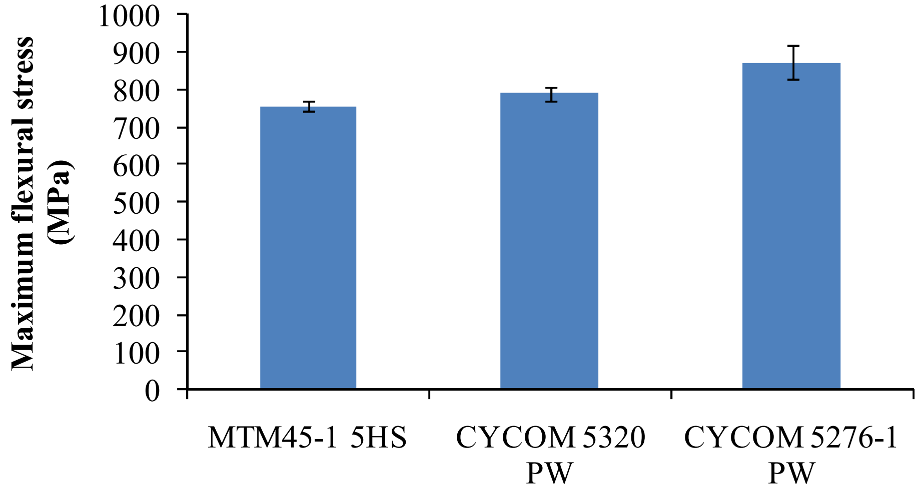

Figure 5.19: Maximum flexural stress of representative parts under 3-point bending load.

Figure 5.20: 3-point bending failed coupons. Top: MTM45-1 5HS (Part A) failed on the compressive side. Bottom: CYCOM5320 PW (Part C) failed on the tensile side.

In compression, the three materials showed similar results. The autoclave prepreg was slightly more resistant, but failures of all materials were all around 440 MPa. Although the autoclave had higher flexural and compression strengths, these results show that OOA prepregs have similar mechanical properties. Moreover, the higher porosity of CYCOM5320 was not clearly detrimental to its mechanical properties. A picture of a typical failed coupon is shown in Figure 5.22.

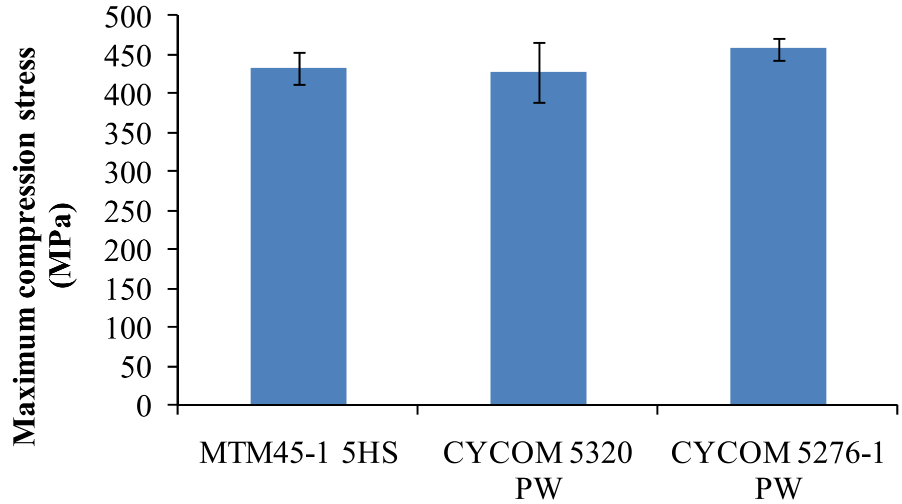

Figure 5.21: Maximum compression stress of representative parts under compressive load.

Figure 5.22: Compression failed coupon. CYCOM5276-1 PW (Part E).

The cores of the sandwich parts were tested in flatwise tension. All the coupons failed in the middle of the core, and not at the core/skin interfaces (see Figure 5.23). That means the adhesive was strongly bonding the core and the skins together. When curing a sandwich part under full vacuum, the adhesive foams and concerns are raised about the strength of the bond. These flatwise tension tests show that the adhesive bonding is stronger than the core itself.

Figure 5.23: Visualisation of the failed core after testing on the MTM45-1 sandwich part.

5.6.4 Glass Transition Temperature (T_g)

The measured T_gs are given in Table 5.5. The two post-cured OOA prepregs had a T_g above 190°C. CYCOM5276-1 had a lower T_g of 169.5°C. With a post-cure, OOA prepregs can have a glass transition temperature as high as autoclave prepregs. The DMA measurements of the storage modulus that gave the T_g values are given in Appendix C.

Table 5.5: Glass transition temperatures of monolithic representative parts.

MTM45-1 (180°C post-cure)	196 (±0.5) °C
CYCOM5320 (180°C post-cure)	191 (±0.5) °C
CYCOM5276-1 (180°C cure, no post-cure)	169.5 (±0.5) °C

5.6.5 Pressure Sensors

Whereas having a good accuracy, the miniature pressure sensors were found not to be very robust to use. The problems did not come from the pressure cell itself, but rather from the wiring between the cell and the data acquisition interface. The wires were brittle and soldered on a small surface at the back of the pressure cell. Consequently, solder joints failed when placing the sensors, applying the vacuum in the bag or heating up the oven. Also, the wires were sometimes crushed by the oven door. For these reasons, almost half of the measurements could not be interpreted. Figure 5.24 shows the most interesting pressure measurements. During the vacuum hold, the core and bag pressures were low. When the oven was heated up, the core pressure increased up to 450 mbar before going down and was as low as bag pressure by the end of the cure. During cure, the exit of the entrapped air from the core can be related to the high void content measured in the sandwich skins, especially the top skin (bag side). The other measurements are reported in Appendix B.

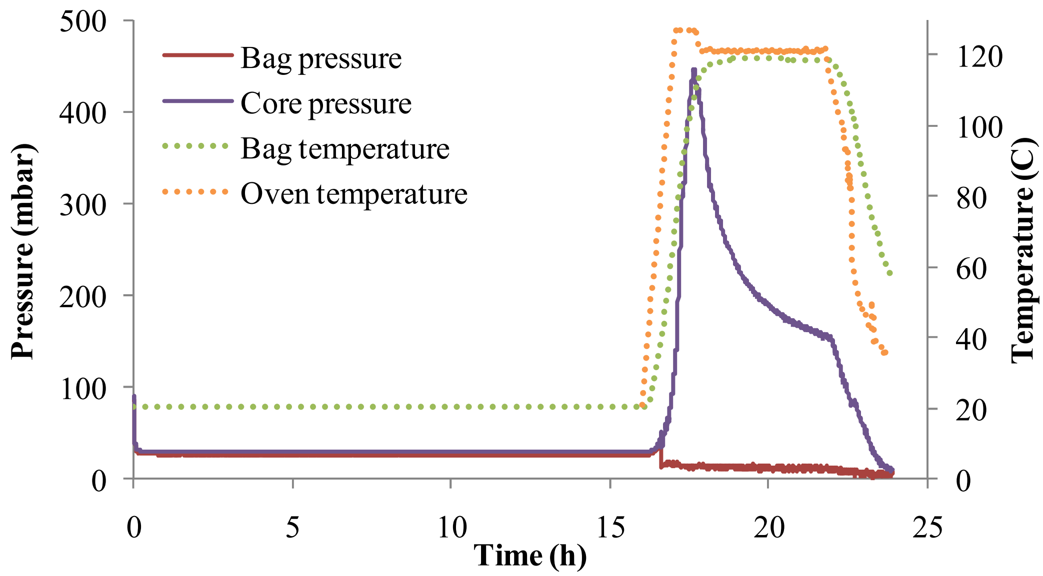

Figure 5.24: Pressure measurements during vacuum hold and cure for Part B: MTM45-1 sandwich part.

6 Conclusion

6.1 Summary and conclusions

This research investigated some aspects of out-of-autoclave technology. Two common features were studied in preliminary experiments: ply drop-offs and tight Z-shape corners. With the knowledge gained from these experiments and other studies done by students of this collaborative project, representative parts were designed and manufactured. Monolithic and sandwich parts were manufactured with MTM45-1 5HS and CYCOM5320 PW, and one monolithic part was manufactured in an autoclave with CYCOM5276-1 PW. Thanks to porosity measurements, thickness measurements in tight corners, mechanical testing and Tg measurements, capacities and limitations of out-of-autoclave technology were investigated and compared with autoclave technology. The following conclusions can be drawn from this research:

1. **Ply drop-offs do not have a detrimental effect on porosity.** There is no crucial need for the partial plies to be in direct contact with edge breathing.
2. **Thickness deviation at corners is a combined consequence of consumable bridging, prepreg's high bulk factor, and prepreg's shearing behaviour.** Corner thickening is observed in concave corners. Convex corners can lead to corner thickening or thinning depending on the boundary conditions of the corner.
3. **OOA prepregs are very sensitive to the time spent at room temperature.** A long out time leads to low tack and higher porosity.
4. **OOA prepregs can have performances similar to autoclave prepregs.** The tests on the representative parts showed that both technologies can produce void-free complex parts. The mechanical properties of OOA prepregs are very close to autoclave prepregs. The T_g of OOA prepregs

was higher than the autoclave prepreg. Manufacturing parts with a uniform thickness in tight corners is a challenge with both technologies.

5. **The best manufacturing technology is specific to each laminate.** Prepreg technology is a solution of choice because it combines several advantages, but OOA and autoclave technologies have limitations. Some parts – with sharp angles for example – would be better manufactured by VARTM, or one of the many existing processes for composite materials.

6.2 Future work

Further knowledge would be gained by scaling up the parts by an order of magnitude, to get to the size of primary structures of aircrafts. Scale up effects should be noticeable, in terms of porosity for example. However, such tests require equipments that are rarely available to academic research.

A way to measure the compaction pressure would be beneficial to quantify the pressure gradient between flanges, convex and concave corners, and relate it to resin migration.

More studies on complex corners need to be performed and repeated a large number of times to account for variability and get statistically robust data.

In the near future, the same representative parts will be manufactured with “fresh” CYCOM5320, and a sandwich part will be manufactured in an autoclave with CYCOM5276-1.

References

[1] W. Roeseler, *et al.*, "Composite materials: the first 100 years," presented at the 16th ICCM, Kyoto, Japan, 2007.

[2] A. Shindo, "Polyacrylonitrile (PAN)-based Carbon Fibers," in *Comprehensive Composite Materials*, K. Anthony and Z. Carl, Eds., ed Oxford: Pergamon, 2000, pp. 1-33.

[3] M. W. Hyer and S. R. White, *Stress analysis of fiber-reinforced composite materials*. Boston, Mass.: WCB McGraw-Hill, 1998.

[4] J. C. Seferis, *et al.*, "Prepregging and autoclaving of thermoset composites," in *Comprehensive Composite Materials*. vol. 2, E. Science, Ed., ed, 2000.

[5] J.-A. E. Manson, *et al.*, "Composite Processing and Manufacturing - An Overview," in *Comprehensive Composite Materials*. vol. 2, E. Science, Ed., ed, 2000.

[6] G. Bond, *et al.*, "Non-autoclave prepreg manufacturing technology," in *International SAMPE Symposium and Exhibition*, Menphis, TN, 2008.

[7] J. Kratz, "Processing Composite Sandwich Structures using Out-of-Autoclave Technology," Master of Engineering, Mechanical Engineering, McGill University, Montreal, 2009.

[8] M. Brillant, "Out-of-Autoclave Manufacturing of Complex Shape Composite Laminates," Master of Engineering, Mechanical Engineering, McGill, Montreal, QC, 2010.

[9] M. Brillant and P. Hubert, "Out-of-autoclave processing of complex shape laminates," in *International SAMPE Symposium and Exhibition*, Seattle, WA, 2010.

[10] J. Kratz, *et al.*, "Out of autoclave honeycomb structures: the behaviour of entrapped air during cure," in *International SAMPE Symposium and Exhibition*, Seattle, WA, 2010.

[11] B. Louis, "Gas transport in out-of-autoclave laminates," Master of Applied Science, Materials Engineering, The University of British Columbia, Vancouver, 2010.

[12] A. C. Loos and G. S. Springer, "Curing of Epoxy Matrix Composites," *Journal of Composite Materials,* vol. 17, pp. 135-169, January 1, 1983 1983.

[13] P. Hubert and A. Poursartip, "A Review of Flow and Compaction Modelling Relevant to Thermoset Matrix Laminate Processing," *Journal of Reinforced Plastics and Composites,* vol. 17, pp. 286-318, March 1, 1998 1998.

[14] E. Ruiz, "Course Notes, MEC6318: Composite Manufacturing, Ecole Polytechnique de Montréal," ed, 2009.

[15] C. Ridgard, "Out of Autoclave Composite Technology for Aerospace, Defense and Space Structures," in *International SAMPE Symposium and Exhibition*, Baltimore, MD, 2009.

[16] J. Boyd, "Vacuum bag only composite manufacturing," SAMPE tutorial2008.
[17] Y. Eom*, et al.*, "Stress-initiated void formation during cure of a three-dimensionally constrained thermoset resin," *Polymer Engineering & Science,* vol. 41, pp. 492-503, 2001.
[18] Y. Gu*, et al.*, "Theoretical and experimental analysis on void formation in epoxy composite laminates," in *International SAMPE Symposium and Exhibition*, Cincinnati, Ohio, USA, 2007.
[19] J. Kardos*, et al.*, "Void growth and resin transport during processing of thermosetting — Matrix composites," ed, 1980, pp. 101-123.
[20] V. Michaud*, et al.*, "Low pressure processing of high fiber content composites," in *The 8th International Conference on Flow Processes in Composite Materials (FPCM8)*, Douai, FRANCE - 11 – 13 July 2006, 2006.
[21] K. J. Ahn*, et al.*, "Permeation measurements through prepreg laminates," *Sampe Journal,* vol. 27, pp. 19-25, Nov-Dec 1991.
[22] A. R. A. Arafath*, et al.*, "Gas transport in prepregs: model and permeability experiments," in *17th ICCM*, Edinburgh, Scotland, 2009.
[23] B. Louis*, et al.*, "Gas permeability measurements of out of autoclave prepreg MTM45-1/CF2426A," in *International SAMPE Symposium and Exhibition*, Seattle, WA, 2010.
[24] K. Hsiao and G. Fernlund, "CYCOM5320 in-plane and out-of-plane permeability," 2010.
[25] J. Kratz, "CYCOM5320 facesheet permeability," 2010.
[26] G. Bond and J. Luner, "Design of experiments evaluation of processing parameters for non-autoclave composite prepreg," The Boeing Company2008.
[27] F. Bonjour*, et al.*, "Vacuum bag processing of large composite structures for America's cup class boats," in *International SAMPE Symposium and Exhibition*, Paris, 2003.
[28] S. S. Tavares*, et al.*, "Non-autoclave processing of sandwich structures: the role of prepreg through thickness air permeability," in *16th ICCM*, Kyoto, Japan, 2007.
[29] S. S. Tavares*, et al.*, "Vacuum-bag processing of sandwich structures: Role of honeycomb pressure level on skin-core adhesion and skin quality," *Composites Science and Technology,* vol. 70, pp. 797-803, 2010.
[30] S. S. Tavares*, et al.*, "Non-autoclave processing of honeycomb sandwich structures: Skin through thickness air permeability during cure," *Composites Part A: Applied Science and Manufacturing,* vol. 41, pp. 646-652, 2010.
[31] G. Fernlund*, et al.*, "Experimental and numerical study of the effect of caul-sheets on corner thinning of composite laminates," *Composites Part A: Applied Science and Manufacturing,* vol. 33, pp. 411-426, 2002.
[32] P. Hubert and A. Poursartip, "Aspects of the Compaction of Composite Angle Laminates: An Experimental Investigation," *Journal of Composite Materials,* vol. 35, pp. 2-26, January 1, 2001 2001.

[33] K. J. Ahn and G. Bond, "Non-autoclave prepreg technology for primary aerospace structures," in *International SAMPE Symposium and Exhibition*, Witchita, KA, 2009.
[34] K. R. Bernetich, "Evaluation of detail part fabrication using out-of-autoclave prepreg," in *International SAMPE Symposium and Exhibition*, Seattle, WA, 2010.
[35] A. D. Botting*, et al.*, "Effect of ply-drop configuration on delamination strength of tapered composite structures," *Aiaa Journal,* vol. 34, pp. 1650-1656, Aug 1996.
[36] A. Mukherjee and B. Varughese, "Design guidelines for ply drop-off in laminated composite structures," *Composites Part B: Engineering,* vol. 32, pp. 153-164, 2001.
[37] ASTM, "Standard test methods for constituent content of composite materials," in *D 3171 - 06*, ed, 2006.
[38] M. t. staff, "MS54XX Miniature SMD Pressure Sensor," ed. Bevaix, Switzerland, 2010.

Appendix A: Manufacturing Steps

Some of the manufacturing steps are illustrated in this appendix. No pictures of the autoclave part could be taken.

Figure A.1: Placing the 1st layer (Part A MTM45-1 monolithic).

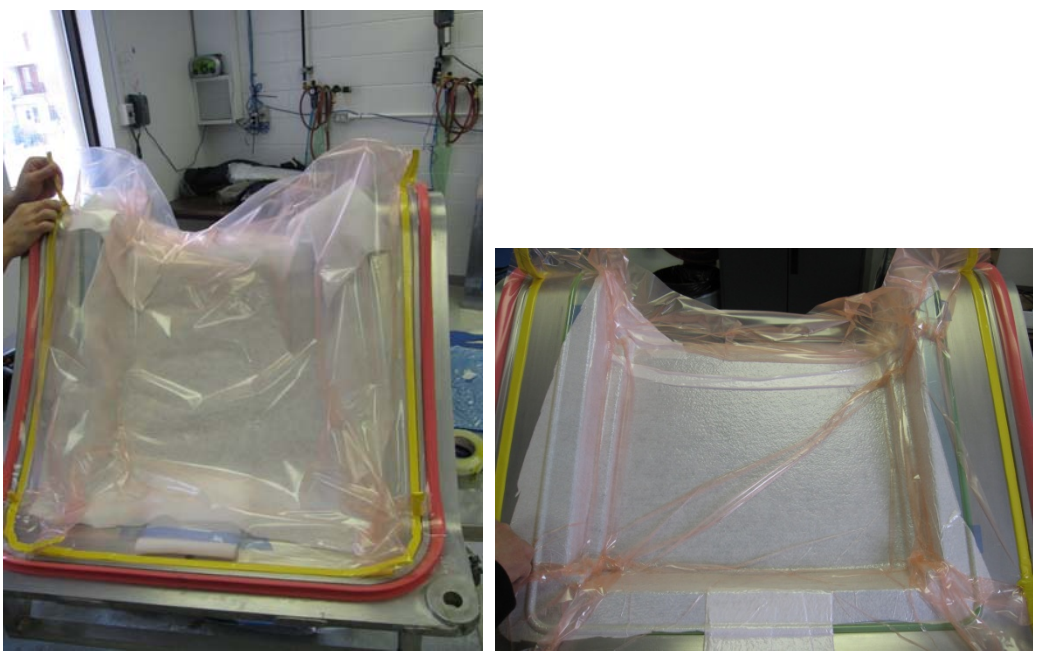

Figure A.2: Debulk between 1st and 2nd layers (Part A MTM45-1 monolithic).

Figure A.3: Placing the 2nd layer (Part C CYCOM5320 monolithic).

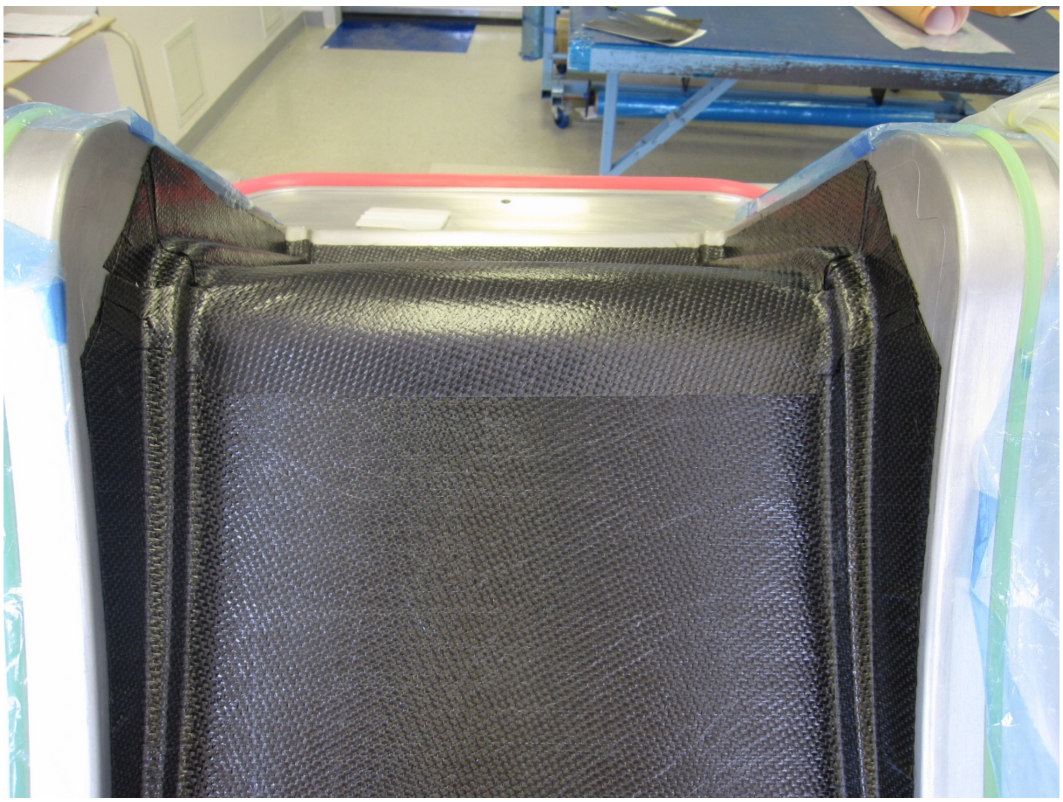

Figure A.4: Placing the 4th layer (PART B MTM45-1 sandwich).

Figure A.5: Placing the partial plies (Part D CYCOM5320 sandwich).

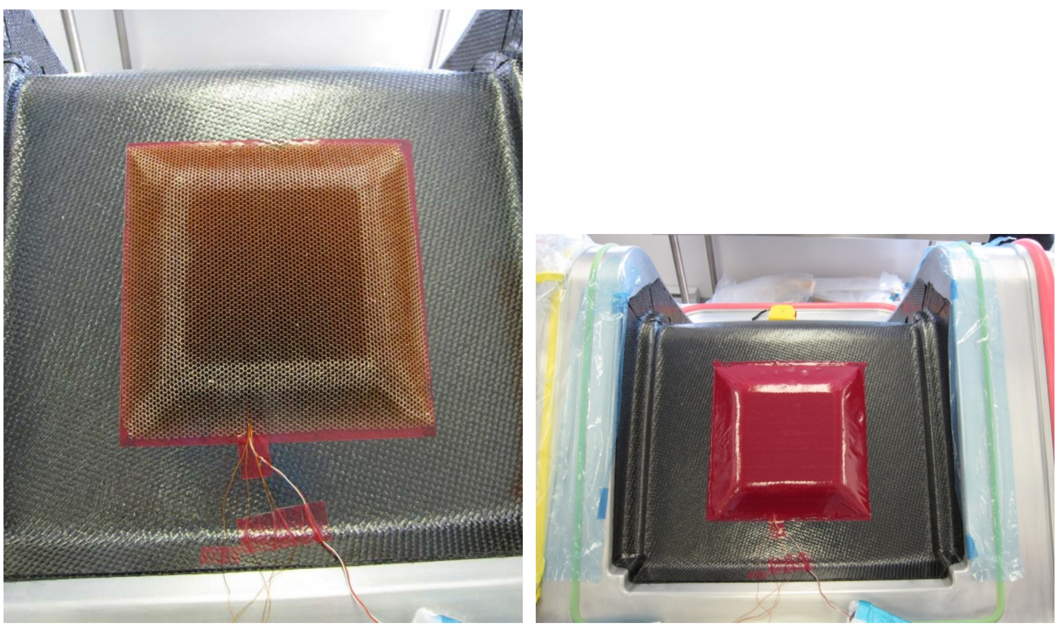

Figure A.6: Placing the honeycomb core (Part B MTM45-1 sandwich).

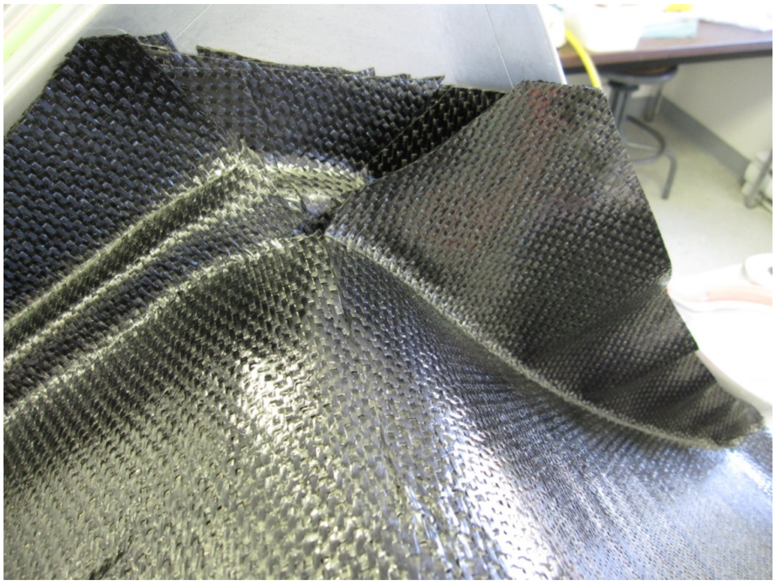

Figure A.7: Placing the 7th layer (Part B MTN45-1 sandwich).

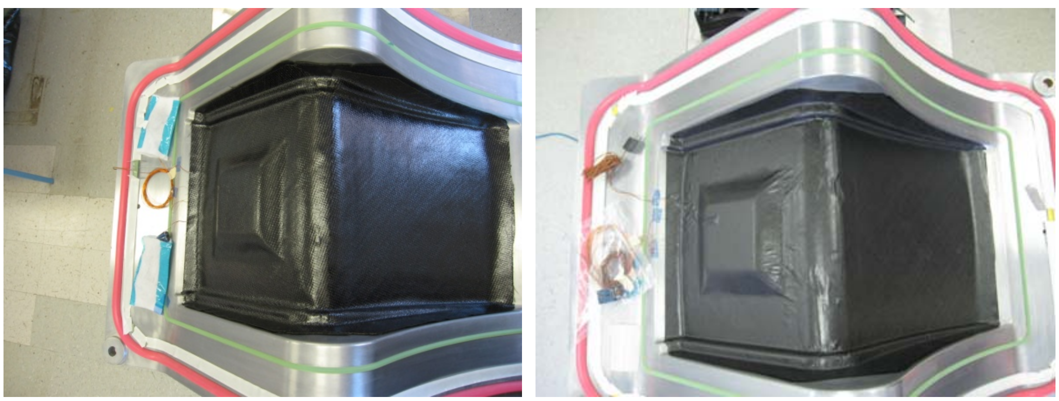

Figure A.8: Part B MTM45-1 sandwich (left) and Part D CYCOM5320 (right) with all plies laid up.

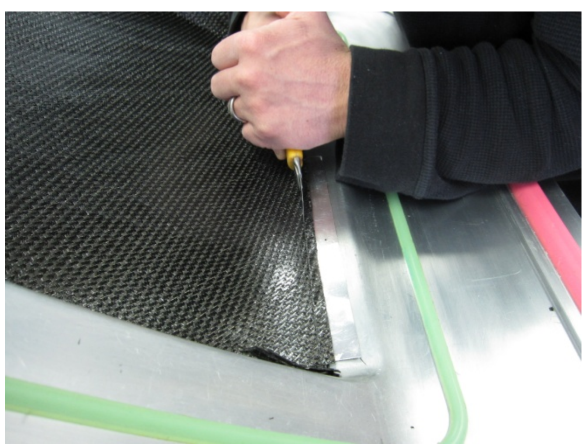

Figure A.9: Edge trimming (Part A MTM45-1 monolithic).

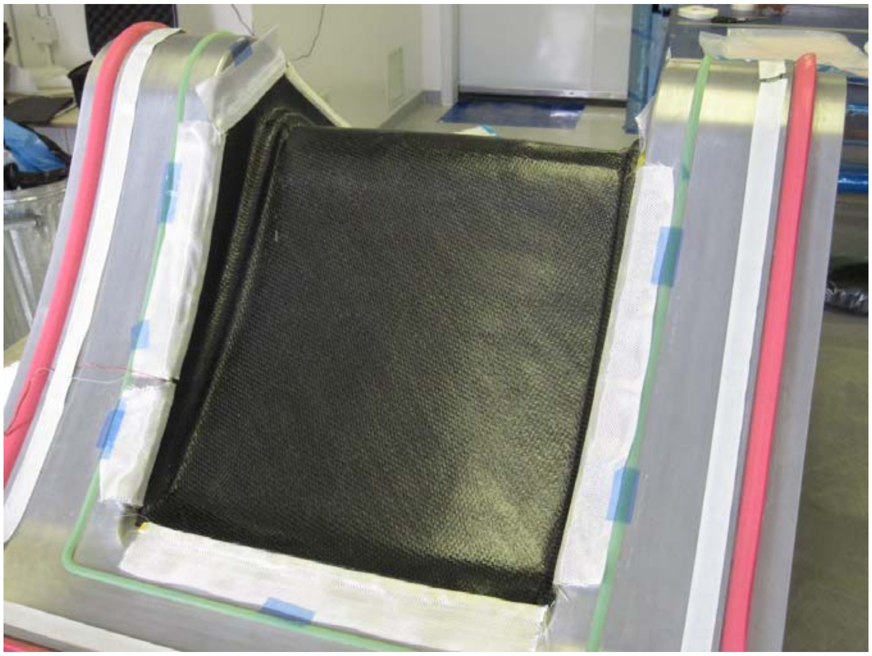

Figure A.10: Edge breathing (Part B MTM45-1 sandwich).

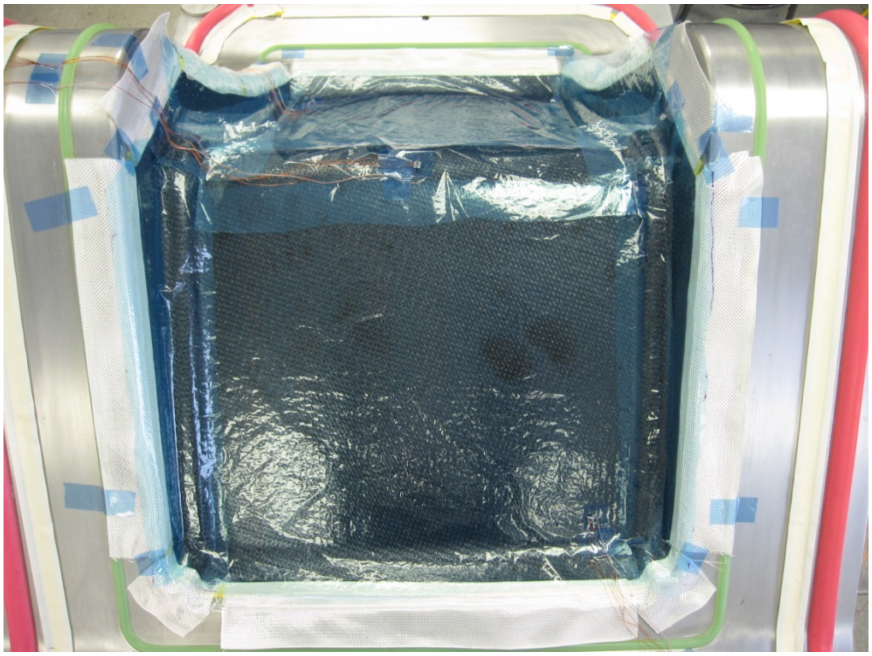

Figure A.11: Release film (Part A MTM45-1 monolithic). Pressure sensors can be seen.

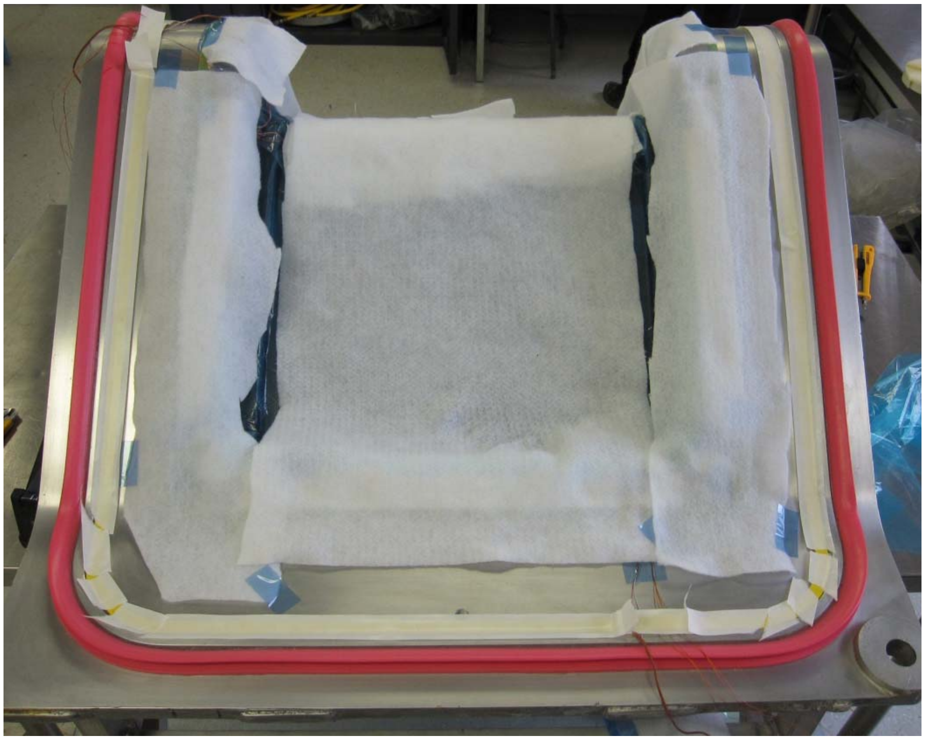

Figure A.12: Breather (Part C CYCOM5320 monolithic). No breather in the tight corners.

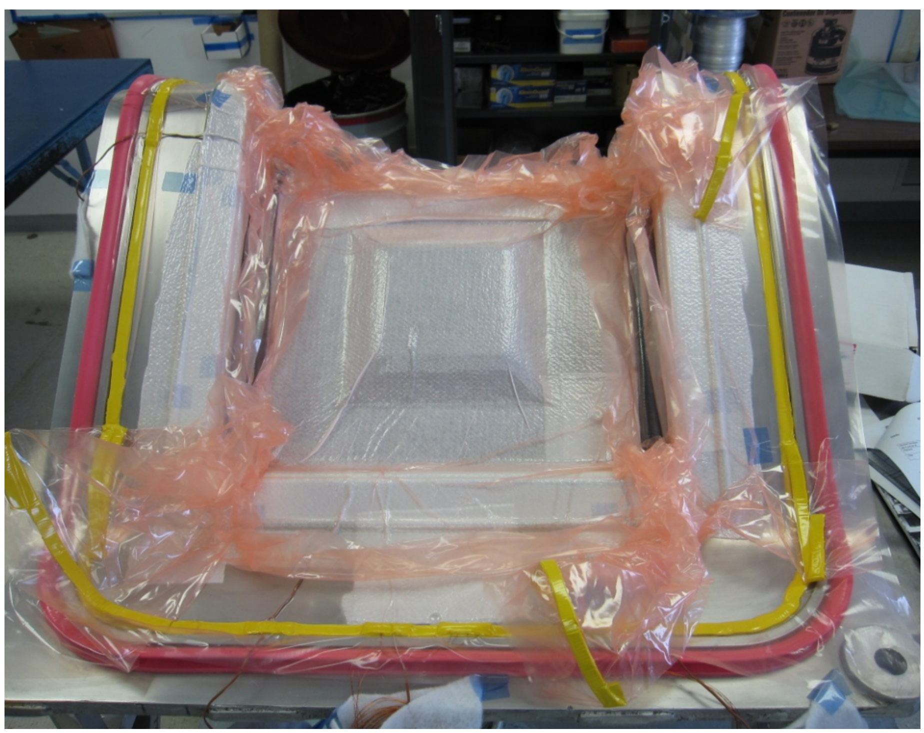

Figure A.13: Final bag (Part D CYCOM532- sandwich). The part is ready to be cured.

Appendix B: Pressure Measurements

As discussed in 5.6.5, the miniature pressure sensors were not very robust. As a consequence, several measurements are not shown because they are meaningless. Furthermore, the measurements of the first representative part (CYCOM5320 monolithic) were affected by the bag touching the membrane of the sensors, thus increasing the pressure readings. This is the reason why the pressure seems to be so high in the graph below. The vacuum pressure measurement shows that the bag pressure was certainly low (below 40 mbar).

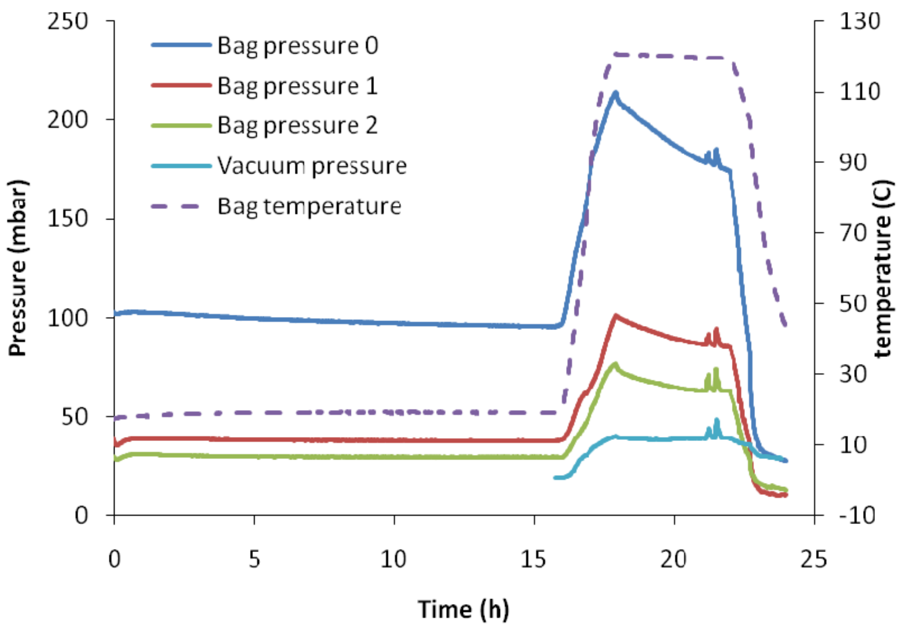

Figure B.1: Pressure measurements during cure of the MTM45-1 monolithic part.

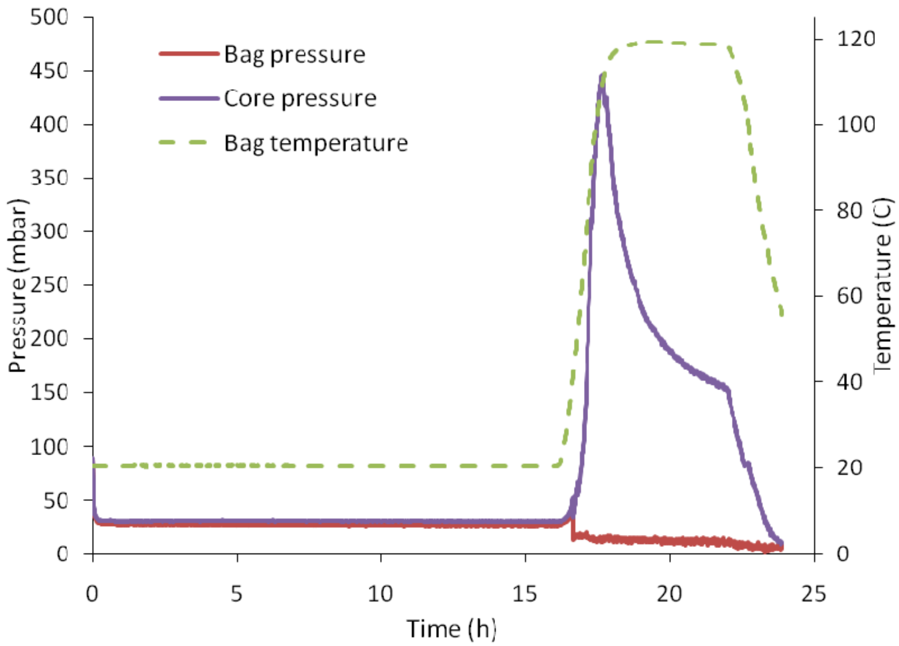

Figure B.2: Pressure measurements during cure of the MTM45-1 sandwich part.

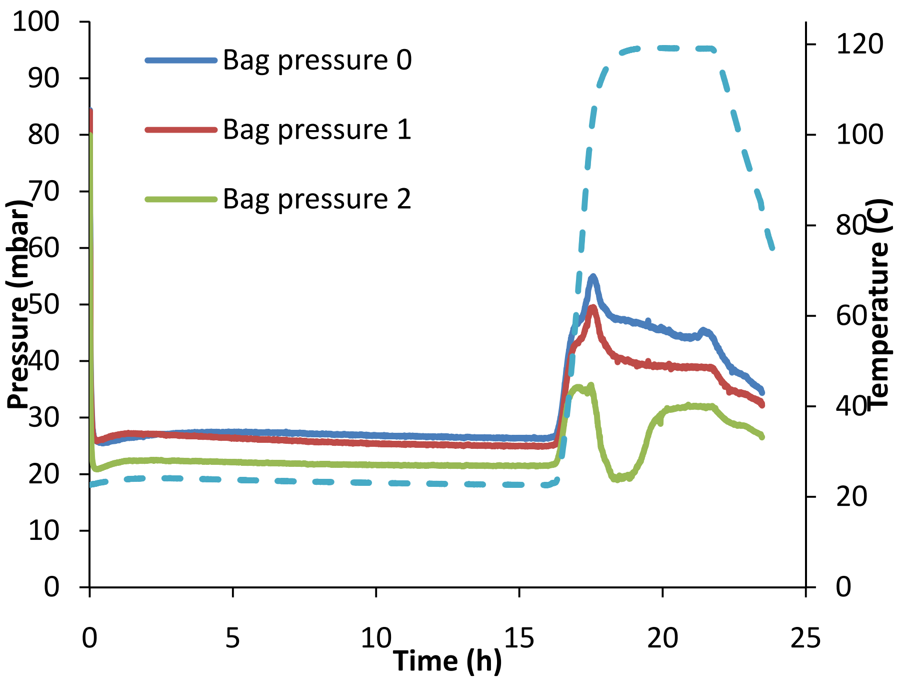

Figure B.3: Pressure measurements during cure of the CYCOM5320 sandwich part.

Appendix C: T_g Measurements

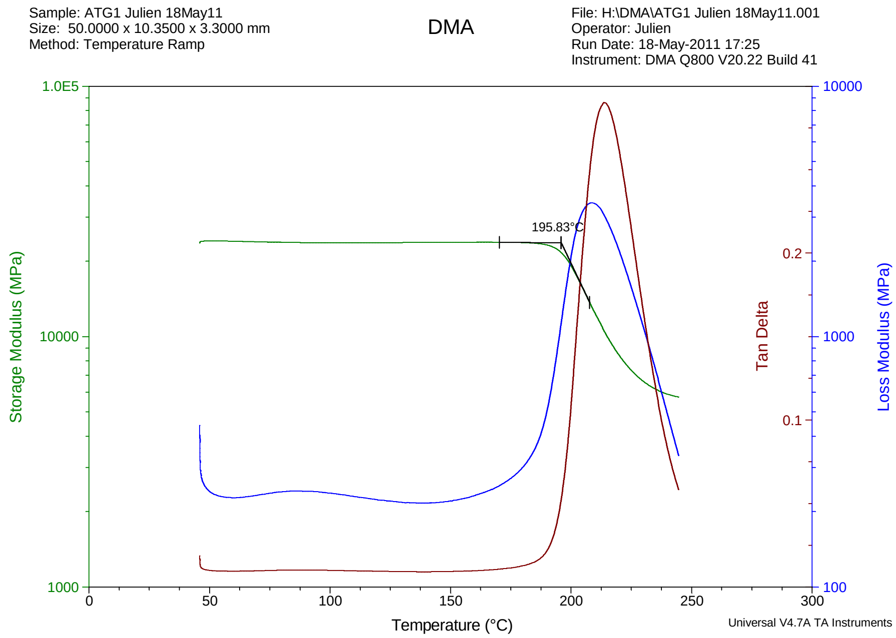

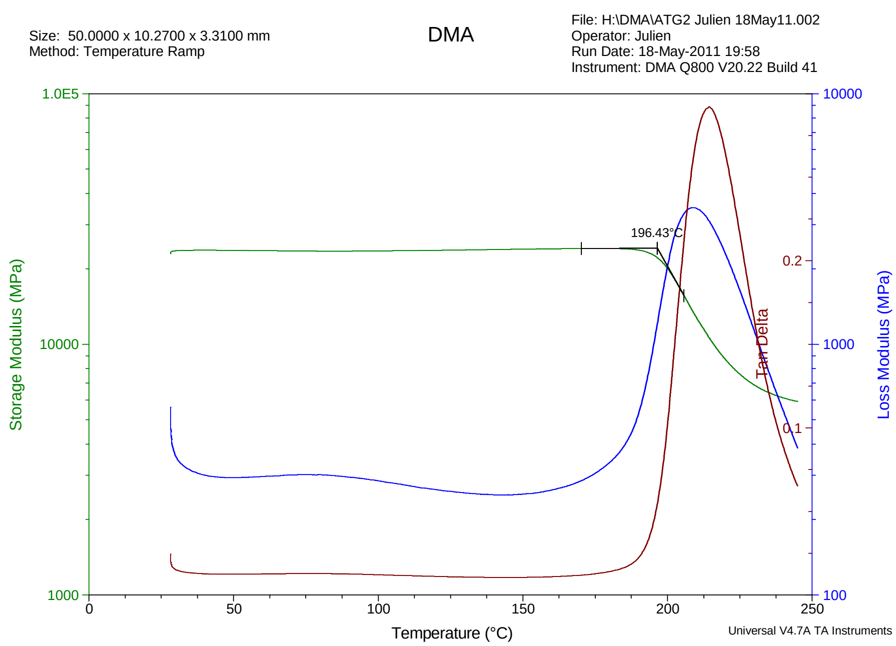

Figure C.1: T_g measurements of the MTM45-1 monolithic part.

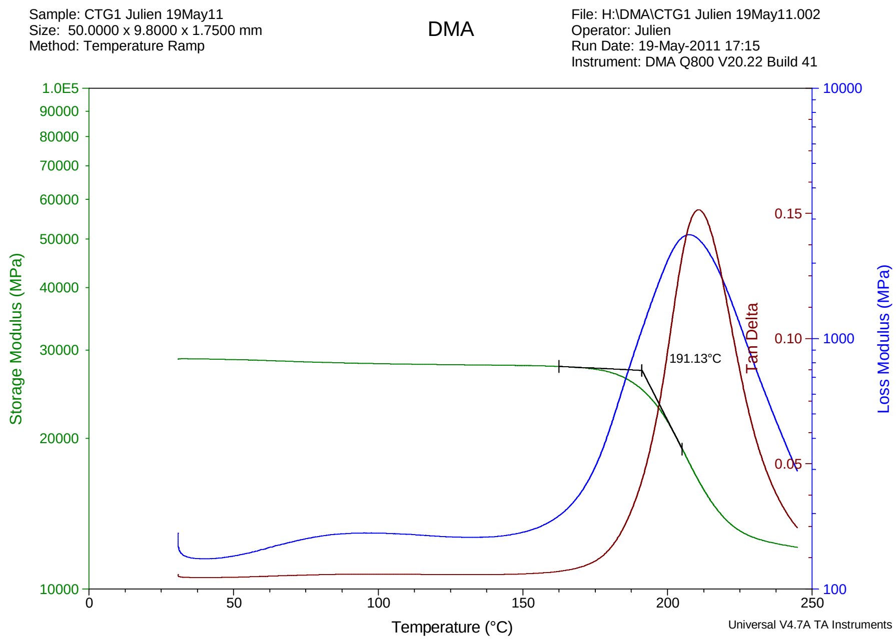

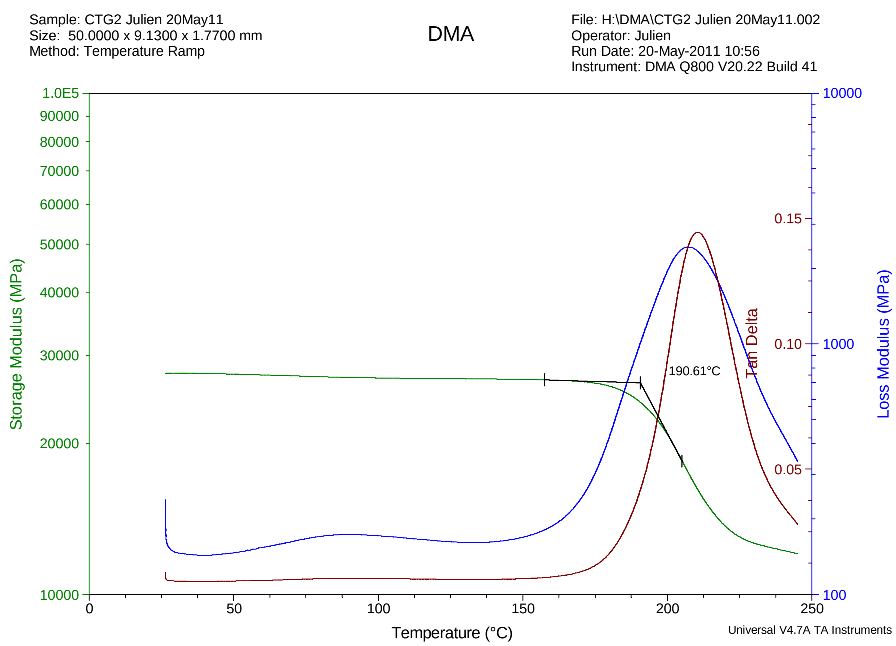

Figure C.2: T_g measurements of the CYCOM5320 monolithic part.

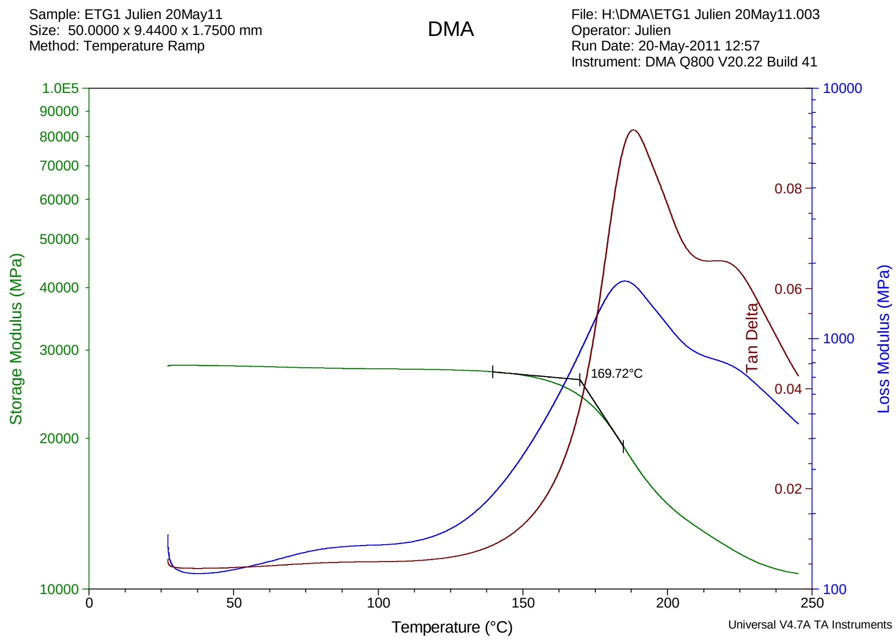

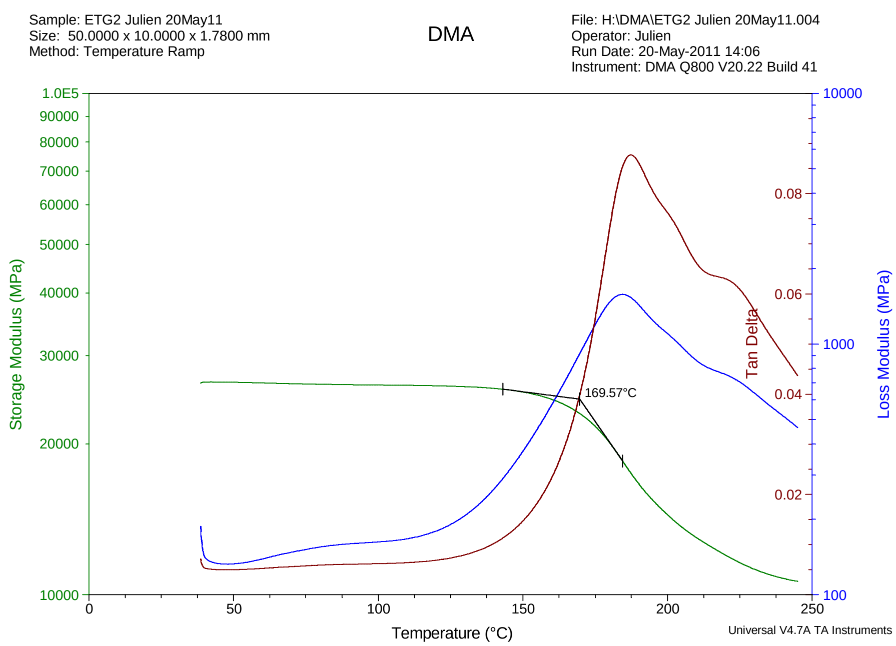

Figure C.3: T_g measurements of the CYCOM5276-1 monolithic part.